



142
457
THS

This is to certify that the
thesis entitled

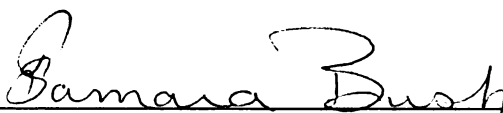
A METHOD FOR PREDICTION OF SEATED SPINAL
CURVATURES

presented by

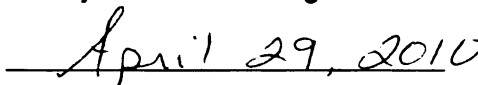
SAMUEL THOMAS LEITKAM

has been accepted towards fulfillment
of the requirements for the

M.S. degree in Engineering Mechanics



Major Professor's Signature



Date

MSU is an Affirmative Action/Equal Opportunity Employer

LIBRARY
Michigan State
University

PLACE IN RETURN BOX to remove this checkout from your record.
TO AVOID FINES return on or before date due.
MAY BE RECALLED with earlier due date if requested.

DATE DUE	DATE DUE	DATE DUE

A METHOD FOR PREDICTION OF SEATED SPINAL CURVATURES

By

Samuel Thomas Leitekam

A THESIS

**Submitted to
Michigan State University
in partial fulfillment of the requirements
for the degree of**

MASTER OF SCIENCE

Engineering Mechanics

2010

ABSTRACT

A METHOD OF PREDICTION OF SEATED SPINAL CURVATURES

By

Samuel Thomas Leitkam

The purpose of this research was to determine if lumbar curvature could be quantified by using only measurements made on the anterior portion of the body. To do this, 31 subjects were tested in four static seated positions as well as dynamic seated postures using a motion capture system. Anterior measurements were used to quantify the relative positions of the ribcage and pelvis in a measure called “openness angle”. Posterior measurements of the lumbar curvature were quantified in a measure called “lumbar angle”. The relationship between the openness angle and the lumbar angle was evaluated using a linear model and a second-order polynomial model for both the static positions and the dynamic postures.

The relationship between the openness angle and the lumbar angle is fit well by both the linear model and the polynomial model in both the static and dynamic cases. Predictions of static lumbar angles of a population developed from linear and polynomial models from a separate population were found to be statistically indistinguishable from the actual lumbar angles. Subject specific predictions of static lumbar angles were also found to be indistinguishable from actual lumbar angles when the subjects’ dynamic models were used for prediction.

These results show reliable predictions of lumbar curvature are possible in static postures by using openness angle in conjunction with a previously determined first or second order calibration model.

This thesis is dedicated to my family in every form it takes.

ACKNOWLEDGEMENTS

I'd like to acknowledge the many people who made this possible. First and foremost, I'd like to thank the subjects who volunteered their time and without whom there would be only be theory. I'd also like to thank my advisor, Dr. Tamara Reid Bush, for giving me the opportunity, balancing the perfect amount of patience and pressure, and for all of the guidance and advice along the way.

In addition, I'd like to thank my family, friends, and best friend for their infinite support and keeping me attached to reality. I'd like to thank my committee members, Dr. Joseph Vorro and Dr. Neil Wright, for lending me their time and advice so that this thesis could evolve into a far more complete, polished and precise piece of work than it was when I first thought I was done. Lastly, I'd like to thank Brad Rutledge, Katie Friederichs, Trevor Deland, and everyone else in the Biomechanical Design and Research Lab for all of their help. Thank you all.

TABLE OF CONTENTS

INTRODUCTION.....	1
LITERATURE REVIEW	4
Technology	4
Standing vs. Seated	7
METHODS.....	9
Data Collection	9
<i>Subject pool</i>	9
<i>Anatomical measures</i>	10
<i>Markers and motion tracking</i>	11
<i>Test conditions</i>	15
<i>Static positions</i>	15
<i>Continuous motion</i>	17
Analysis	19
<i>Hip joint center</i>	19
<i>Lumbar angle</i>	22
Statistical Analysis Methods	25
<i>Distinct static positions</i>	25
<i>Anthropometric correlation to openness/lumbar angle slope</i>	26
<i>Predictive capacity</i>	27
RESULTS.....	31
Openness and Lumbar Angles	31
Distinct Static Positions	33
Relationship between Openness and Lumbar Angles	34
<i>Static</i>	34
<i>Dynamic</i>	42
Anthropometric Correlation to Openness/Lumbar Angle Slope	53
Predictive Capacity	54
<i>Static data predicting static positions for test population</i>	54
<i>Dynamic data predicting dynamic positions for the test population</i>	56
<i>Static data predicting dynamic positions for the test population</i>	59
<i>Dynamic data predicting static positions for the test population</i>	62
<i>Static data predicting dynamic positions within a subject</i>	65
<i>Dynamic data predicting static positions within a subject</i>	66
DISCUSSION AND CONCLUSIONS.....	67
Openness and Lumbar Angles	67
Distinct Static Positions	69
Observations between openness and lumbar angles	70
<i>Static</i>	70

<i>Dynamic</i>	72
Anthropometric Measures Related to Slope	73
Predictive Capacity	73
<i>Static data predicting static positions for the test population</i>	74
<i>Dynamic data predicting dynamic positions for the test population</i>	74
<i>Static data predicting dynamic positions for the test population</i>	75
<i>Dynamic data predicting static positions for the test population</i>	75
<i>Static data predicting dynamic positions within a subject</i>	76
<i>Dynamic data predicting static positions within a subject</i>	77
APPENDIX	84
A1. Subject Questionnaire	84
A2. Individual Subject Measurements	86
A3. Calibration Measurements	87
A4. Lumbar radius calculation	88
A5. Dynamic Openness and Lumbar Angles (deg)	92
BIBLIOGRAPHY	117

LIST OF TABLES

Table 1. Height, weight, and age of the subjects.....	9
Table 2. Height, weight, and age of the subjects as divided by gender	9
Table 3. Subject seated dimensions and pelvic dimensions (all values in cm)	11
Table 4. Static openness angles for each subject at each posture	31
Table 5. Static lumbar angles for each subject at each posture.....	32
Table 6. Dynamic maximum, minimum, and range values for openness and lumbar angles.....	33
Table 7. Probabilities that each pair of positions is the statistically the same as determined by a paired t-test	33
Table 8. Slope, linear r^2 and polynomial r^2 values for each subject as determined by best fit line	41
Table 9. Summary table of slope, intercept and r^2 for 15 dynamic subjects.....	47
Table 10. Pearson Product Moment Correlation Coefficients for Slope vs. each anthropometric measure	53
Table 11. Paired t-test values comparing predicted dynamic lumbar angles vs. actual lumbar angles for a prediction model based off the same subject's static data	65
Table 12. Paired t-test values comparing predicted static lumbar angles vs. actual static lumbar angles for a subject prediction model based off of the same subject's dynamic data	66
Table 13. Prediction methods summary table	78

LIST OF FIGURES

Figure 1. Motion capture data collection configuration with global coordinate system and origin shown	12
Figure 2. Retroreflective markers applied to the posterior at C7, T12, MidPSIS while standing erect with additional markers spaced approximately 3cm apart between C7 and MidPSIS	13
Figure 3. Retroreflective markers applied to the subject's anterior and lateral sides	14
Figure 4. Basic posture assumed by the subject with head over pelvis, feet flat on floor, and gaze forward	15
Figure 5. Static postures assumed by the subjects. Clockwise from top left: Maximum Lumbar Lordosis, Maximum Lumbar Kyphosis, "Straight and Tall", "Comfortable"	17
Figure 6. Diagram of the "openness" angle as calculated from the positions of HJC, ASIS, Sternum marker and C7	22
Figure 7. Calculation diagram for circumradius and lumbar angle.....	24
Figure 8. Diagram of the lumbar angle as calculated from the positions of T12, LU, and Mid-PSIS	25
Figure 9 (a-ee). Openness Angle vs. Lumbar Angle for each individual subject using static postures with included linear and second order polynomial best fits	34
Figure 10 (a,b). a) Linear best fit plots for subjects 1-15.....	40
Figure 11 (a-o). Openness Angle vs. Lumbar Angle for each individual subject using static postures with included linear and second order polynomial best fits	42
Figure 12 (a-o). Dynamic and Static data plotted as Openness vs. Lumbar Angle for each subject with sufficient dynamic data.....	48
Figure 13. Graphical representation of linear predictive model developed from the static openness and lumbar angle data of subjects S01-S16	54
Figure 14. Predicted static lumbar angle values compared to actual static lumbar angle values for linear static model applied to the openness angles of subjects S17-S31	55

Figure 15. Graphical representation of polynomial predictive model developed from the static openness and lumbar angle data of subjects S01-S16	55
Figure 16. Predicted static lumbar angle values compared to actual static lumbar angle values for polynomial static model applied to the openness angles of subjects S17-S31	56
Figure 17. Graphical representation of linear predictive model developed from the first eight subjects in the dynamic data group.....	57
Figure 18. Predicted dynamic lumbar angle values compared to actual dynamic lumbar angle values for linear dynamic model applied to the openness angles of the last seven subjects in the dynamic data group.....	57
Figure 19. Graphical representation of polynomial predictive model developed from the first eight subjects in the dynamic data group.....	58
Figure 20. Predicted dynamic lumbar angle values compared to actual dynamic lumbar angle values for polynomial dynamic model applied to the openness angles of the last seven subjects in the dynamic data group.....	59
Figure 21. Graphical representation of linear population predictive model developed from all of the static openness and lumbar angle data	60
Figure 22. Predicted dynamic lumbar angle values compared to actual dynamic lumbar angle values for linear static population model applied to the openness angles of the entire dynamic data group.....	60
Figure 23. Graphical representation of polynomial population predictive model developed from all of the static openness and lumbar angle data.....	61
Figure 24. Predicted dynamic lumbar angle values compared to actual dynamic lumbar angle values for polynomial static population model applied to the openness angles of the entire dynamic data group.....	62
Figure 25. Graphical representation of linear population predictive model developed from all of the dynamic openness and lumbar angle data	62
Figure 26. Predicted static lumbar angle values compared to actual static lumbar angle values for linear dynamic population model applied to the openness angles of the entire static data group	63
Figure 27. Graphical representation of polynomial population predictive model developed from all of the dynamic openness and lumbar angle data.....	64

Figure 28. Predicted static lumbar angle values compared to actual static lumbar angle values for polynomial dynamic population model applied to the openness angles of the entire static data group	65
Figure 29. Diagram for radius calculation	88

LIST OF SYMBOLS AND ABBREVIATIONS

a	distance between MidPSIS and T12 lumbar markers
ASIS	Anterior Superior Iliac Spine
b	distance between MidPSIS and LU lumbar markers
c	distance between T12 and LU lumbar markers
C7	seventh cervical vertebra
\bar{G}_{name}	global position vector of marker “name”
HJC	Hip Joint Center
IVD	Intervertebral Disc
\bar{L}_D	local pelvis depth vector
\hat{L}_{Dunit}	local pelvis depth unit vector
\bar{L}_H	local pelvis height vector
\hat{L}_{Hunit}	local pelvis height unit vector
\bar{L}_W	local pelvis width vector
\hat{L}_{Wunit}	local pelvis width unit vector
LBP	Lower Back Pain
LU	most eccentric lumbar marker
MidPSIS	Midpoint between the right and left PSIS
MRI	Magnetic Resonance Imaging
\bar{P}	Pelvis vector
PD	Pelvic Depth

PH	Pelvic Height
PSIS	Posterior Superior Iliac Spine
PW	Pelvic Width
\bar{Q}_{name}	translated and rotated global position vector of marker “name”
r	radius of calculated lumbar semicircle
\bar{R}	Ribcage vector
T12	twelfth thoracic vertebra
\bar{T}_{name}	translated global position vector of marker “name”
α	lumbar angle
ϕ	YZ-plane rotation angle
θ	openness angle

INTRODUCTION

Lower back pain (LBP) is a widespread and costly problem that results in significant compensation claims and lost time at work. Several studies have shown that the problem is prevalent in across different populations around the world and across many different types of industry including, but not limited to, helicopter pilots, tractor drivers, bus drivers, factory workers, commercial travelers, dental hygienists and steel industry workers [1, 2].

This high prevalence of LBP can become costly for society [3]. A large part of this cost comes from workers compensation claims alone [4]. However, it is not limited to just the compensation cost. In Great Britain, in 1998, 1632 million pounds were spent covering medical care associated with LBP including physiotherapists, hospital costs, medication, community care, and radiology [5]. In the US, the figures are even more staggering: The National Institute for Occupational Safety and Health (NIOSH) estimates that low back pain costs American industry \$14 billion dollars annually [6].

This back pain can be linked to seating [3, 7, 8]. It has been shown that people who had jobs that required durations of static postures, such as being in a static seated position, were more likely to develop back pain [9]. Researchers have tested many hypotheses for the cause of lower back pain, ranging from reduced blood flow in the region and reduced exercising of the intervertebral discs (IVD) to increased pressure and forces in the IVD and forces in the zygapophysial joints [10]. While the results are often inconsistent, the constant through the research is that extended periods of static posture are unhealthy for the lower back.

However, static postures are not the only option while seated. It has been shown that a dynamic posture can be good for the body. Research has shown that a dynamic posture can decrease vertebral disc degeneration over time [8]. Similarly, it has also been shown that rotational body dynamics can have a positive influence the subject's LBP [11]. It is presumed that this is due to the increase in movement of the fluid into and out of the avascular IVDs. Other research has shown that this increased activity should occur in moderation as LBP occurs from not only low levels of back activity but also high levels of back activity [2, 12].

Knowing this, it then becomes important to assess measures to prevent LBP by ways of promoting healthier, dynamic postures. It has been suggested that dynamic chairs offer potential advantage over simple static chairs [7]. Whereas simple chairs support one static posture, dynamic chairs offer the possibility of supporting a wide range of postures with a single chair. However, to confirm this, researchers need to understand how the spinal curvature changes as people move through a full range of spinal articulations. Once researchers understand this motion pattern, engineers can begin to design for dynamic motions of a seat that will accommodate a range of anthropometry.

The problem then becomes measuring the human in a dynamic seat without changing the human/seat interface. Understanding of the human/seat interface is crucial to gaining a full knowledge of healthy and unhealthy seating. Of specific importance is understanding and quantifying the change in spinal curvature with different seated positions. Currently, there is no scientifically accepted research that addresses a means to predict posterior human spinal curvatures over a comfortable range of motion while the human's back is obscured by a seatback.

Therefore, the purpose of this research was to determine if a relationship exists between physical structures of the body that can be measured with anterior markers and sagittal plane lumbar curvature. To address this, four distinct goals were formed:

1. A relationship exists between anterior body measurements and posterior curvatures, determined through four unique seated static postures.
2. A relationship exists between anterior body measurements and posterior curvatures, determined through a dynamic range of seated motion.
3. The relationship between the anterior measurements and posterior lumbar curvatures identified in the static postures holds true for the dynamic range of motion in the same seated environment.
4. The relationship between the anterior measurements and posterior lumbar curvatures identified in the dynamic range of motion holds true for the static postures in the same seated environment.

LITERATURE REVIEW

A vast amount of research has been conducted on the human spine. The spine has been studied in many cases as site of discomfort or failing health [13-16], ergonomics [17, 18], the study of balance [19], gait analyses [20], predictive modeling [19, 21-23], and spinal stability [19, 21]. Back and spine research employs many different methods to accomplish these quantifications including radiographs, magnetic resonance imaging (MRI), inclinometers, and three-dimensional (3D) motion capture amongst others [17, 24, 25]. While there are many ways to investigate the spine, each has its own associated benefits and drawbacks.

Technology

The use of radiographs, which have been used as far back as 1957 [26], is the most prevalent method used in spinal research. It is still widely used today as a method to determine the position of each vertebra, particularly in a sagittal plane [13, 27-29]. Radiographs are sometimes preferred because of the precision of measurement of positions of the vertebrae in living human subjects. However, the drawbacks are that the positions must be taken statically, and it requires the subject be exposed to radiation.

MRI's are also commonly used to determine the relative positions and orientations of the vertebrae. MRI's have the added benefit being able to reconstruct 3D images so any plane, sagittal or otherwise can be viewed. This too, has been used by several studies [30-32]. However, in large part this too has the drawback of only being able to produce static images. There are MRI machines capable of capturing dynamic

data of a vertically supported subject, but they are expensive and not widely available. In addition, the space inside most MRI machines is limited, restricting the range of motion and positions that can be measured.

Another common source of spinal measurement data comes from the use of an inclinometer. Several studies use this, primarily as a means to quantify the sacral angle [33, 34]. This has the benefit of being a quick, non-invasive measure that can be performed on live subjects. However, it has been shown by Bierma et al. [35] that these measurements do not concur with radiographic data. They showed that the mean difference between sacral inclination angle as measured by inclinometer and a radiograph was 23.12 degrees with a standard deviation of 8.56 degrees. In addition, inclinometer measurements must be taken statically, and require access to the subject's back by the researcher.

Three dimensional (3D) motion capture is another data collection method that presents its own set of benefits and drawbacks. By using cameras that track spherical shaped markers attached to the subject, this method presents the opportunity to collect continuous positional data that is non-invasive, making it the choice of several spinal researchers [14, 19, 36-38]. Criticisms of this method arise because the markers must be applied to the skin over the spinous processes of the vertebrae and are therefore subject to shifting of the skin over the bony landmark. This problem is common to all motion capture data collection.

However, several studies have shown that the relative movement between the markers placed on the skin and the position the spinous process through ranges of movement is minimal on the spine [30, 39]. Using sets of markers attached to both the

skin and the vertebrae at the level of T12, Stinton et al. [40] showed that the maximum difference in measured rotation angles between the skin and bone markers was 1.4 degrees, while the average was 0.4 degrees. This was over a range of flexion motion of 14.4 degrees.

Additionally, Mörl and Blickhan [30] used MRI with markers affixed over the L3 and L4 vertebrae to show that there is a strong linear relationship ($0.916 < r < 0.993$, $p < 0.0001$) between the position of the spinous process and corresponding marker through several seated postures.

Although 3D motion capture has many benefits, if one is interested in studying spinal articulation in a seated position, the motion system presents a unique challenge. In order for a marker to be tracked, there must be a clear line of sight between it and the cameras. In a seated environment, a seatback creates an obstruction that occludes the view of markers on a subject's back therefore making the markers immeasurable. Therefore, in order to directly measure the subject's back in a seated environment with this method the seat must either not have a back, or have a back that has been specifically designed for the lab environment. Because these direct methods cannot be effectively and consistently applied to understanding the interface between a subject's back and seatback of many different commercially available chairs, this research seeks to develop a method to infer the measurements of the back by establishing a correlation to anterior measurements that can easily be obtained with 3D motion capture.

Standing vs. Seated

A majority of the literature discusses measuring and quantifying spinal curvature in a standing position. For example, in a standing position, several studies have been conducted to establish a normative database of lumbar spine ranges of motion [33, 41]. Guangyan Li and Peter Buckle composed an overview paper of many of the posture-based techniques used prior to 1999 [34] including pen-and-paper based methods, video-taping computer based observational methods and direct methods such as goniometers and inclinometers.

However, while many have investigated standing postures there are only a limited few studies that actually address seated spinal curvatures. Of particular note there were studies by Black [36], Walsh [38], and Dunne [17]. This group of researchers studied the various effects of spinal curvatures and the ways in which to quantify it.

The research by Black et al. [36] used 4 distinct seated positions to determine the effect of posture on the cervical spine. They showed that lumbar posture could be correlated to the movements of the cervical spine. While Black's particular research focused on the cervical region of the spine, it provided a precedent for techniques to be used in the current study. This research established the ability to correlate positions of the lumbar spine to positions elsewhere in the body.

Walsh et al. [38] performed research in 2006 that employed motion capture data of the thoracic and lumbar spine to develop a single variable threshold model of the spine. This model was used to determine posture based on overall flexion of the spine. They found that the best indicator of total posture was the vector from the fourth lumbar vertebra to the seventh cervical vertebra. This method was then used by Dunne et al. [17]

in 2007 to verify a wearable method of posture monitoring. In relation to the current study, this showed that a single variable model can be used to determine a relationship about the spine. The current research seeks to expand upon the findings of Black, Walsh and Dunne to determine a relationship as it not only relates to posture, but to the curvature of the lumbar region of the human back.

Several other works, though not necessarily concerning specifically to seated spinal curvature, also had a distinct influence on the experimental design of the current research discussed here.

Janik et al. [29] showed that the lumbar spine can be well fit by an ellipse. To accomplish this, they used digitized standing radiographs of 50 healthy individuals. By measuring the positions of the superior and inferior posterior margins of the bodies of the lumbar vertebrae, they were able to fit approximately 85 degrees of an ellipse to the lumbar spine, from the inferior margin of twelfth thoracic vertebra to the superior margin of first sacral vertebra. The accuracy produced was a least squared error of 1.2 mm per point along the path. The methods produced by this group were slightly modified for use in the current research.

When modeling the lumbar spine, researchers have considered the ribcage to act as a rigid body [19, 22]. The assumptions made are that the movements of the thoracic vertebrae are minimal when compared to the movements of the lumbar vertebrae and have little influence on the movement of the lumbar spine. These assumptions were also adopted by the current study.

METHODS

Data Collection

Subject pool

Participants for this study were young healthy adults free of back pain or spinal injuries. Following the subject's written consent (IRB# 06-764), a questionnaire (A1) was administered verbally to the subjects to assure each was healthy and lacking obvious physical ailments that would preclude them from the study. A total of 31 subjects, 16 female and 15 male, were tested with an average age of 23.4 years (1.9 years) . The average height and weight of the subjects was 1.68m (0.11m) and 663 N (151 N) respectively. Table 1 and Table 2 show the ranges and distributions for these data. A table with these data for each subject can be found in the appendix (A2).

Table 1. Height, weight, and age of the subjects

	Height (cm)	Weight (N)	Age (years)
	Total	Total	Total
Min	150	400	20
Max	185	1000	27
Average	168	663	23.4
SD	<i>10.8</i>	<i>151</i>	<i>1.9</i>

Table 2. Height, weight, and age of the subjects as divided by gender

	Height (cm)		Weight (N)		Age (years)	
	Female	Male	Female	Male	Female	Male
Min	150	165	400	609	20	20
Max	175	185	814	1000	26	27
Average	160	177	562	771	23.1	23.7
SD	<i>7.8</i>	<i>5.3</i>	<i>101</i>	<i>118</i>	<i>1.9</i>	<i>1.9</i>

Anatomical measures

A variety of additional anthropometric measures were taken including seated height, seated buttocks width, pelvic width, pelvic height, and pelvic depth. These measures were used to quantify the physical characteristics of each of the subjects and the subject pool in general. The method for collection of each of these measurements is described below.

- The seated height was taken with the subjects sitting on a stool with their backs against a wall. The seated height was then measured as the distance from the top of the seat pan to the top of their head.
- The seated buttocks width was measured using anthropometers at the widest part of the hips while the subject was seated.
- Pelvic width was measured as the lateral distance between the subject's left and right anterior superior iliac spines (ASIS) in a standing position.
- Pelvic depth was measured as the anterior to posterior distance between the subject's right ASIS and right posterior superior iliac spine (PSIS) in a standing position.
- Pelvic height was measured as the inferior to superior distance between the subject's pubic symphysis and his/her right ASIS in a standing position.

A summary of these data can be seen in Table 3 while subject specific data can be found in the appendix (A2).

Table 3. Subject seated dimensions and pelvic dimensions (all values in cm)

	Seated Height	Seated Buttocks Width	Pelvic Width	Pelvic Height	Pelvic Depth
Min	29	30.5	20	5.5	11.5
Max	37	46	28	12.5	19.5
Average	33.9	37.4	23.3	8.4	15.1
SD	2.00	3.19	1.91	1.78	1.93

Markers and motion tracking

After all anthropometric measurements were gathered, retroreflective motion tracking markers were applied to each subject so that 3D motion data could be captured during the testing process. The motion system used was a 6 camera Qualisys Motion Tracking System (Gothenburg, Sweden) with marker sizes of 13mm and 19mm in diameter. The 13mm markers were used on the subject's back to allow for the highest possible density of markers to be distinguished given the limitations of the system. The 19mm markers were used on the subject's anterior to reduce the possibility that the markers could be obscured by clothing or excess skin. All data were captured at 30 Hz.

A global Cartesian coordinate system was established within the testing space as defined by the motion tracking software. The origin of the system was chosen during calibration of the system to be the left posterior corner of the stool's seat. The orientation of the coordinate system was arranged such that the X-axis was oriented horizontally from subject left to subject right; the Y-axis was oriented horizontally from posterior to anterior; and the Z-axis was vertical from inferior to superior. The coordinate system was the same for all subjects. A calibration of the system was performed each day prior to data collection.

The accuracy of the system and configuration seen in Figure 1 was evaluated in both length and angular measurements. The same camera configuration used for all data collection was used to capture several premade marker arrays with known lengths and angles. It was tested on two different days with a new calibration each day to ensure repeatability. The greatest standard deviation in a known length was 1.64 mm. The greatest standard deviation in angle for a 5 second motion file of the known angles was 0.38 degree. All of these data are located in the appendix (A3).

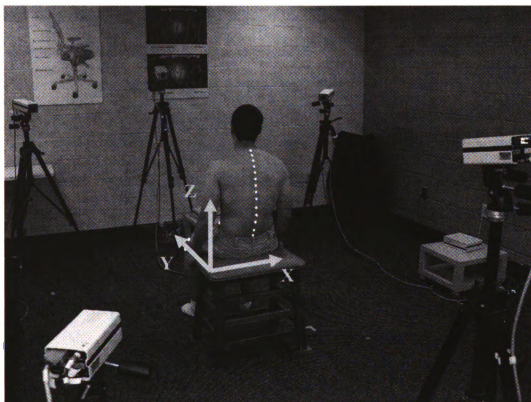


Figure 1. Motion capture data collection configuration with global coordinate system and origin shown

The 13mm markers were attached along the subject's back over specific anatomical positions. The most superior back marker was placed over the spinous process of the seventh cervical vertebra (C7). Then the spinous processes of the thoracic vertebrae were palpated down to the twelfth thoracic vertebra (T12) and a marker was

placed over that bony landmark. Next, a marker was placed between the right and left PSIS's (MidPSIS). Once that was completed, additional markers were placed between C7 and T12 and also between T12 and MidPSIS such that the markers were even spaced approximately 3 cm apart. This was chosen as the spacing that would allow the most data to be gathered by the system without exceeding the system's capability to distinguish between separate markers. It should be noted that these intermediate markers were not placed on the back over any distinct spinous processes, but rather to give the highest allowable linear density for data collection. These markers were used to monitor the motion of the back and can be seen in Figure 2.

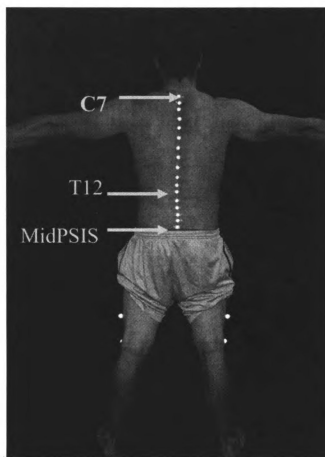


Figure 2. Retroreflective markers applied to the posterior at C7, T12, MidPSIS while standing erect with additional markers spaced approximately 3cm apart between C7 and MidPSIS

To monitor the movement of the ribcage and pelvis, markers were also applied to the anterior side of the subject. A three-marker pod was placed over the subject's sternum with the most superior portion of the pod being affixed just inferior to the sternal notch. A fourth marker was also placed just superior to the sternal notch. Additionally, markers were affixed over the subject's left and right ASIS, over the lateral epicondyles of each femur, and on each thigh. These can be seen in Figure 3.

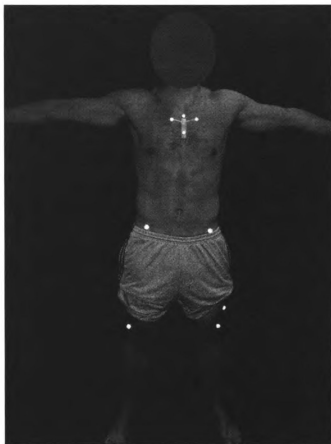


Figure 3. Retroreflective markers applied to the subject's anterior and lateral sides

The markers on the subject's ASIS's, MidPSIS, and knees were used to calculate the position and orientation of the pelvis throughout the various test conditions.

Test conditions

To quantify a full range of seated spinal articulations for each subject, measurements were taken in several different ways. Data were collected in two test conditions:

- 1) Four static positions, and
- 2) Dynamic ranges of motion

Both conditions are described in detail below, but for all testing, subjects were asked to sit with their feet flat on the floor, shoulder width apart, having their head above their pelvis with a forward gaze, and arms at their sides, as seen in Figure 4.

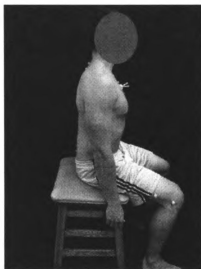


Figure 4. Basic posture assumed by the subject with head over pelvis, feet flat on floor, and gaze forward

Static positions

The goal of the four static postures was to determine the full range of motion for each individual while in the seated position. Two extreme and two intermediate postures were used to obtain this full range data,

The extreme postures were taken as:

- 1) **Maximum Lumbar Lordosis (Max. Lord.):** a maximally lordotic self-selected position.
- 2) **Maximum Lumbar Kyphosis (Max. Kyph.):** a maximally kyphotic self-selected position.

The intermediate postures were taken as:

- 3) **Comfortable (Comfort):** a self-selected position that the subject assumed when asked to “sit comfortably”
- 4) **Straight and Tall (S&T):** A self-selected position that the subject assumed when asked to “sit straight and tall”.

The purpose of the two intermediate postures was to obtain two measurement positions that were located between the two extreme postures. All four postures can be seen below in Figure 5 and were taken as the average of three seconds of data while the subject maintained each position.

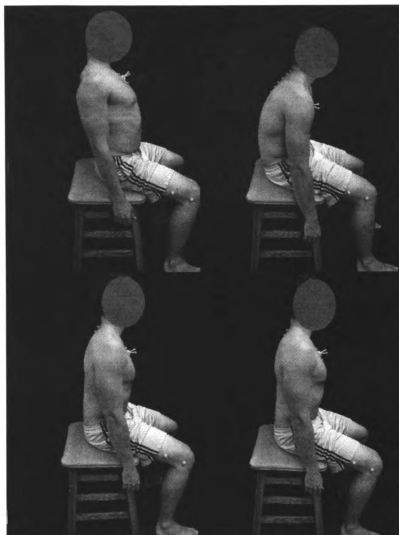


Figure 5. Static postures assumed by the subjects. Clockwise from top left: Maximum Lumbar Lordosis, Maximum Lumbar Kyphosis, “Straight and Tall”, “Comfortable”

Continuous motion

The continuous motion files were collected to show the complete continuous trajectory of movement ranging from maximum kyphosis to maximum lordosis. These data were captured while the subject moved from a comfortable position to a lordotic position, to a kyphotic position, and back again to the comfortable position. The subject was verbally queued throughout the motions to ensure a full cycle was completed within

the data collection timeframe and the subject was able to pause at the extreme positions. The total duration of data capture for each continuous motion file was 20 seconds to ensure a full cycle through the motions was possible. The only data that were used for analysis were the data that occurred during the verbal instruction.

Once all of the positions and motions had been collected, the data were processed in the motion capture software. Each marker was identified and labeled, tracked throughout its trajectory, and exported to a spreadsheet in the form of the global XYZ coordinates.

For the continuous capture dynamic motion data, only subjects with the most complete motion files were used. Due to the unforeseen occlusion of some key markers, most notably the ASIS markers, some motion trajectories were not completely tracked through the entire motion. This meant that for some subjects the necessary calculations for analysis could not be made at all points in time. Therefore, the inclusion criteria for the dynamic files were that at least 75% of the trajectory was tracked and the end-ranges of motion were clearly distinguished, as noted by the pauses at the extreme postures. These criteria left only 15 of the original 31 subjects in the dynamic data pool.

Analysis

Hip joint center

The first calculation was of each of the subject's hip joint centers (HJC). The HJC locations were calculated by both the Seidel method [42] and then, secondly, by the method developed by Bush and Gutowski [43]. In practice, a reference file would be taken with posterior markers and the Seidel Method would be used to compute the HJC. Then, using these data and the relationships formed between the calculated HJC, knee marker and ASIS marker, the posterior markers could be removed and the Bush Method would be used while the subject was seated in a chair. This is important because one of the end goals of this research was to be able to predict posterior motions without having any posterior markers measured.

For these calculations, anatomical directional vectors were developed on the subject's pelvis, such that the width vector was oriented from the subject's left ASIS to the right ASIS, the depth vector was oriented from the MidPSIS to the midpoint between the subject's left and right ASIS, and the height vector was oriented 90 degrees from both the width and depth vectors in a superior direction. The vector notation for these calculations can be seen in equation set 1.

$$\begin{aligned}\bar{L}_W &= \bar{G}_{RASIS} - \bar{G}_{LASIS} \\ \bar{L}_D &= (\bar{G}_{LASIS} + \bar{G}_{RASIS}) / 2 - \bar{G}_{MidPSIS} \\ \bar{L}_H &= \bar{L}_W \times \bar{L}_D \\ \hat{L}_{Wunit} &= \frac{\bar{L}_W}{|\bar{L}_W|} \quad \hat{L}_{Dunit} = \frac{\bar{L}_D}{|\bar{L}_D|} \quad \hat{L}_{Hunit} = \frac{\bar{L}_H}{|\bar{L}_H|}\end{aligned}\tag{1}$$

The HJC was then calculated as a position relative to the subject's corresponding ASIS using the local pelvis vectors and the subject's pelvic measurements. According to Seidel [42] the position of the HJC in relation to the ASIS is 14% of the subject's pelvic width in the medial direction, 34% of the subject's pelvic depth in the posterior direction and 79% of the subject's pelvic height in the inferior direction.

For the right HJC, this meant starting at the position of the right ASIS, the right HJC was 14% of the subject's pelvic width in the negative X direction, 34% of the subject's pelvic depth in the negative Y direction and 79% of the subject's pelvic height in the negative Z direction. This calculation can be seen in equation set 2

$$\begin{aligned}
 PW &= \text{Pelvic Width} \\
 PD &= \text{Pelvic Depth} \\
 PH &= \text{Pelvic Height} \\
 \bar{G}_{RHJC} &= \bar{G}_{RASIS} - PW * 0.14 * \hat{L}_{Wunit} - PD * 0.34 * \hat{L}_{Dunit} - PH * 0.79 * \hat{L}_{Hunit}
 \end{aligned} \tag{2}$$

For the left HJC, this meant starting at the position of the left ASIS, the left HJC was 14% of the subject's pelvic width in the direction of the width vector, 34% of the subject's pelvic depth in the negative direction of the depth vector and 79% of the subject's pelvic height in the negative direction of the height vector. This calculation can be seen in equation 3.

$$\bar{G}_{LHJC} = \bar{G}_{LASIS} + PW * 0.14 * \hat{L}_{Wunit} - PD * 0.34 * \hat{L}_{Dunit} - PH * 0.79 * \hat{L}_{Hunit} \tag{3}$$

Then, by Bush and Gutowski's method, it was again calculated without the MidPSIS marker by using the known length from the respective ASIS to the HJC and from the lateral condyle marker to the HJC, as both distances should be constant.

Openness angle

Once the HJC were determined, it was possible to calculate the “openness” angle (θ). This was the measure used to quantify the relative orientations of the pelvis and the ribcage. To calculate this angle, all data were viewed in the YZ (sagittal) plane to eliminate any medial/lateral dependence or skewing. Once this was established, two vectors were computed, one through the pelvis and one through the thorax. The pelvis vector (\vec{P}) was calculated originating at the average of the right and left HJC and passing through the average of the right and left ASIS, seen in equation 4.

$$\vec{P} = \left(\frac{\vec{G}_{LASIS} + \vec{G}_{RASIS}}{2} \right) - \left(\frac{\vec{G}_{LHJC} + \vec{G}_{RHJC}}{2} \right) \quad (4)$$

The ribcage vector (\vec{R}) was then created originating at the sternum pod and passing through the C7 marker, seen in equation 5.

$$\vec{R} = \vec{G}_{C7} - \vec{G}_{MidSternum} \quad (5)$$

The angle created by these two vectors, seen in equation 6, was then calculated as the “openness”. A diagram how this angle was calculated can be seen below in Figure 6.

$$\theta = \cos^{-1} \left(\frac{\vec{P} \cdot \vec{R}}{|\vec{P}| |\vec{R}|} \right) \quad (6)$$

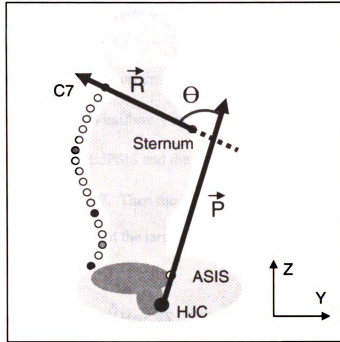


Figure 6. Diagram of the “openness” angle as calculated from the positions of HJC, ASIS, Sternum marker and C7

The openness angle was chosen because it can be calculated using markers that are primarily on the anterior side of the subject and can all be obtained while a subject is in a chair with a back. The C7 marker is on the posterior side of the subject, but most seatbacks do not extend that high, so it is still a viable marker in seating research.

Lumbar angle

The second angle to be calculated was an angle on the posterior side of the subject. This angle, referred to as the lumbar angle, was meant to capture the contour of the lower back at the same time the “openness” angle was quantifying the relative

orientations of the ribcage and pelvis. It was calculated by taking the positions of the markers at T12 and MidPSIS and the most eccentric marker between them (LU) and then using those points to create a 3 point arc.

LU was calculated by first translating the positions of all markers uniformly so that the MidPSIS marker was at the origin and each marker was renamed \bar{T}_{name} . Next, all marker positions were rotated uniformly in the sagittal plane such that T12 was positioned vertically over the MidPSIS and the markers were renamed \bar{Q}_{name} by the calculations seen in equation set 7. Then the LU marker was chosen to be the marker between MidPSIS and T12 that had the largest magnitude y-value.

$$\begin{aligned}
 \bar{T}_{name} &= \bar{G}_{name} - \bar{G}_{MidPSIS} \\
 \text{Rotation Angle} = \phi &= \tan^{-1} \left(\frac{\bar{T}_{T12} \cdot \hat{j}}{\bar{T}_{T12} \cdot \hat{k}} \right) \\
 \bar{Q}_{name} &= \begin{bmatrix} Q_{nameX} \\ Q_{nameY} \\ Q_{nameZ} \end{bmatrix} = \begin{bmatrix} 1 & 0 & 0 \\ 0 & \cos \phi & -\sin \phi \\ 0 & \sin \phi & \cos \phi \end{bmatrix} \begin{bmatrix} T_{nameX} \\ T_{nameY} \\ T_{nameZ} \end{bmatrix} \quad (7)
 \end{aligned}$$

Once LU was defined, it was possible to calculate a circumradius of a circle that would contain all 3 points (MidPSIS, T12, LU) as seen in Figure 7. This was calculated using the known distances between the three points in the sagittal plane, seen in equation 8, and using the algebraic equations 9 and 10

$$\begin{aligned}
 |\bar{G}_{MidPSIS} - \bar{G}_{T12}| &= a \\
 |\bar{G}_{MidPSIS} - \bar{G}_{LU}| &= b \\
 |\bar{G}_{T12} - \bar{G}_{LU}| &= c
 \end{aligned} \quad (8)$$

$$r = \frac{a * b * c}{\sqrt{(a + b + c)(-a + b + c)(a - b + c)(a + b - c)}} \quad (9)$$

$$\alpha = 2 * \sin^{-1} \left(\frac{a/2}{r} \right) \quad (10)$$

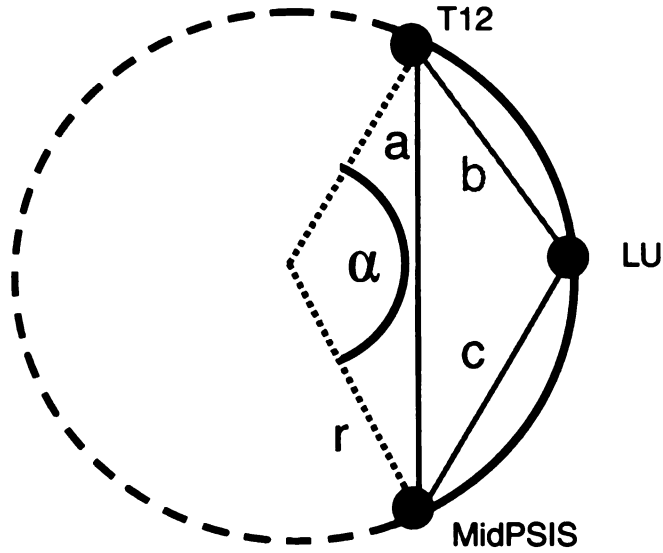


Figure 7. Calculation diagram for circumradius and lumbar angle

Once this radius was determined (derivation found in Appendix A4) it was possible to calculate the angle of the whole circle that the 3 points formed. The equation defining this relationship can also be seen above. A diagram for the lumbar angle (α) is shown in Figure 8. In the case of a kyphotic lumbar position, where the LU marker was posterior to the line between the T12 marker and the MidPSIS marker, the lumbar angle was considered to be negative.

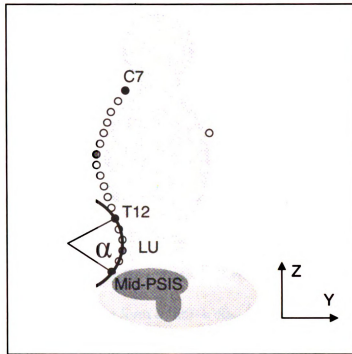


Figure 8. Diagram of the lumbar angle as calculated from the positions of T12, LU, and Mid-PSIS

Statistical Analysis Methods

Distinct static positions

Before the relationship between the static measurements was evaluated, it was necessary to confirm that each of the four postures were different from one another. This analysis was conducted for both of the major measurements: openness angle and lumbar angle. Upon the suggestion of a statistician, successive positions were tested using a paired t-test, for both openness and lumbar angles. The null hypothesis was that position A and position B were not statistically different.

Relationship between openness and lumbar angles

Given openness and lumbar angles that were distinct across each of the static positions, the next step of analysis was to determine if a relationship existed between the two angles across all the positions. This was performed on the static and dynamic data with two separate models, a linear model and a second order polynomial model.

For the linear model, it was hypothesized that this was a linear relationship and therefore the measure chosen to test this was a linear r^2 correlation. Specifically, it was hypothesized that with openness as the independent variable and lumbar angle as the dependent variable, a model of the form $\alpha = m\theta + b$ could be developed and the r^2 value would tell how well the data fit that model. In this case, α is the lumbar angle, θ is the openness angle and “m” and “b” are the coefficients forming the relationship.

For the polynomial model, a second hypothesis was that the relationship between the openness and lumbar angles followed a relationship of the form $\alpha = U\theta^2 + V\theta + W$, where again, α was the lumbar angle and θ was the openness angle and “U”, “V”, and “W” were the coefficients forming the relationship. This was calculated as a best fit polynomial and evaluated again with an r^2 correlation.

These models were applied to both the static and dynamic data.

Anthropometric correlation to openness/lumbar angle slope

Once the linear relationship between openness angle and lumbar angle was established, it was necessary to determine if any anthropometric measures had any influence on the relationship. This was tested by using a Pearson product moment correlation test. For the static sample size of 31 subjects at a significance level of 0.05,

the critical value of the correlation was 0.355. For the dynamic sample size of 15 subjects, at a significance level of 0.05, the critical value of correlation was 0.514. These critical values were found by first finding critical t-values for confidence and prediction intervals associated with the degrees of freedom and levels of significance required in each set of data. Then the t-values were converted to r, by way of equation 11 for a test of linear association in a bivariate normal population, where N is the number of subjects [44]. Any values larger than the critical values are considered to be statistically significant.

$$t = \frac{r\sqrt{N-2}}{\sqrt{1-r^2}} \quad (11)$$

Predictive capacity

In order to test the predictive capacity of the relationships between the openness angle and the lumbar angle, predictive models had to be developed from one group and tested on another group. This lead to six total predictive combinations that were tested:

1. Static data predicting static positions for a test population
2. Dynamic data predicting dynamic positions for a test population
3. Static data predicting dynamic positions for a test population
4. Dynamic data predicting static positions for a test population
5. Static data predicting dynamic positions within a subject
6. Dynamic data predicting static positions within a subject

Static data predicting static positions for a test population

For the static to static predictive capacity measurement, the total static data set was split into two groups. The first group consisted of the first 16 subjects and the second group consisted of the last 15 subjects. From the all of the data points in the first group, linear and second order predictive models of the form $\alpha = m\theta + b$ and $\alpha = U\theta^2 + V\theta + W$ were formed. These models were then applied to all of the openness values in the second group, creating a linear and second order “predicted lumbar angle” for each openness datum in the second group. Finally, paired t-tests were performed to test the actual lumbar angles vs. the predicted lumbar angles to determine if the predicted lumbar angles were statistically different from the actual lumbar angles.

Dynamic data predicting dynamic positions for a test population

A similar procedure was executed for all of the dynamic data. The subject pool was split into two groups. The first group consisted of the first eight subjects with sufficient dynamic data, and the second group consisted of the last seven subjects with sufficient dynamic data. All of the data from the first group were used to produce a linear prediction model of the form $\alpha = m\theta + b$ and a second order polynomial model of the form $\alpha = U\theta^2 + V\theta + W$. These models were then applied to the second group’s openness angle values to produce a “predicted lumbar angle” for each openness angle in the second group for each model. The predicted lumbar angles were then compared to the actual lumbar angles across each openness angle in the second group’s data using paired t-tests to determine if the predicted lumbar angles were statistically different from the actual lumbar angles.

Static data predicting dynamic positions for a test population

For these models, all of the static data and all of the complete dynamic data were utilized. The static data from all subjects were used to form linear and second order predictive models of the form $\alpha = m\theta + b$ and $\alpha = U\theta^2 + V\theta + W$. These two models were then applied to all of the openness values in all of the complete dynamic subjects, creating a linear and second order “predicted lumbar angle” for each openness datum in the dynamic data group. Then, paired t-tests were performed to test if the actual lumbar angles were statistically different than the predicted lumbar angles.

Note that these models were different than the models developed for the “static to static” prediction because all of the subjects (S01-S31) were used instead of just the first half (S01-S16) to build the models.

Dynamic data predicting static positions for a test population

For these models, all of the static data and all of the complete dynamic data were utilized. The dynamic data from all subjects with complete data sets were used to form a linear and a second order predictive model of the forms $\alpha = m\theta + b$ and $\alpha = U\theta^2 + V\theta + W$. These models were then applied to all of the openness values for all of the static data, creating a linear and second order “predicted lumbar angle” for each openness datum in the static data group. Paired t-tests were performed to test if the actual lumbar angles were statistically different than the predicted lumbar angles.

Note that these models were different than the models developed for the “dynamic to dynamic” predictions because all of the dynamic subjects were used to build these

models instead of just the first half of the dynamic subjects for the “dynamic to dynamic” models.

Static data predicting dynamic positions within a subject

A similar approach was taken to determine if, within a subject, the static data could be used to predict the same subject’s dynamic pattern of movement. To test this, a linear model, of the form $\alpha = m\theta + b$, was fit to the static data of each subject. These models were then used to predict each dynamic lumbar angle using the same subject’s dynamic openness angles. The predicted lumbar angles were compared to the actual lumbar angles by utilizing a paired t-test, for each subject.

Dynamic data predicting static positions within a subject

Additionally, the ability to predict the static positions of a subject based on a model developed from the dynamic data from that same subject was tested. Linear models, of the form $\alpha = m\theta + b$, were developed for each subject based off of their own dynamic data. Then, each model was applied to the same subject’s openness angles for each of the static positions, creating predicted static lumbar angles. The predicted static lumbar angles were then compared to the actual static lumbar angles for each subject using a paired t-test.

RESULTS

Openness and Lumbar Angles

The calculated openness angles for each subject in each static position are given in Table 4.

Table 4. Static openness angles for each subject at each posture
Openness Angle, θ (deg)

Subject	Maximum Lordotic	“Straight and Tall”	“Comfort”	Maximum Kyphotic	Total Range
S01	93.5	91.5	72.4	63.0	30.5
S02	97.3	80.0	63.6	46.4	50.9
S03	133.8	119.5	107.5	89.9	43.9
S04	99.8	96.9	74.1	63.1	36.7
S05	129.5	126.6	82.8	72.2	57.3
S06	98.0	78.4	56.1	40.6	57.3
S07	82.3	81.0	55.0	43.9	38.4
S08	104.5	99.7	95.7	76.2	28.2
S09	131.7	100.1	79.6	46.1	85.6
S10	129.4	115.7	90.8	78.2	51.3
S11	126.8	107.0	94.4	78.5	48.2
S12	111.6	99.3	84.6	67.2	44.4
S13	125.2	94.6	78.0	64.6	60.7
S14	155.2	127.6	112.1	80.5	74.7
S15	88.3	75.9	61.1	22.1	66.2
S16	105.1	87.1	74.2	52.5	52.6
S17	129.3	119.3	101.6	78.8	50.5
S18	100.3	91.0	80.4	66.8	33.5
S19	99.1	92.3	78.0	70.4	28.7
S20	122.7	107.3	75.7	54.0	68.8
S21	113.7	103.7	83.6	46.6	67.1
S22	120.8	111.7	92.5	69.4	51.4
S23	122.0	97.9	80.6	59.1	62.9
S24	118.9	93.5	77.5	50.0	68.9
S25	104.1	92.7	74.1	38.1	66.0
S26	119.3	105.2	82.7	59.8	59.5
S27	129.4	111.0	74.2	52.2	77.2
S28	104.2	79.4	63.4	42.7	61.6
S29	124.4	102.5	92.1	72.4	52.0
S30	116.7	105.6	75.5	71.7	44.9
S31	92.0	91.4	79.1	67.3	24.7
AVG	113.8	99.5	80.4	60.8	53.0
S.D.	16.4	13.8	13.6	15.4	15.4

The calculated lumbar angles for each subject in each static position can be seen below in Table 5. Note that in both the openness angles and lumbar angles, the trend from lowest to highest in terms of the positions, is maximum kyphotic, comfortable, “straight and tall”, and maximum lordotic.

Table 5. Static lumbar angles for each subject at each posture
Lumbar Angle, α (deg)

Subject	Maximum Lordotic	“Straight and Tall”	“Comfort”	Maximum Kyphotic	Total Range
S01	-5.2	-6.7	-9.2	-11.0	5.8
S02	21.9	-10.7	-17.8	-18.9	40.8
S03	29.4	12.1	14.6	-12.8	42.3
S04	34.4	19.0	6.9	-5.9	40.3
S05	49.4	55.5	-16.1	-21.1	76.6
S06	6.8	-11.7	-13.5	-17.5	24.3
S07	20.8	19.6	-4.3	-14.0	34.8
S08	34.8	11.0	8.8	-14.9	49.7
S09	49.6	9.7	-7.6	-17.3	66.9
S10	62.9	34.9	-1.4	-14.6	77.4
S11	15.5	22.6	7.5	-2.1	24.8
S12	34.4	12.9	10.8	-9.1	43.5
S13	17.6	-10.2	-13.2	-19.0	36.6
S14	41.3	31.6	25.7	-21.3	62.6
S15	-19.4	2.8	-12.8	-27.0	29.8
S16	8.0	-5.4	-17.1	-24.3	32.3
S17	61.0	25.3	22.3	-6.7	67.7
S18	-15.7	-4.4	-7.7	-11.9	11.3
S19	3.8	3.2	-5.7	-8.8	12.5
S20	-9.6	4.4	-10.0	-17.2	21.6
S21	35.4	17.9	9.3	-20.4	55.8
S22	32.1	17.8	-10.1	-12.8	44.9
S23	79.6	38.8	12.0	-8.8	88.4
S24	16.1	13.4	3.1	-16.4	32.5
S25	61.4	36.4	13.3	-21.2	82.6
S26	58.4	18.7	-6.5	-13.4	71.8
S27	42.1	13.7	-20.8	-31.1	73.3
S28	-8.5	-5.0	-22.9	-30.7	25.7
S29	9.9	-5.4	-8.3	-9.3	19.2
S30	25.9	25.2	-11.6	-18.3	44.2
S31	-4.3	5.8	-11.3	-18.3	24.2
AVG	25.5	12.7	-3.0	-16.0	44.0
S.D.	25.6	16.5	12.9	6.9	22.8

Table 6 shows the maximum, minimum and range values for the openness and lumbar angles as calculated from the dynamic range of motion data.

Table 6. Dynamic maximum, minimum, and range values for openness and lumbar angles

Subject	Openness Angle, θ (deg)			Lumbar Angle, α (deg)		
	Max	Min	Range	Max	Min	Range
S01	101.5	76.5	25.0	8.5	-6.2	14.7
S04	91.3	59.8	31.5	27.2	-7.9	35.1
S08	102.5	56.3	46.2	33.5	-17.9	51.4
S10	124.5	74.2	50.3	51.3	7.2	44.0
S11	119.1	67.9	51.2	34.6	0.9	33.7
S12	109.6	63.3	46.3	43.3	4.4	38.9
S13	109.5	61.8	47.7	5.9	-20.9	26.8
S17	127.1	80.4	46.7	50.7	8.6	42.1
S18	92.2	57.1	35.1	-5.5	-19.3	13.8
S19	86.9	67.2	19.8	4.5	-9.2	13.7
S21	118.8	51.1	67.7	67.9	-42.4	110.4
S23	125.7	52.2	73.4	81.5	-25.6	107.0
S26	122.9	61.4	61.5	35.7	-16.0	51.6
S28	107.7	36.5	71.2	21.9	-34.5	56.4
S30	115.3	64.0	51.2	28.8	-17.8	46.6
AVG	110.3	62.0	48.3	32.6	-13.1	45.7
S.D.	13.2	11.0	15.9	24.1	14.9	29.0

Distinct Static Positions

The probabilities, as determined by the paired t-test, that each set of positions are the same are seen below in Table 7.

Table 7. Probabilities that each pair of positions is the statistically the same as determined by a paired t-test

Test Condition	Openness Angle	Lumbar Angle
Max. Lord. vs. S&T	<0.0001	0.0003
S&T vs. Comfort	<0.0001	<0.0001
Comfort vs. Max. Kyph.	<0.0001	<0.0001
Max. Lord. vs. Comfort	<0.0001	<0.0001
S&T vs. Max. Kyph.	<0.0001	<0.0001
Max. Lord. vs. Max. Kyph.	<0.0001	<0.0001

Relationship between Openness and Lumbar Angles

Static

A graph for each subject's static data can be seen in **Figure 9 (a-ee)**. Also included in the graphs are the linear and polynomial models with their associated r^2 values. The linear best fit approximations are shown as gray lines, while the second order polynomials are the black curves.

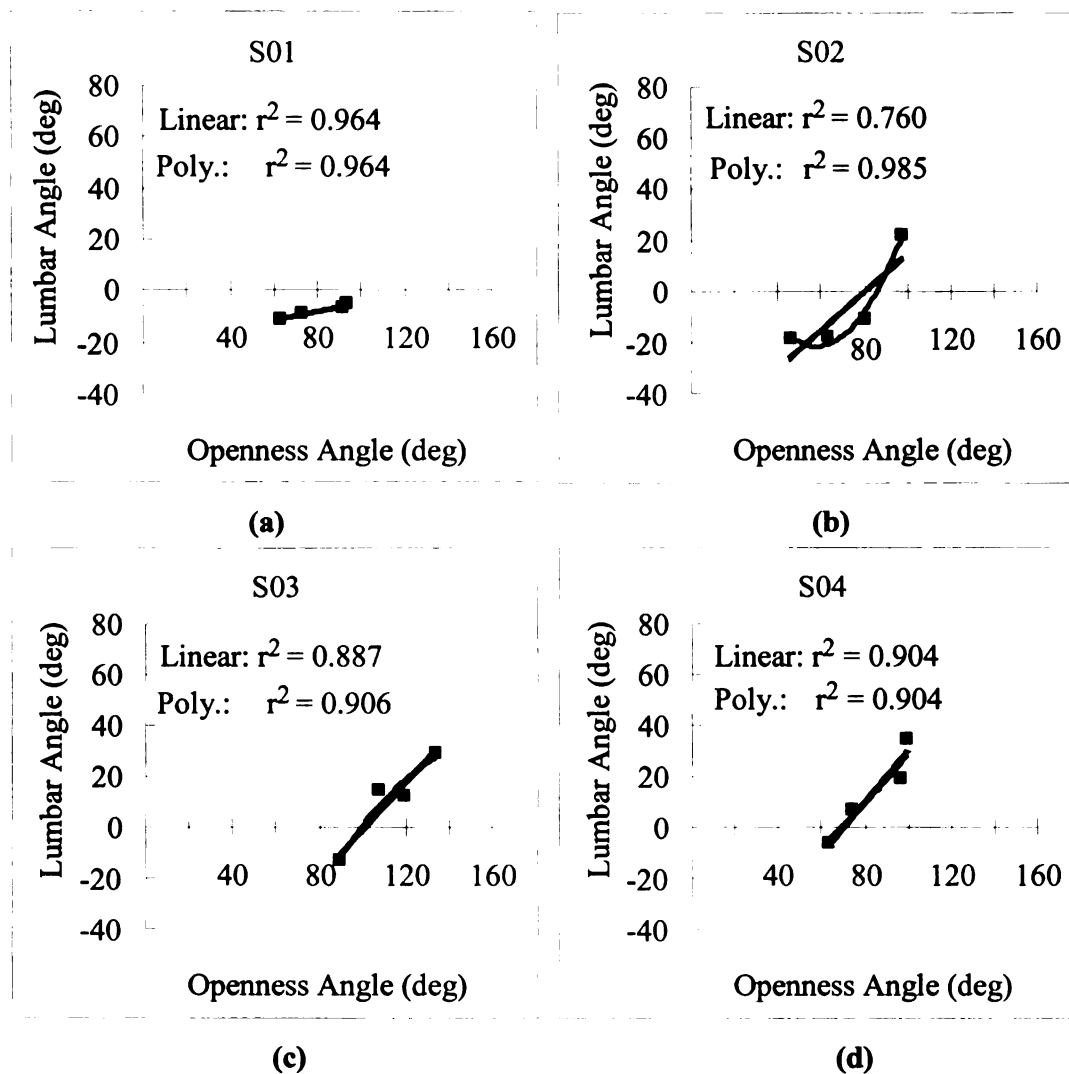


Figure 9 (a-ee). Openness Angle vs. Lumbar Angle for each individual subject using static postures with included linear and second order polynomial best fits

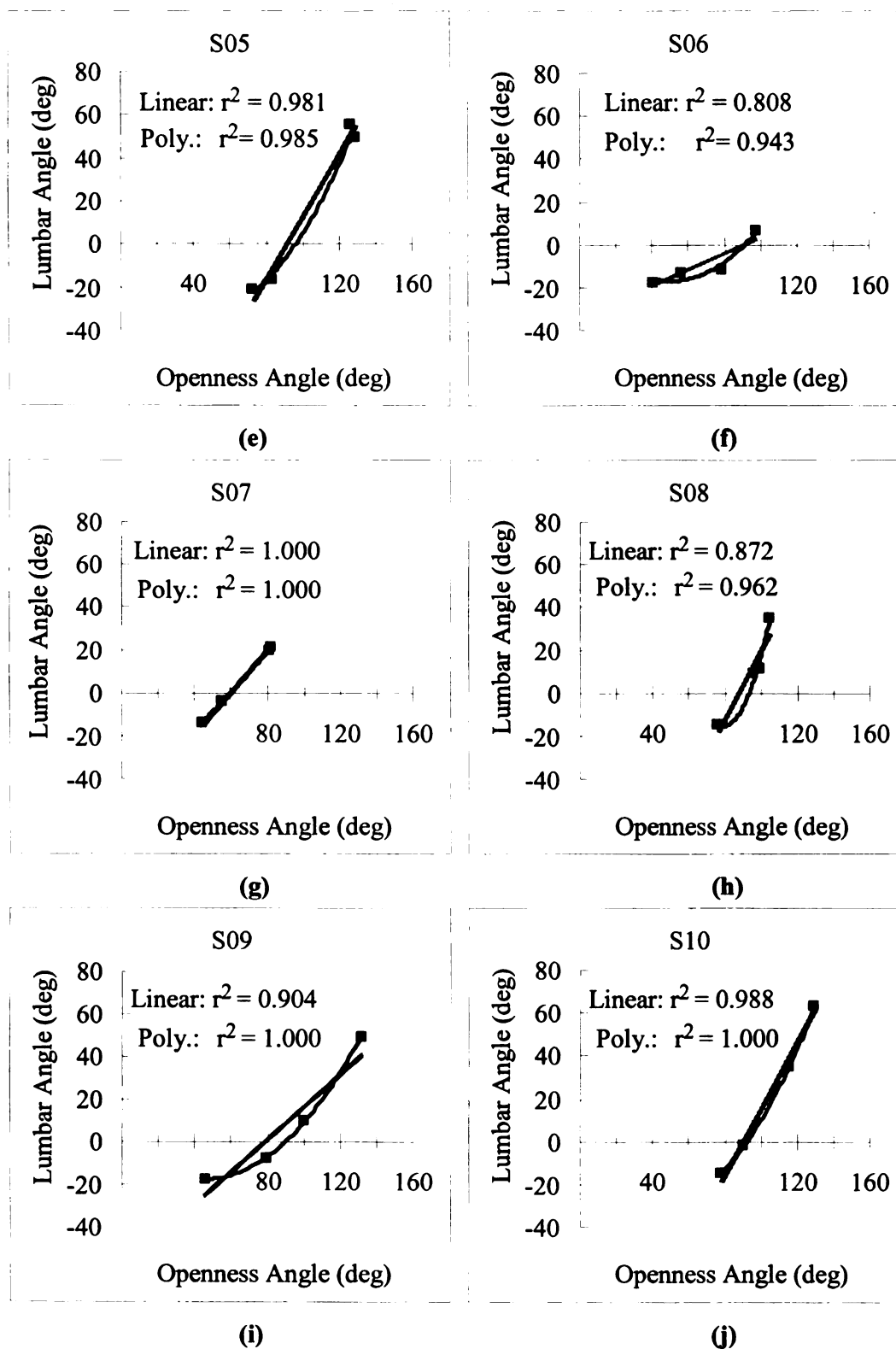


Figure 9 (cont.)

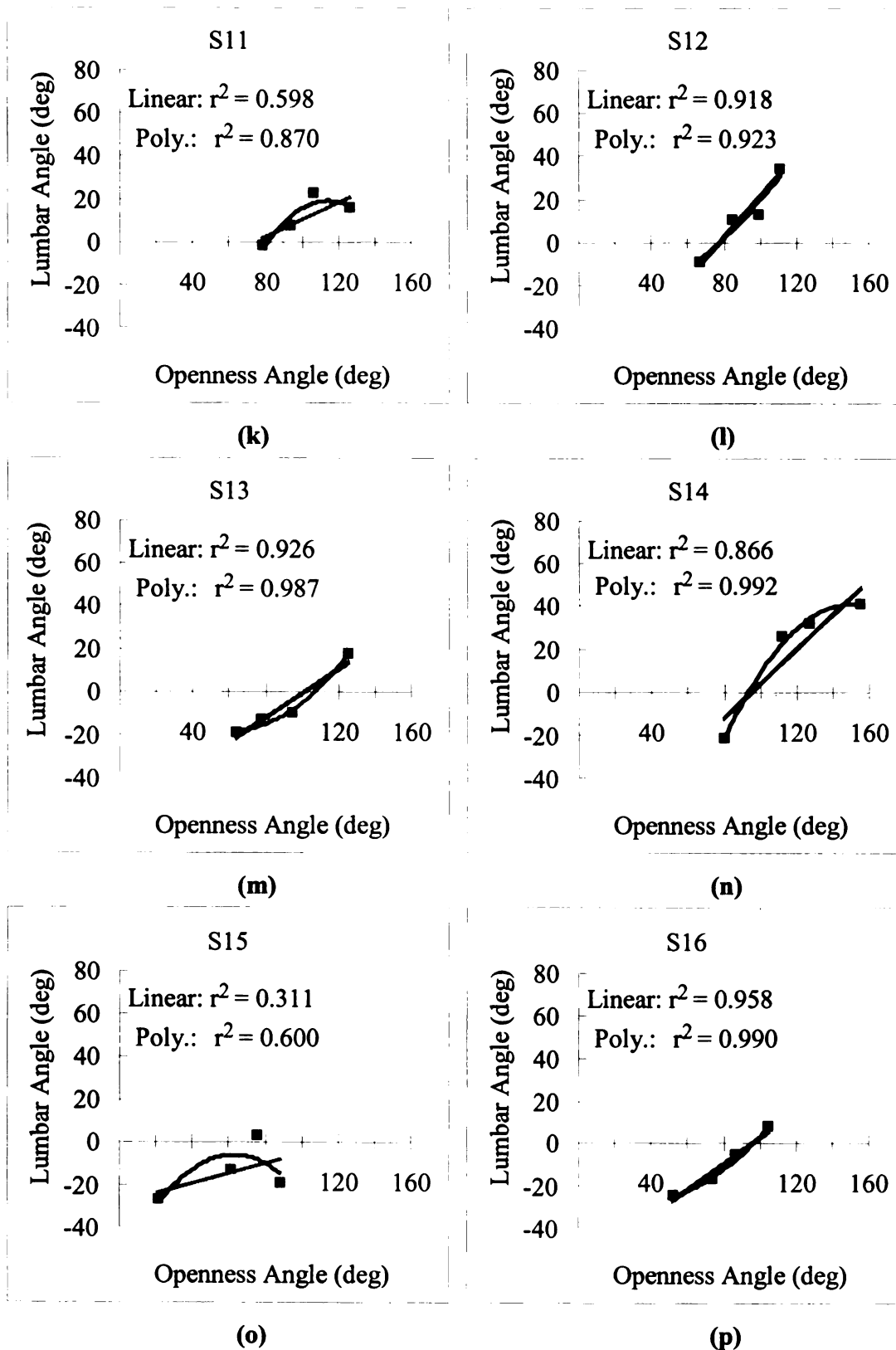


Figure 9 (cont.)

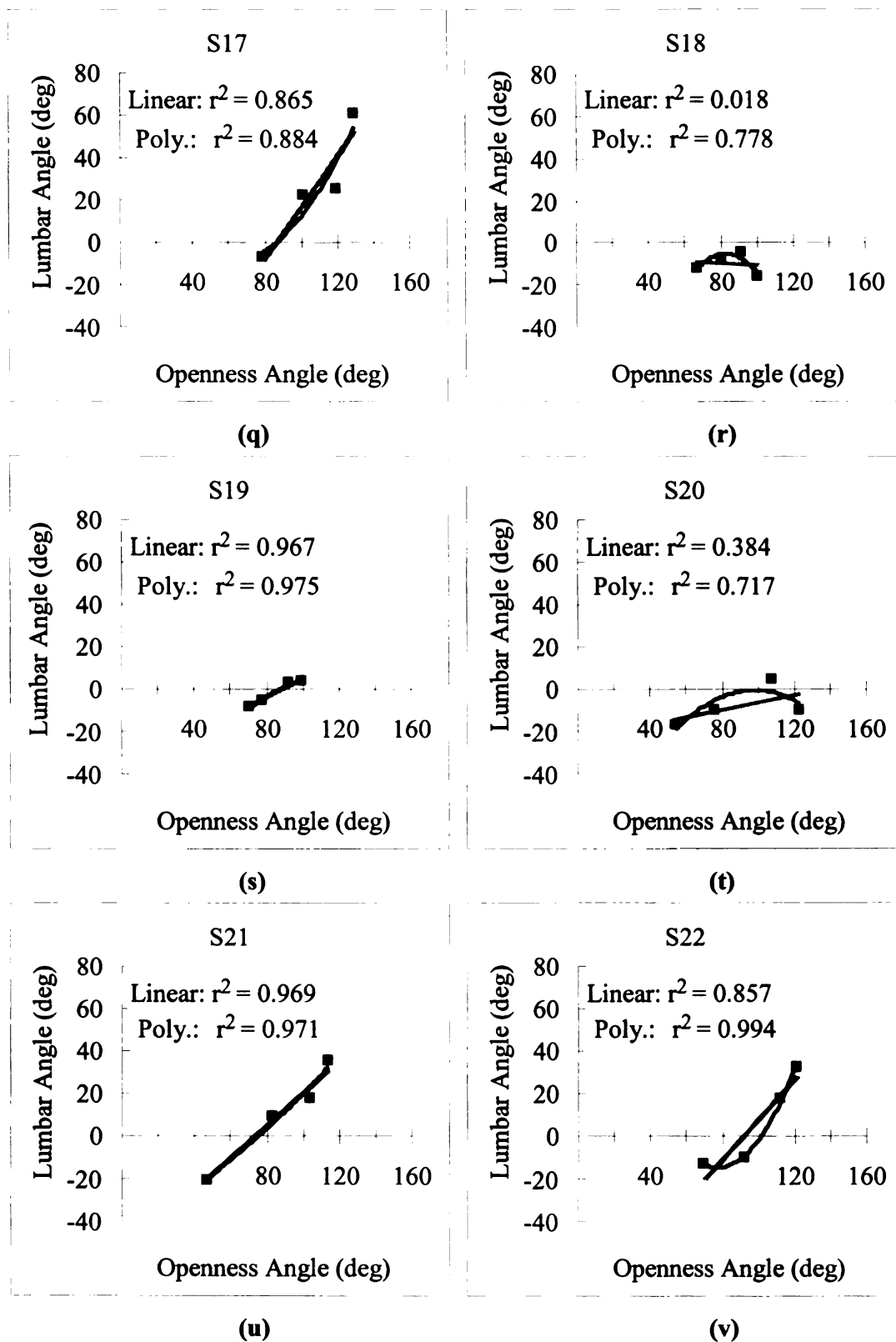


Figure 9 (cont.)

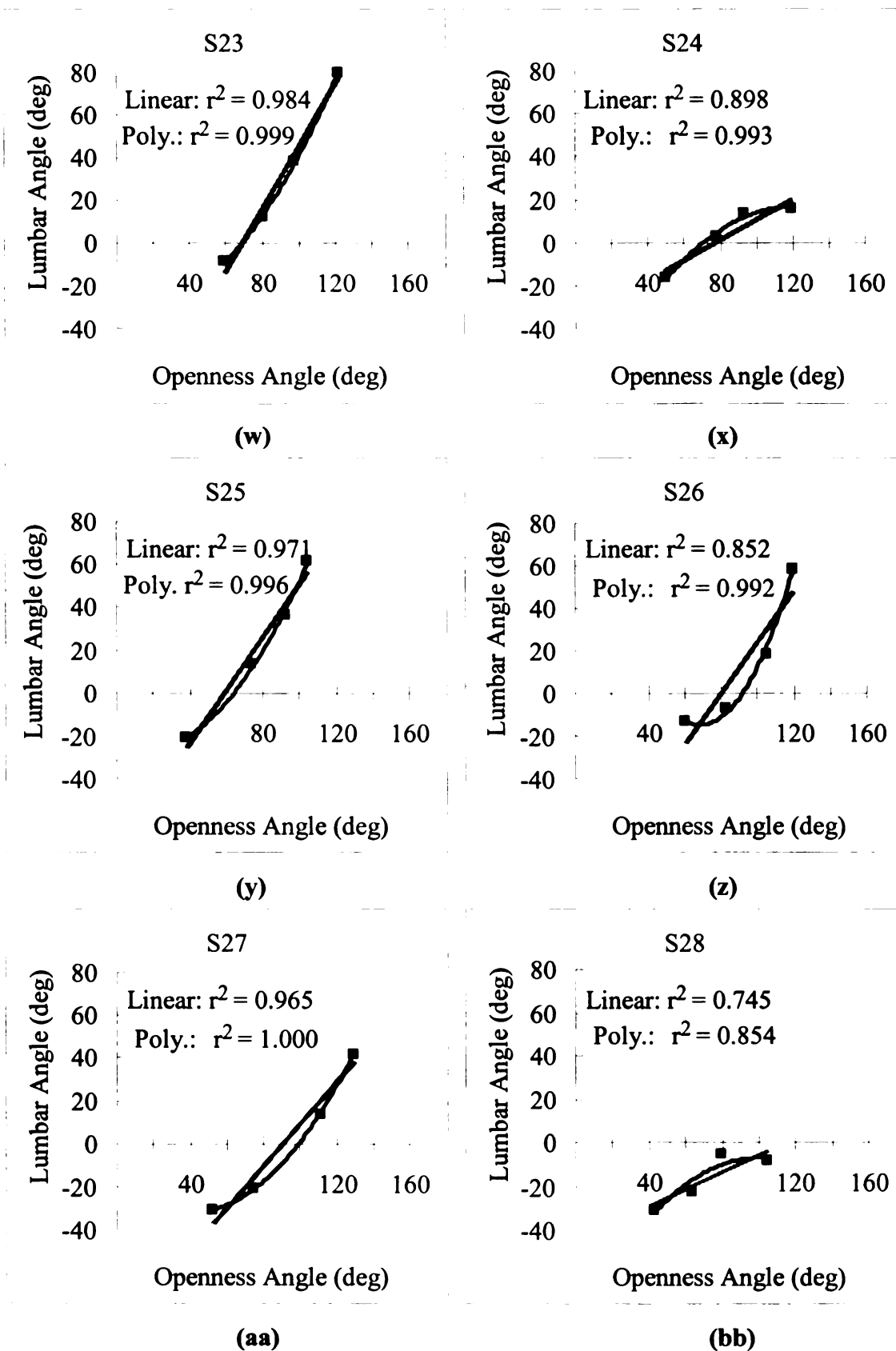


Figure 9 (cont.)

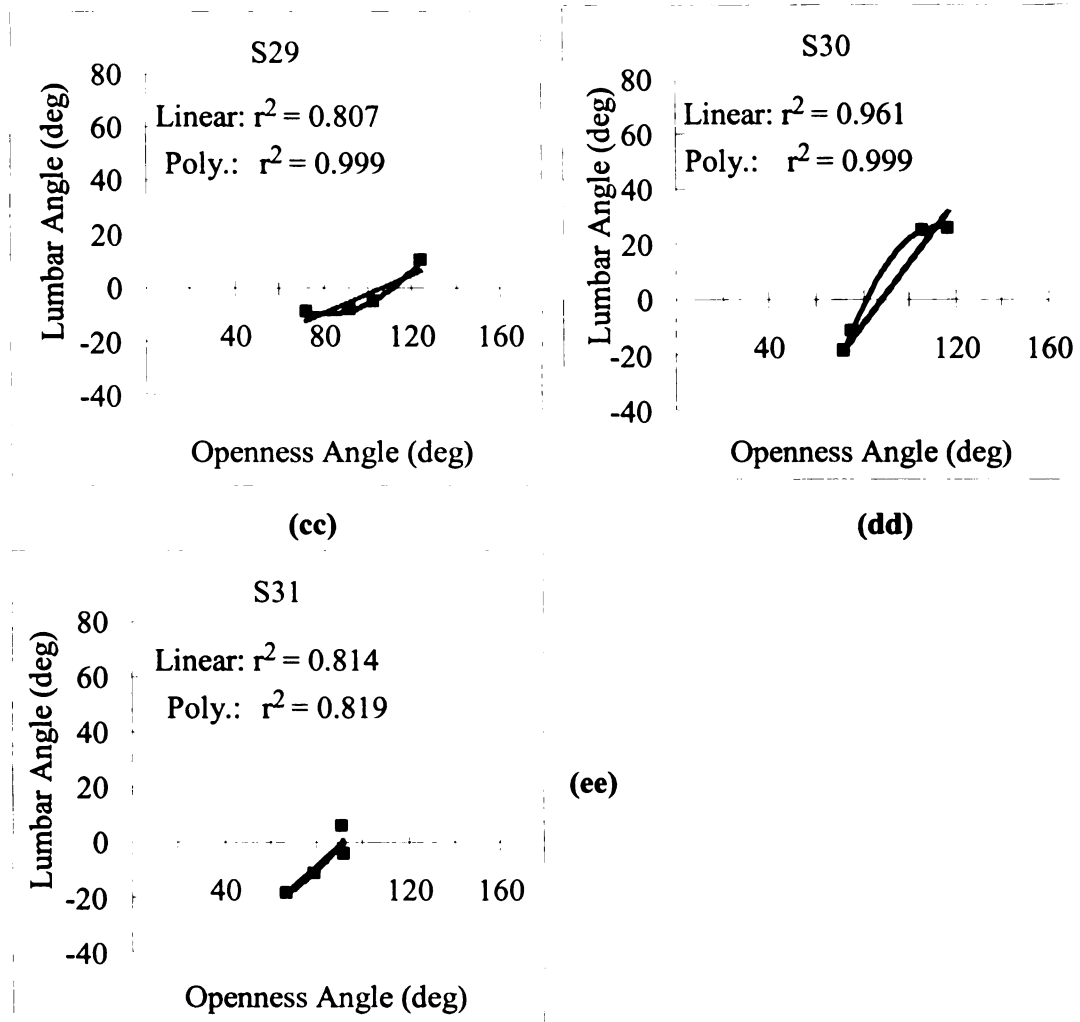
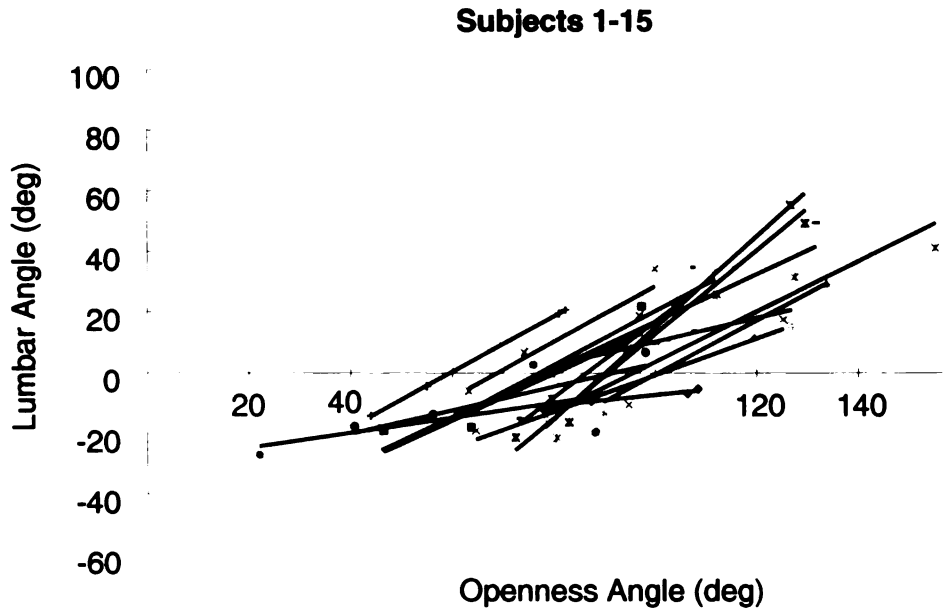
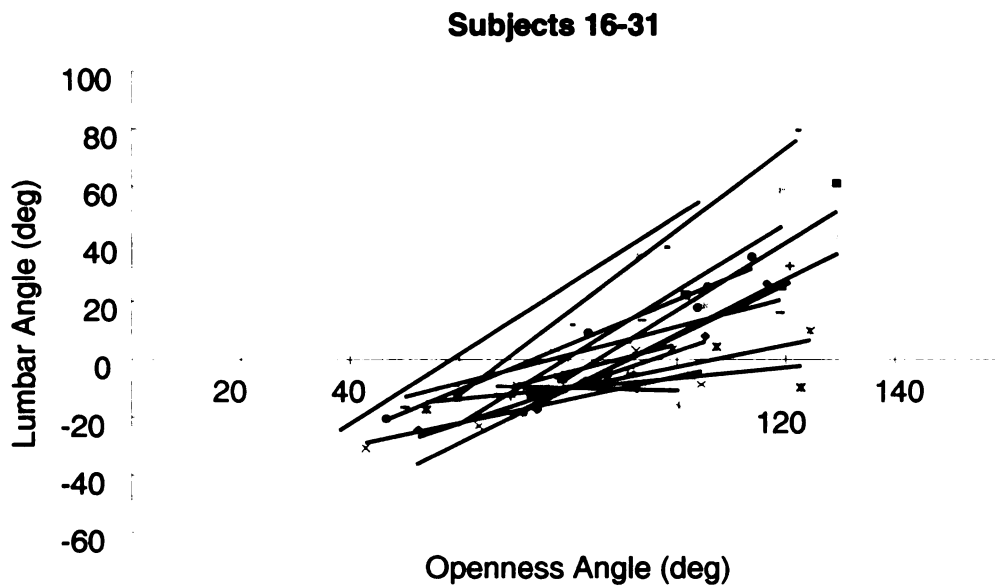


Figure 9 (cont.)

Figure 10 (a,b) shows the linear approximations for all of the subjects. In this case, the data have been split into two graphs for ease of viewing.



(a)



(b)

**Figure 10 (a,b). a) Linear best fit plots for subjects 1-15
b) Linear best fit plots for subjects 16-31**

A summary table displaying the linear slopes and r^2 values for the linear and polynomial model for each subject in the static positions can be seen below in Table 8.

Note that the average linear r^2 value is 0.829, the average polynomial r^2 value is 0.935, and all of the slope values are positive except for one subject.

Table 8. Slope, linear r^2 and polynomial r^2 values for each subject as determined by best fit line

Subject	Linear Slope	Linear r^2	Polynomial r^2
S01	0.171	0.964	0.964
S02	0.767	0.760	0.985
S03	0.888	0.887	0.906
S04	0.919	0.903	0.904
S05	1.380	0.981	0.985
S06	0.386	0.808	0.943
S07	0.909	1.000	1.000
S08	1.532	0.872	0.962
S09	0.782	0.904	1.000
S10	1.503	0.988	1.000
S11	0.404	0.598	0.870
S12	0.891	0.918	0.923
S13	0.599	0.926	0.987
S14	0.830	0.866	0.992
S15	0.246	0.311	0.599
S16	0.625	0.957	0.990
S17	1.163	0.865	0.884
S18	-0.046	0.018	0.778
S19	0.473	0.967	0.975
S20	0.181	0.384	0.717
S21	0.775	0.969	0.971
S22	0.888	0.857	0.994
S23	1.421	0.984	0.999
S24	0.484	0.897	0.993
S25	1.199	0.971	0.996
S26	1.149	0.852	0.992
S27	0.941	0.965	1.000
S28	0.402	0.745	0.854
S29	0.371	0.807	0.999
S30	1.040	0.962	1.000
S31	0.795	0.814	0.819
AVG	0.776	0.829	0.935
S.D.	0.409	0.221	0.096

Dynamic

Graphs for the dynamic data can be seen in Figure 11 (a-o). Also included in the graphs are the graphical representations of the linear and polynomial models with their associated r^2 values. The linear best fit approximations are shown as gray lines, while the second order polynomials are the black curves. Note that in some cases, such as Figure 11 (a), due to the similarities in linear and polynomial models, it appears only the polynomial black curve is visible. Figure 11 (c) provides a good example of a subject where the linear and polynomial models do not overlap.

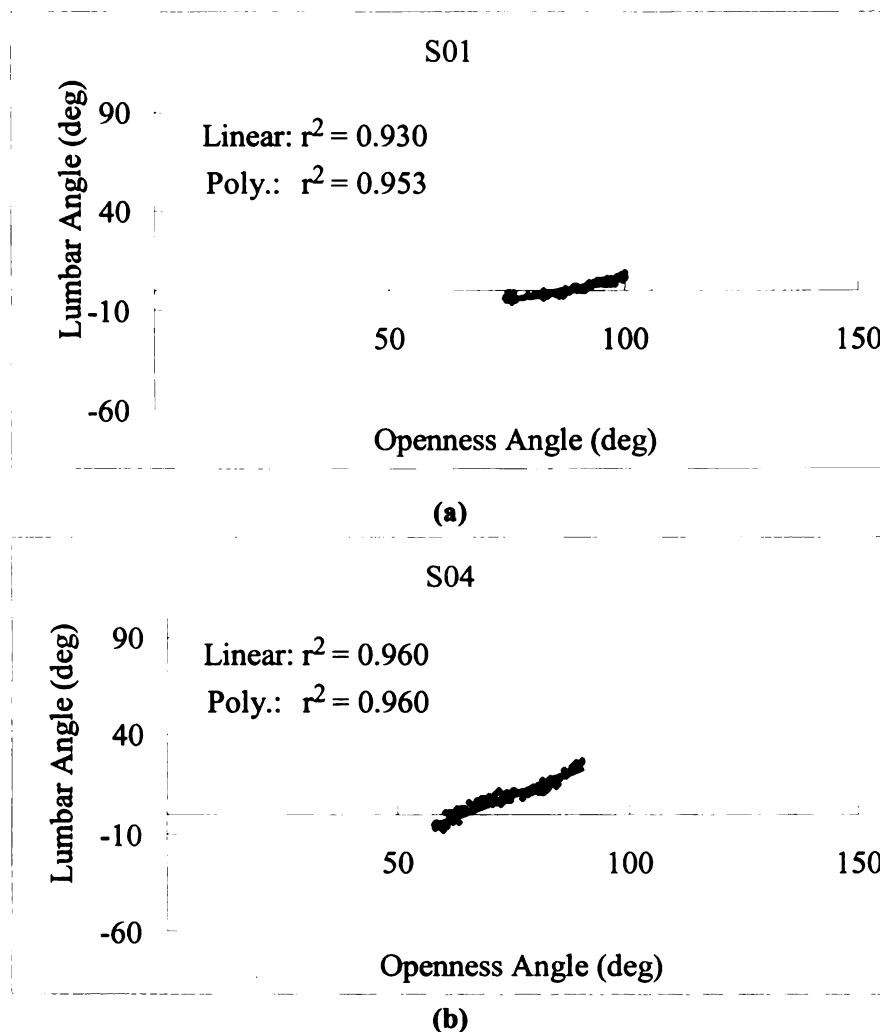
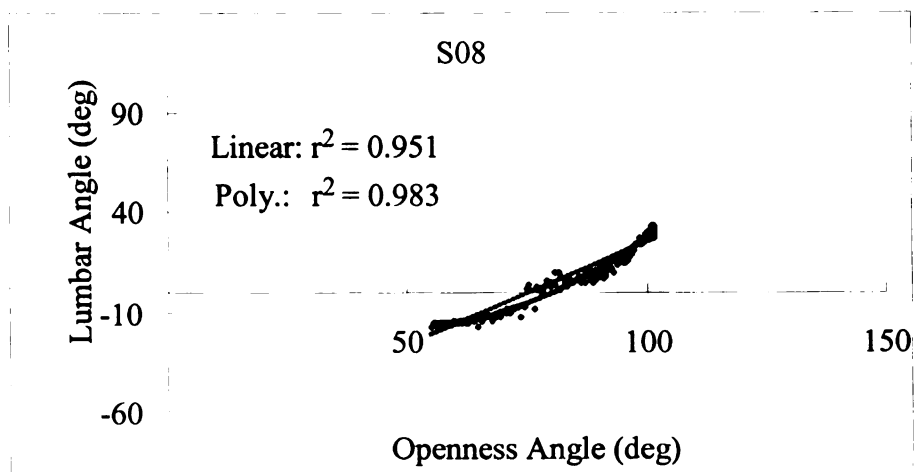
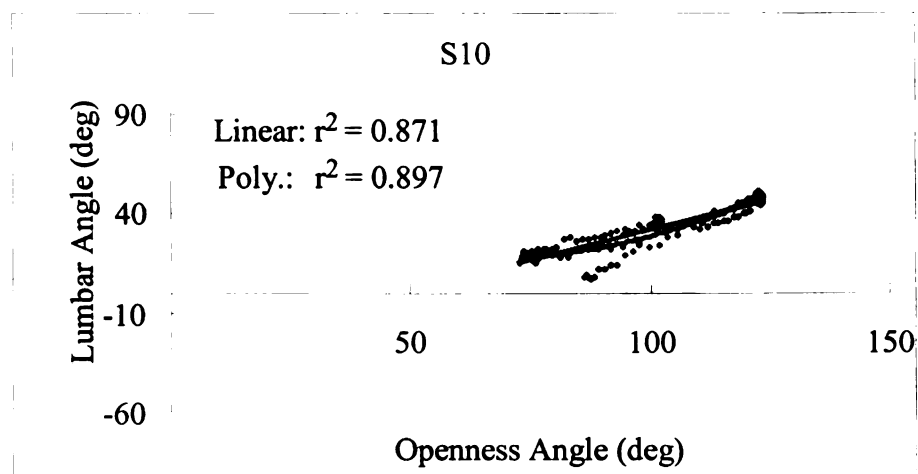


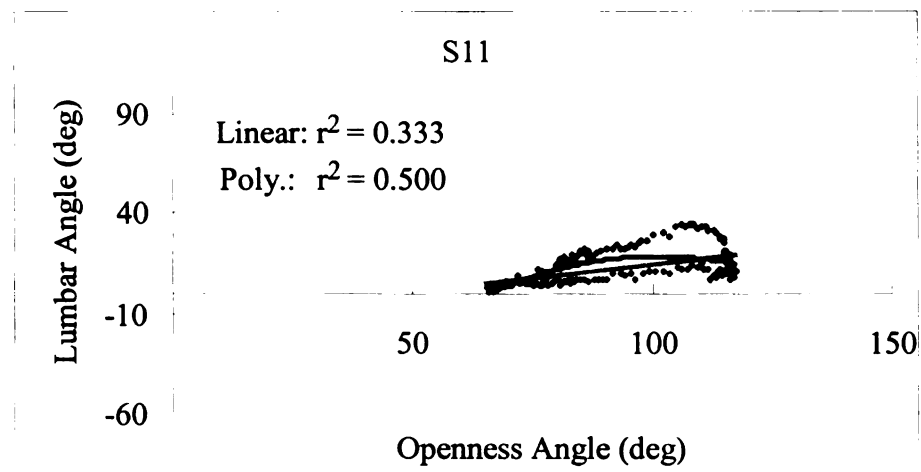
Figure 11 (a-o). Openness Angle vs. Lumbar Angle for each individual subject using static postures with included linear and second order polynomial best fits



(c)

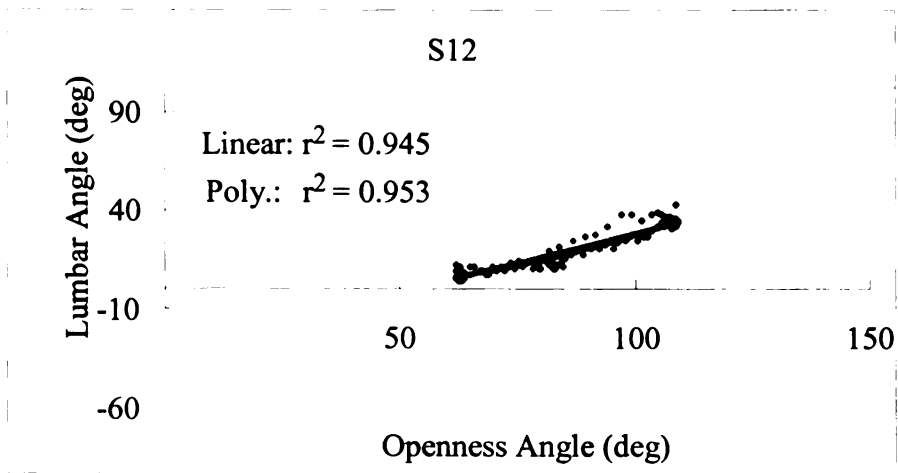


(d)

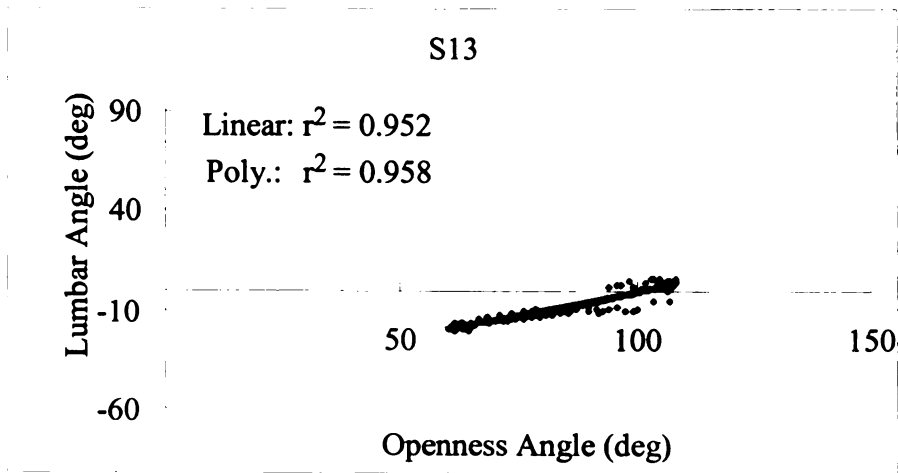


(e)

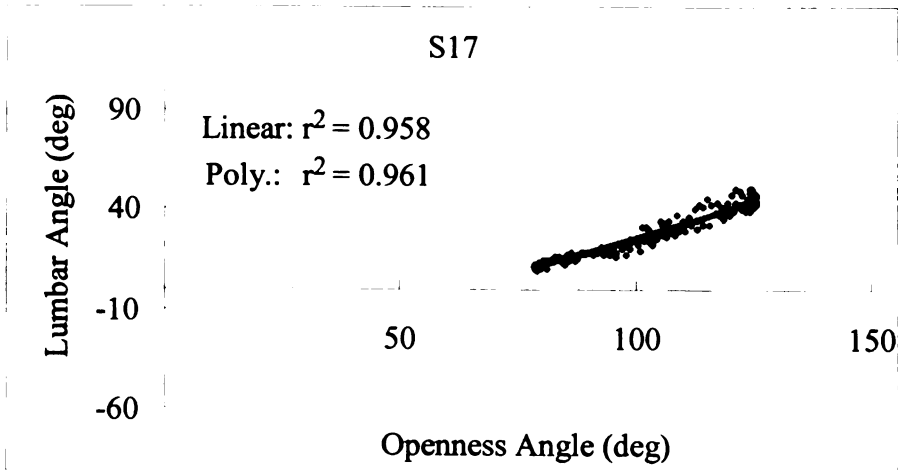
(cont.)



(f)

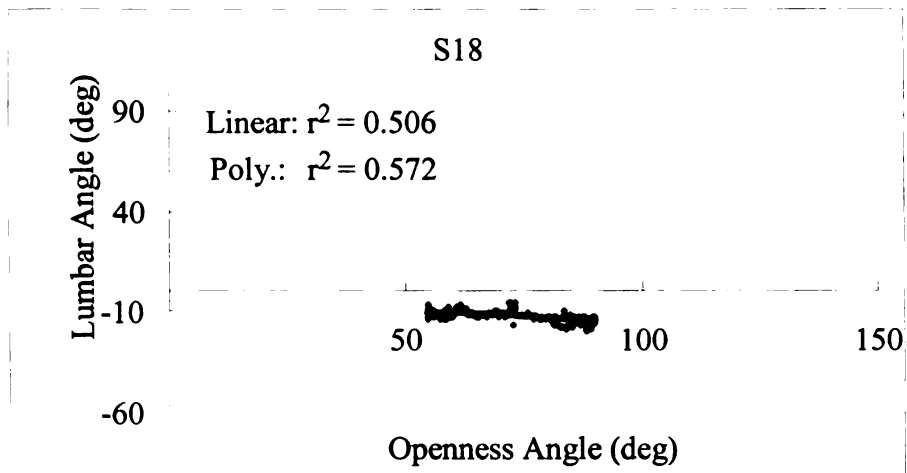


(g)

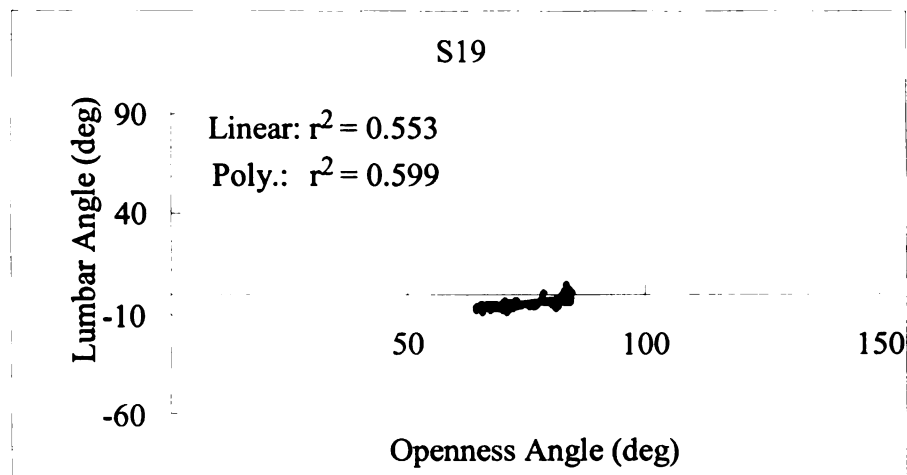


(h)

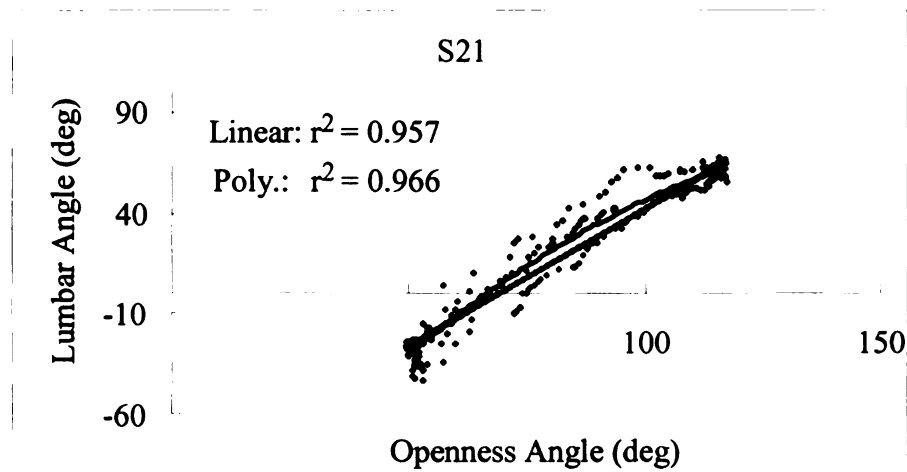
(cont.)



(i)

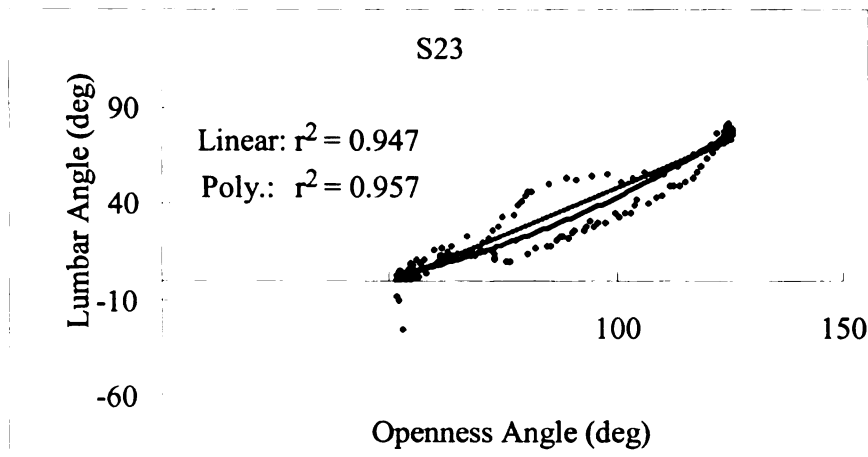


(j)

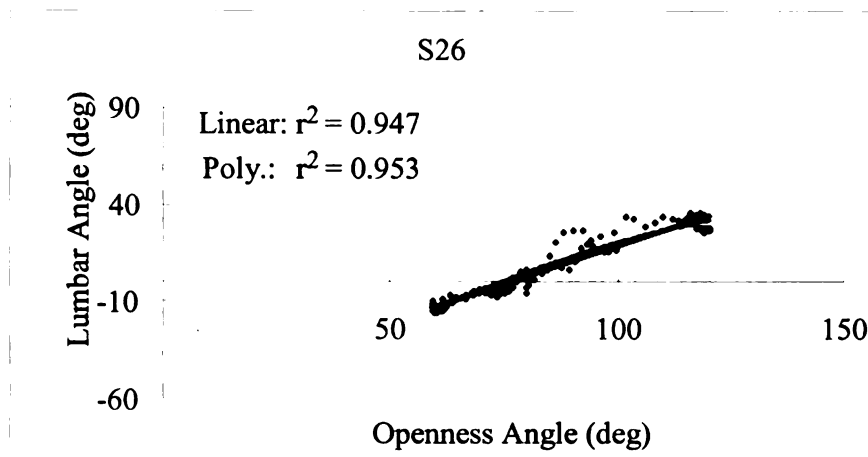


(k)

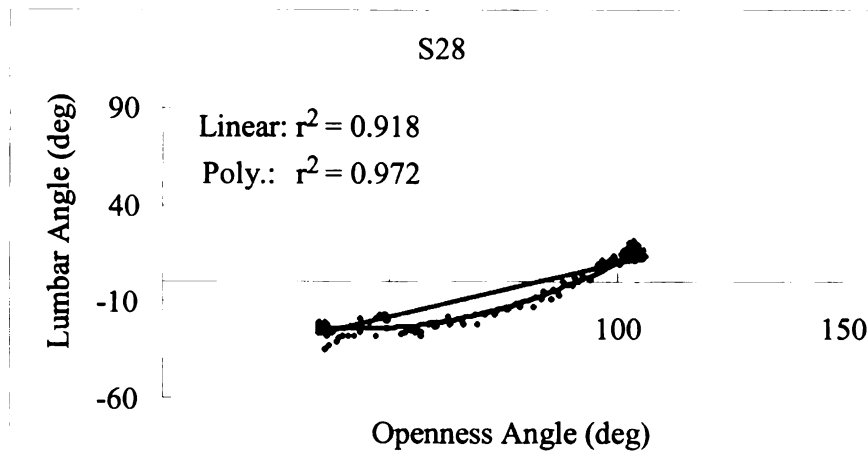
(cont.)



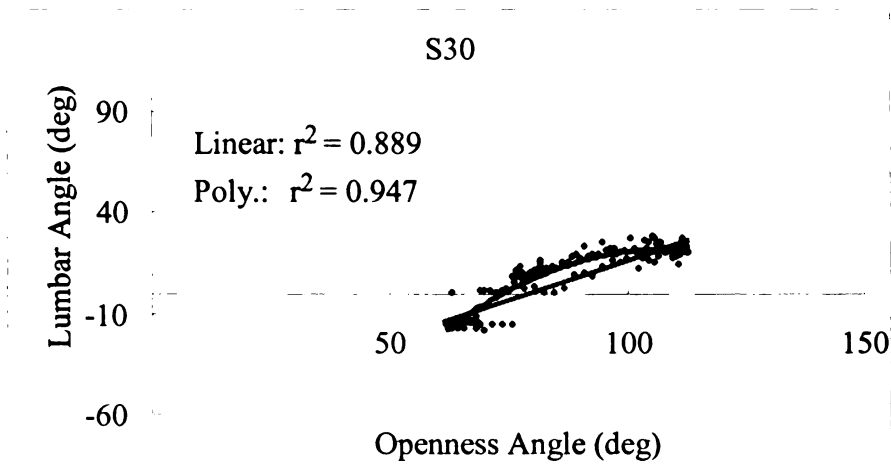
(l)



(m)



(n)
(cont.)



(cont.)

A summary table displaying the linear slopes and r^2 values for the linear and polynomial model for each subject in the dynamic positions can be seen below in Table

9. Note that the average linear r^2 value is 0.841, the average polynomial r^2 value is 0.875, and that all of the slope values are positive except for one subject.

Table 9. Summary table of slope, intercept and r^2 for 15 dynamic subjects

Subject	Linear Slope	Linear r^2	Polynomial r^2
S01	0.435	0.930	0.953
S04	0.931	0.960	0.960
S08	1.042	0.951	0.983
S10	0.619	0.869	0.896
S11	0.265	0.330	0.496
S12	0.608	0.944	0.952
S13	0.483	0.952	0.958
S17	0.740	0.958	0.961
S18	-0.149	0.507	0.573
S19	0.293	0.554	0.600
S21	1.380	0.957	0.966
S23	1.009	0.947	0.957
S26	0.770	0.947	0.954
S28	0.561	0.919	0.972
S30	0.784	0.889	0.946
AVG	0.651	0.841	0.875
S.D.	0.372	0.202	0.167

A graph of the dynamic and static data for each subject with full data sets is shown in Figure 12 (a-o). In this case, the linear and polynomial best fit models have been left off the graphs for visual clarity of the data.

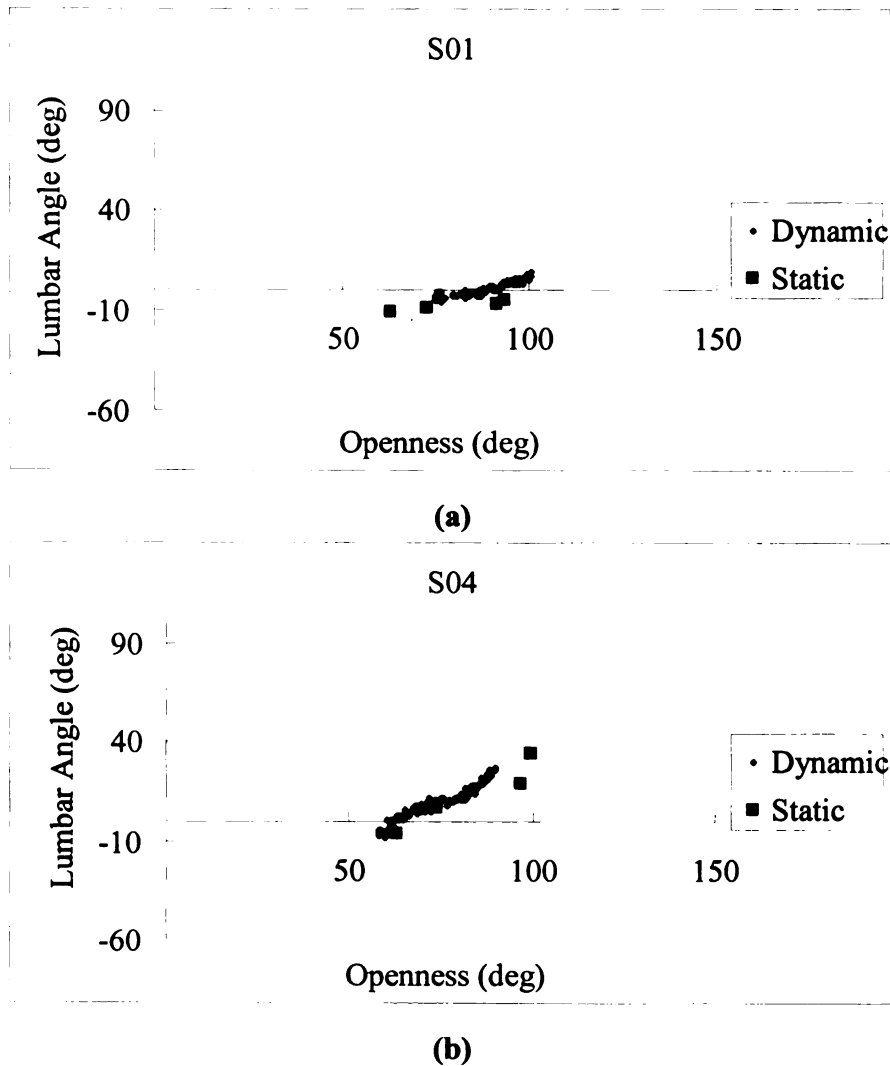
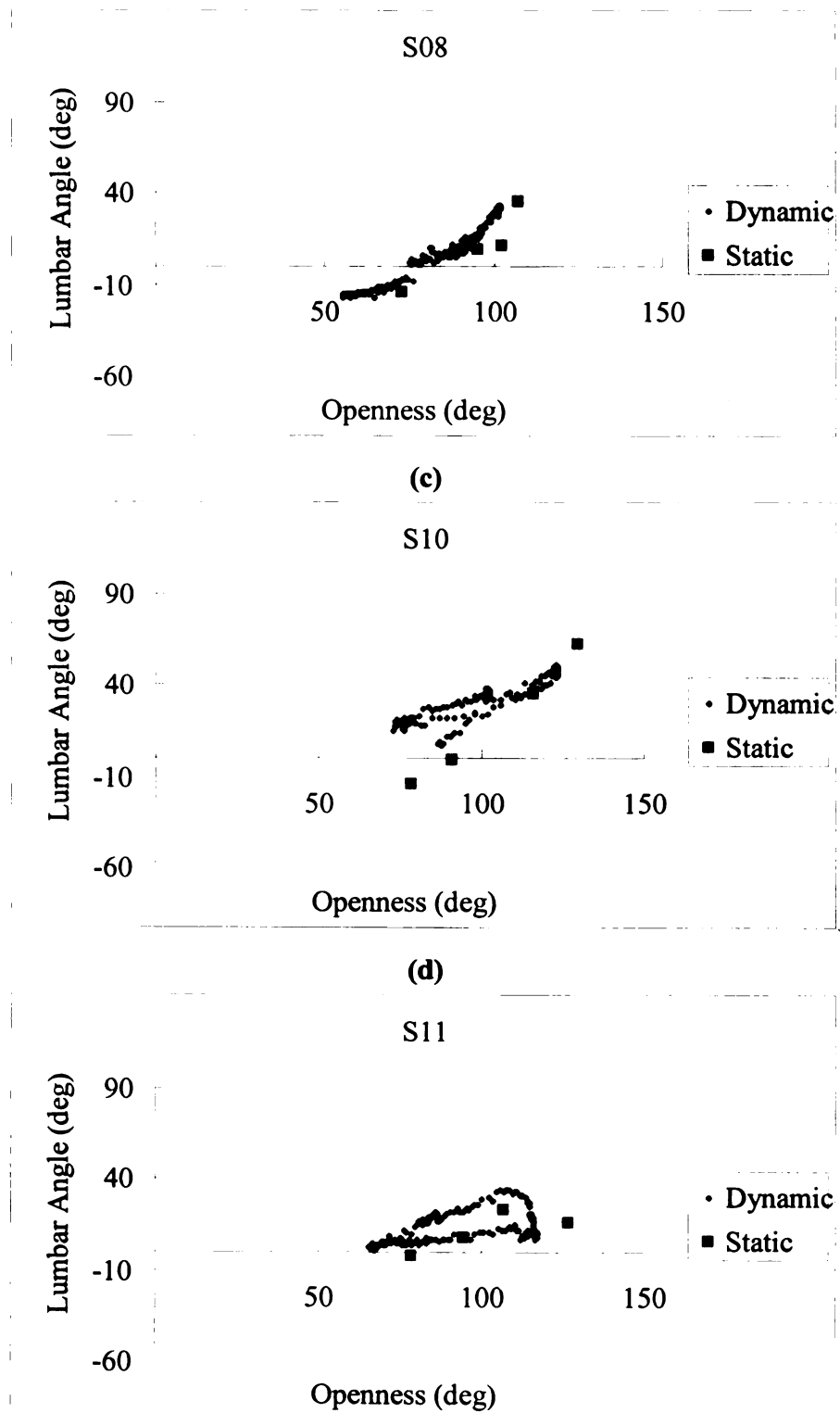
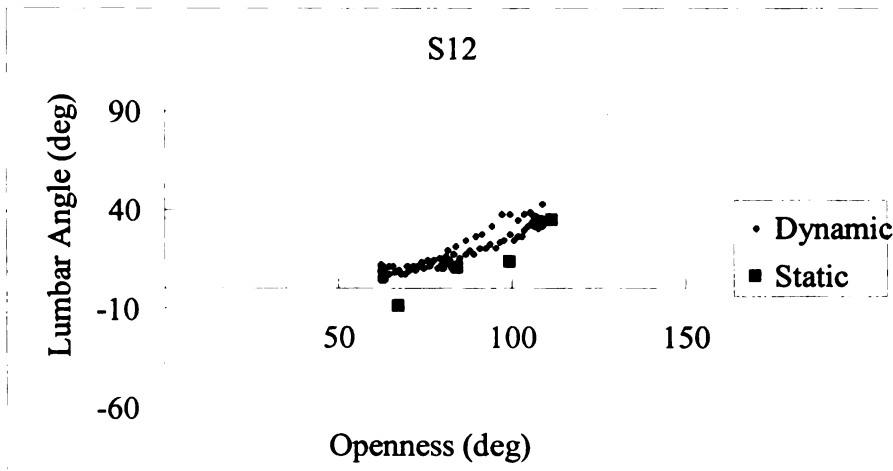


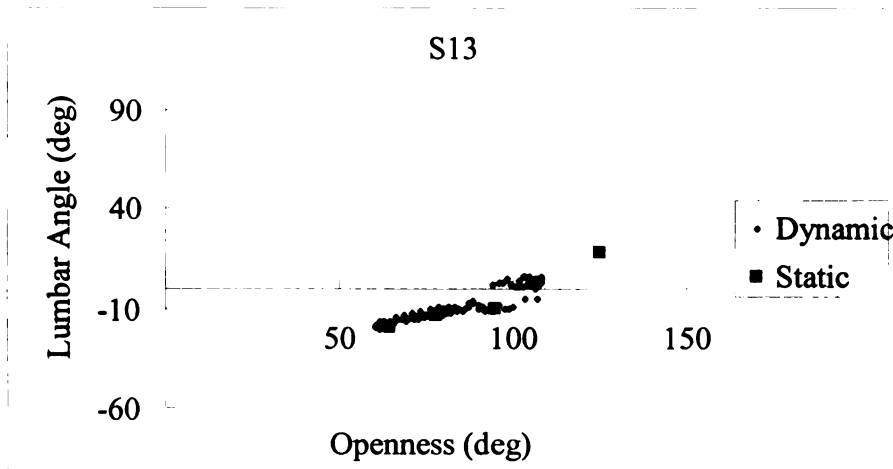
Figure 12 (a-o). Dynamic and Static data plotted as Openness vs. Lumbar Angle for each subject with sufficient dynamic data



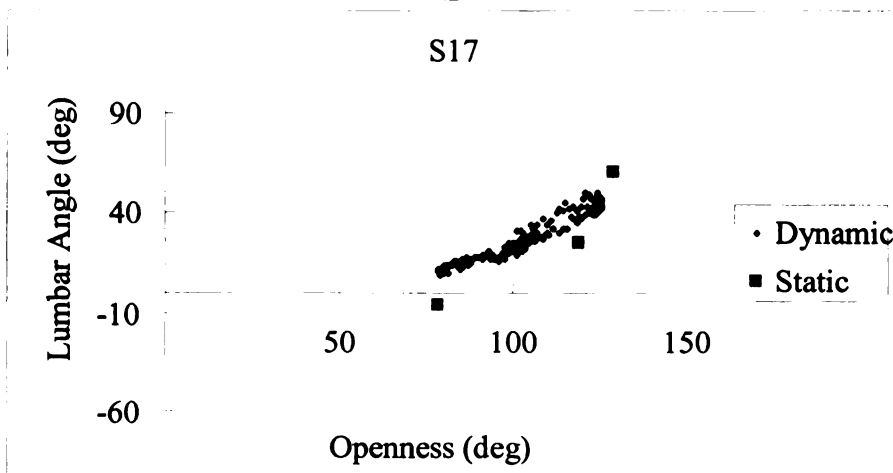
(e)
Figure 12 (cont.)



(f)



(g)

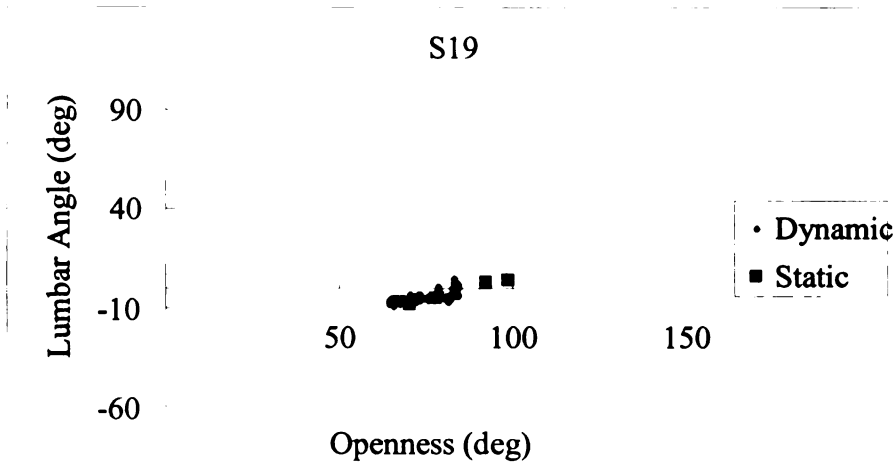


(h)

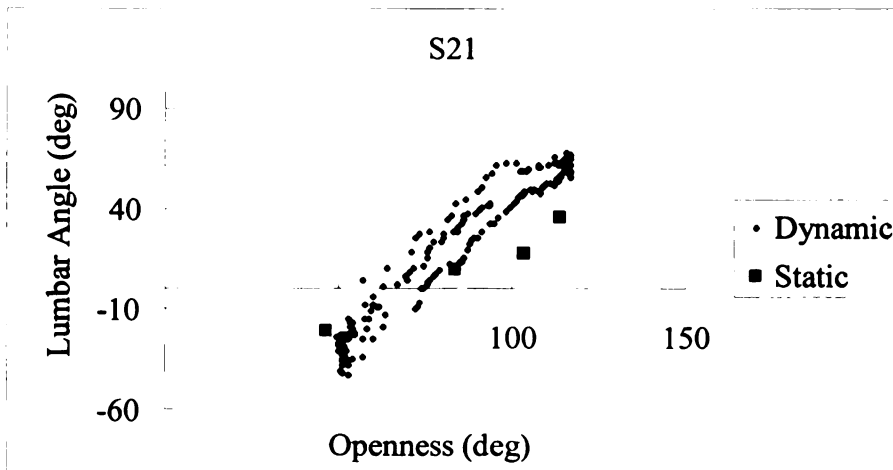
Figure 12 (cont.)



(i)

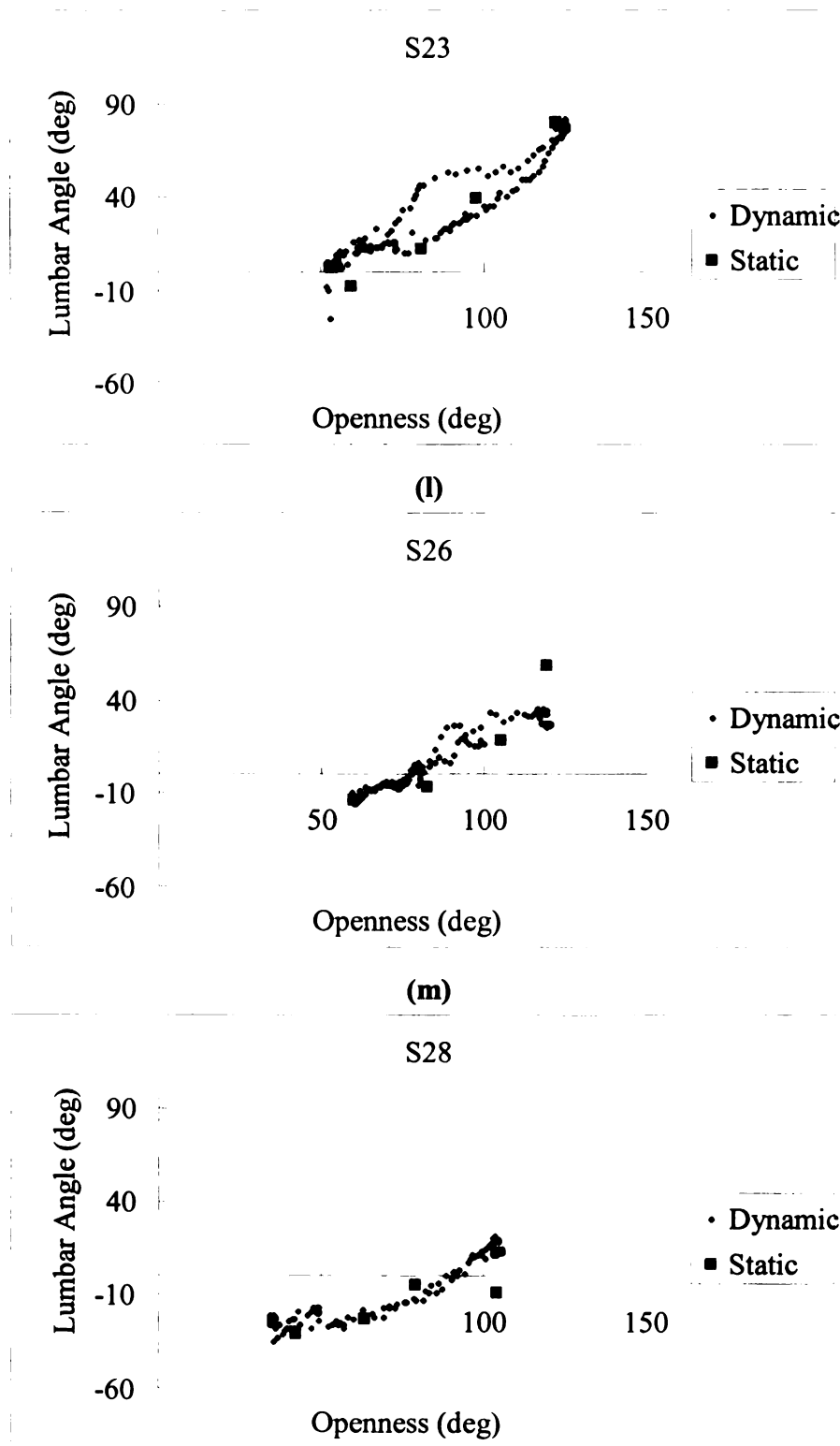


(j)



(k)

Figure 12 (cont.)



(n)
Figure 12 (cont.)

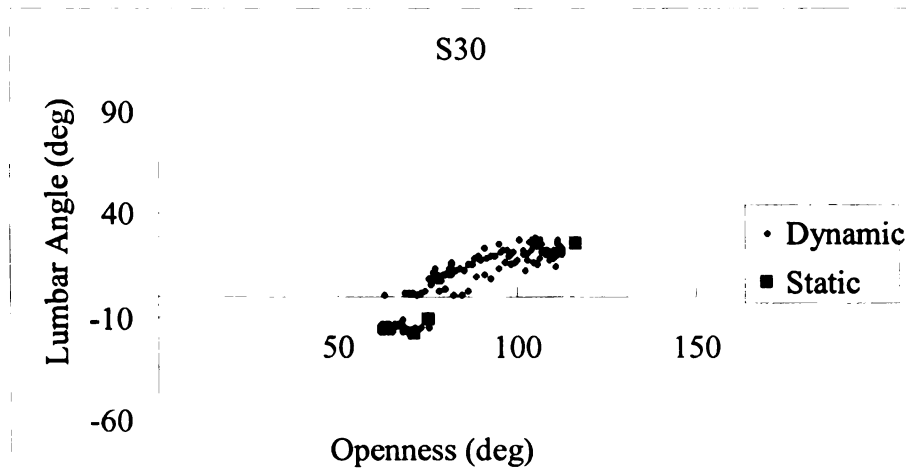


Figure 12 (cont.)

Anthropometric Correlation to Openness/Lumbar Angle Slope

Table 10 shows the correlation coefficients between the anthropometric measures and the slope of the relationship between openness and lumbar angles. Note that only seated height and pelvic depth in the dynamic model have correlation values with an absolute value higher than the critical value.

Table 10. Pearson Product Moment Correlation Coefficients for Slope vs. each anthropometric measure

Openness/Lumbar Slope vs.	Pearson Product Moment Correlation Coefficient	
	Static	Dynamic
Critical	0.355	0.514
Height	-0.010	0.374
Weight	-0.055	0.240
Age	-0.140	-0.226
Seated Height	0.195	0.628
Seated Buttocks Width	0.168	0.458
Pelvic Width	0.315	0.273
Pelvic Height	-0.075	0.330
Pelvic Depth	0.060	0.601

Predictive Capacity

Static data predicting static positions for test population

The linear model developed from the first 16 subjects (S01-S16) was $\alpha = 0.687\theta - 56.1$, where α is the lumbar angle and θ is the openness angle. This model was developed by finding the best fit regression line for all of the static data for the first half of the subjects, as described previously, and can be seen graphically in Figure 13.

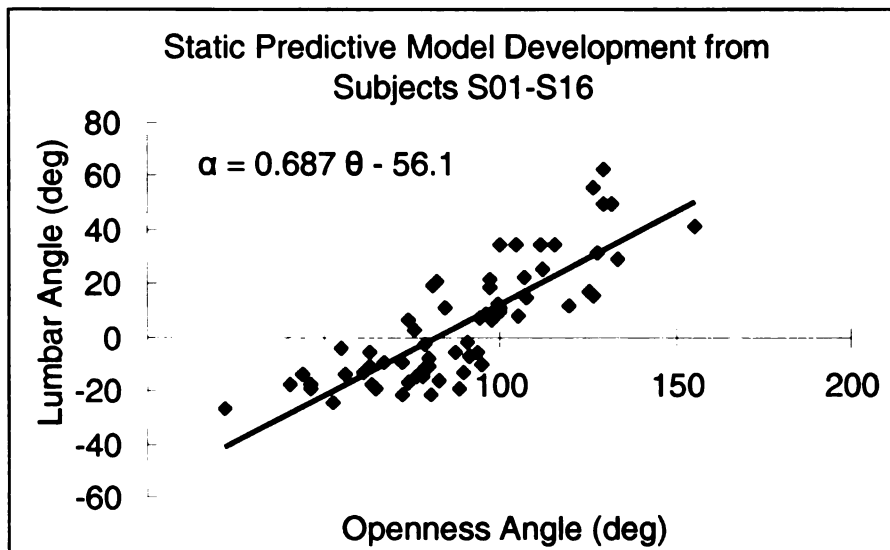


Figure 13. Graphical representation of linear predictive model developed from the static openness and lumbar angle data of subjects S01-S16

Figure 14 shows both the actual data from the second group of subjects (S17-S31), and the predicted values for the same openness angles that were determined by applying the model developed by the first group of subjects.

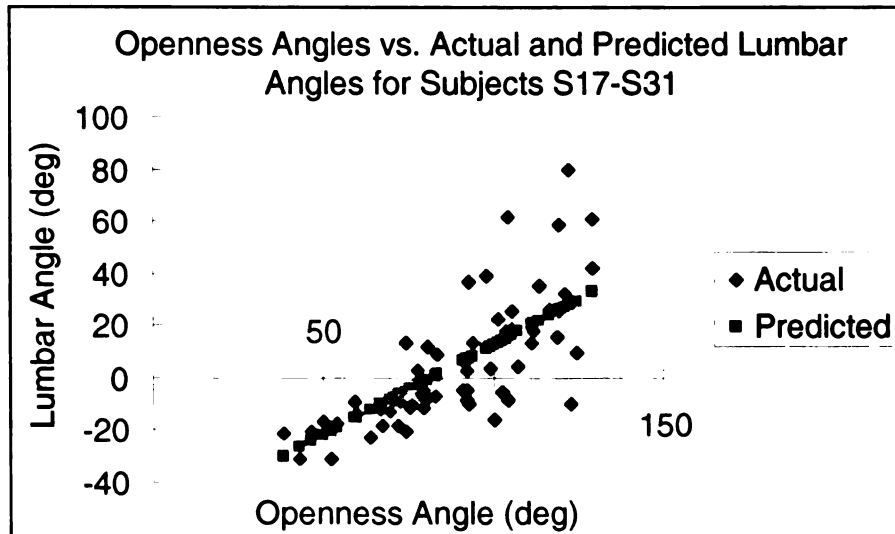


Figure 14. Predicted static lumbar angle values compared to actual static lumbar angle values for linear static model applied to openness angles of subjects S17-S31

Comparing the lumbar angles predicted from the linear model and actual lumbar angles seen in Figure 14 with a paired t-test, the p-value was found to be 0.969.

The second order polynomial model developed from the first group, seen in Figure 15, was found to be $\alpha = 0.003\theta^2 + 0.063\theta - 30.6$, where α is the lumbar angle and θ is the openness angle.

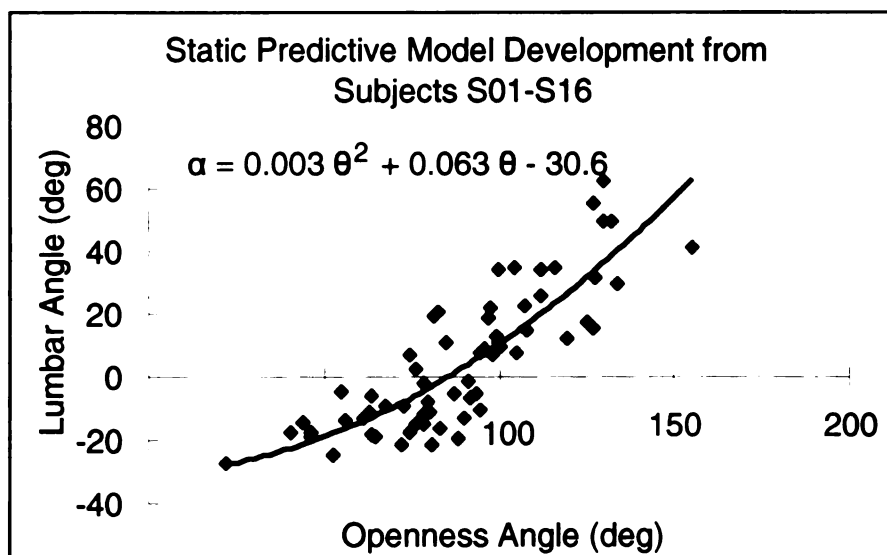


Figure 15. Graphical representation of polynomial predictive model developed from the static openness and lumbar angle data of subjects S01-S16

When this polynomial model, derived from the first group of subjects, was applied to the second group, the predicted values seen in Figure 16 were found. Also shown in Figure 16 are the actual values of lumbar angles for each corresponding openness angle.

The p-value for a paired t-test comparison between the polynomial predicted static lumbar angles and the actual lumbar angles for subjects S17-S31 was found to be 0.827.

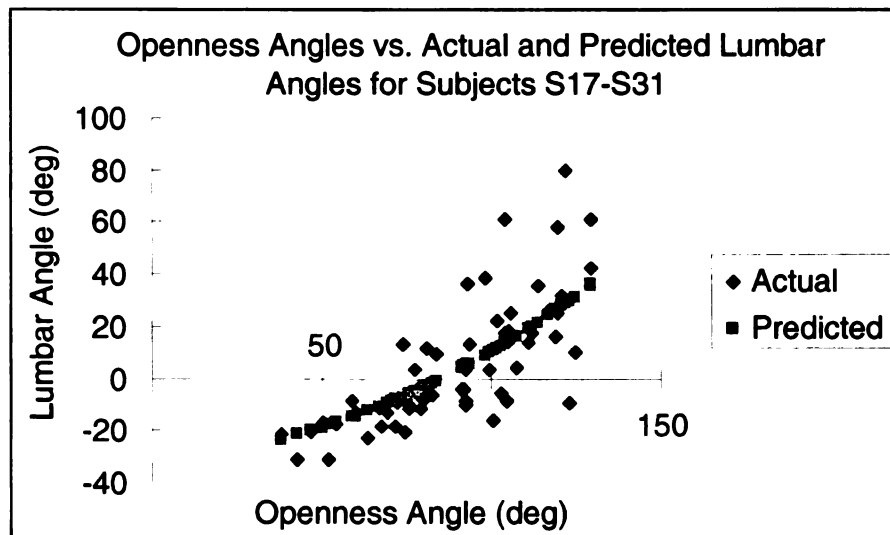


Figure 16. Predicted static lumbar angle values compared to actual static lumbar angle values for polynomial static model applied to the openness angles of subjects S17-S31

Dynamic data predicting dynamic positions for the test population

The linear model developed from the first set of subjects (S01, S04, S08, S10, S11, S12, S13, S17) was $\alpha = 0.754\theta - 57.2$, where α is the lumbar angle and θ is the openness angle. This can be seen graphically in Figure 17.

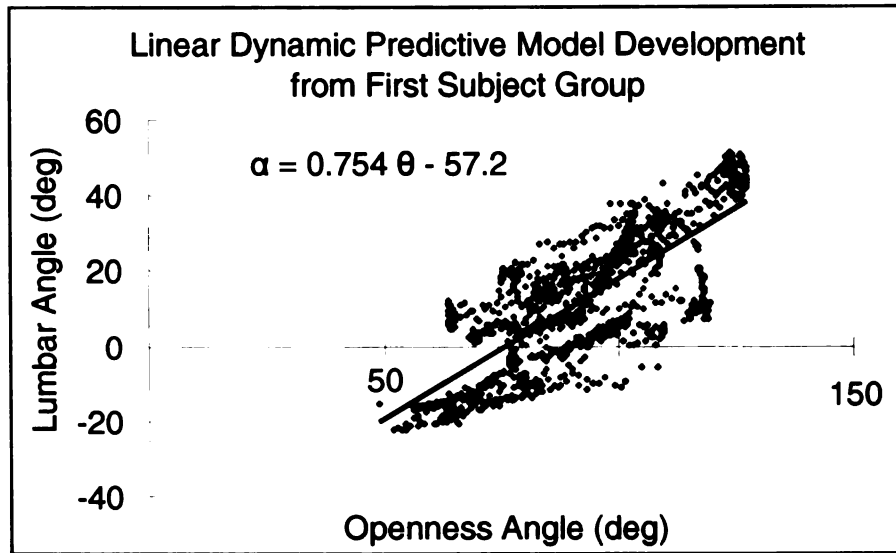


Figure 17. Graphical representation of linear predictive model developed from the first eight subjects in the dynamic data group

Figure 18 shows both the actual data from the second group of dynamic subjects (S18, S19, S21, S23, S26, S28, S30), and the predicted values for the same openness angles that were determined by applying the model developed by the first group of dynamic subjects.

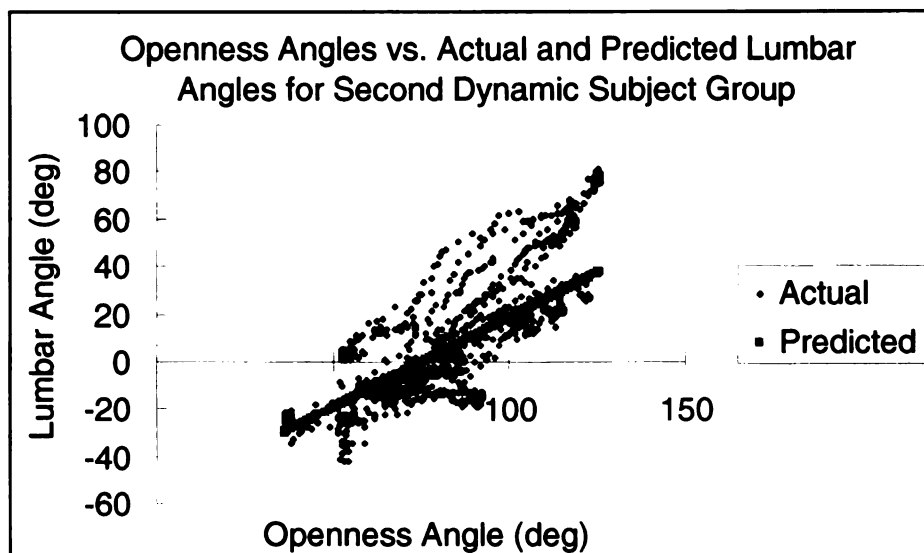


Figure 18. Predicted dynamic lumbar angle values compared to actual dynamic lumbar angle values for linear dynamic model applied to the openness angles of the last seven subjects in the dynamic data group

Comparing the lumbar angles predicted from the dynamic linear model and actual dynamic lumbar angles seen in Figure 18 with a paired t-test, the p-value was found to be less than 0.0001.

The second order polynomial model developed from the first group, seen in Figure 19, was found to be $\alpha = 0.002\theta^2 + 0.34\theta - 39.0$, where α is the lumbar angle and θ is the openness angle.

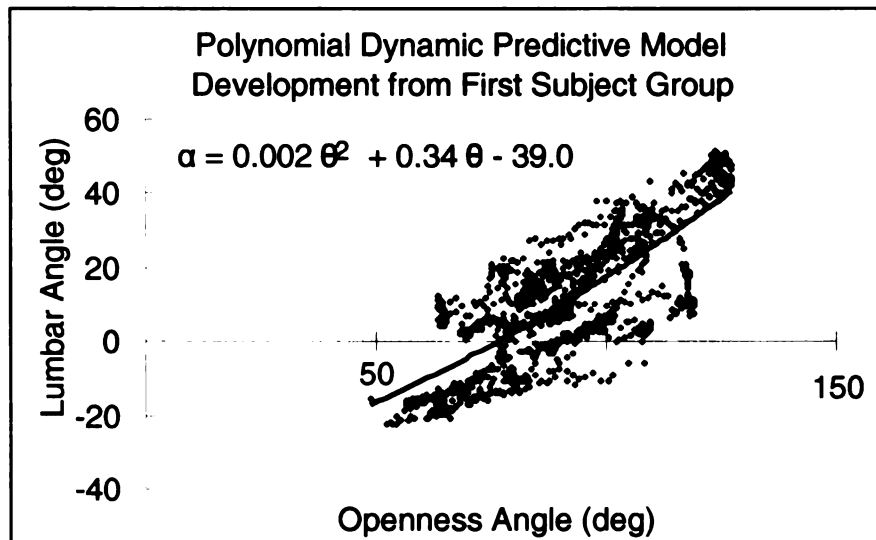


Figure 19. Graphical representation of polynomial predictive model developed from the first eight subjects in the dynamic data group

When this polynomial model, derived from the first group of dynamic subjects, was applied to the second group of dynamic subjects, the predicted values seen in Figure 20 were found. Also shown in Figure 20, are the actual values of lumbar angles for each corresponding openness angle.

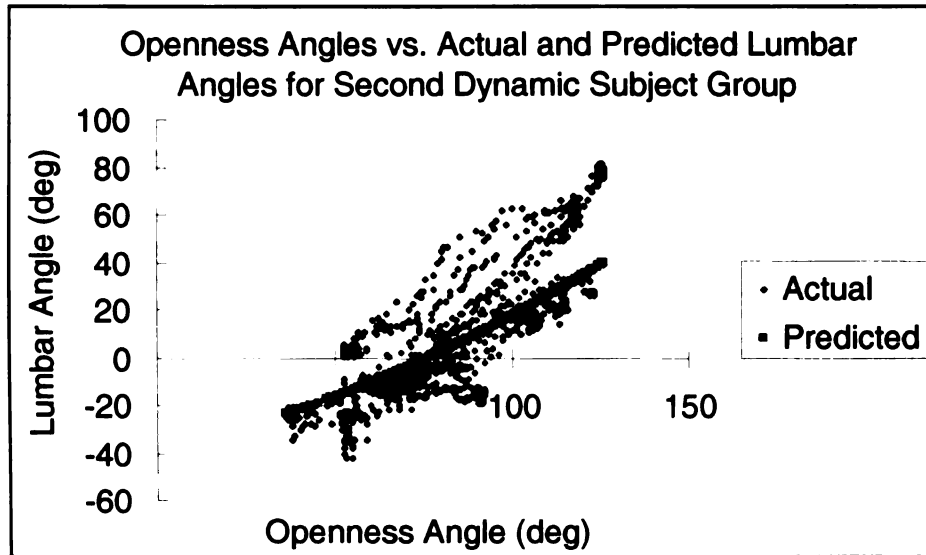


Figure 20. Predicted dynamic lumbar angle values compared to actual dynamic lumbar angle values for polynomial dynamic model applied to the openness angles of the last seven subjects in the dynamic data group

The p-value for a paired t-test comparison between the polynomial predicted dynamic lumbar angles and the actual lumbar angles for the second group of dynamic subjects was found to be 0.002.

Static data predicting dynamic positions for the test population

The linear model developed from the entire static population was $\alpha = 0.723\theta - 59.3$, where α is the lumbar angle and θ is the openness angle. Notice because this was the entire population, as compared to only a subset of the test population, this linear model is slightly different than the static model presented in the “Static predicting Static population” This model was developed by finding the best fit regression line for all of the static data and can be seen graphically in Figure 21.

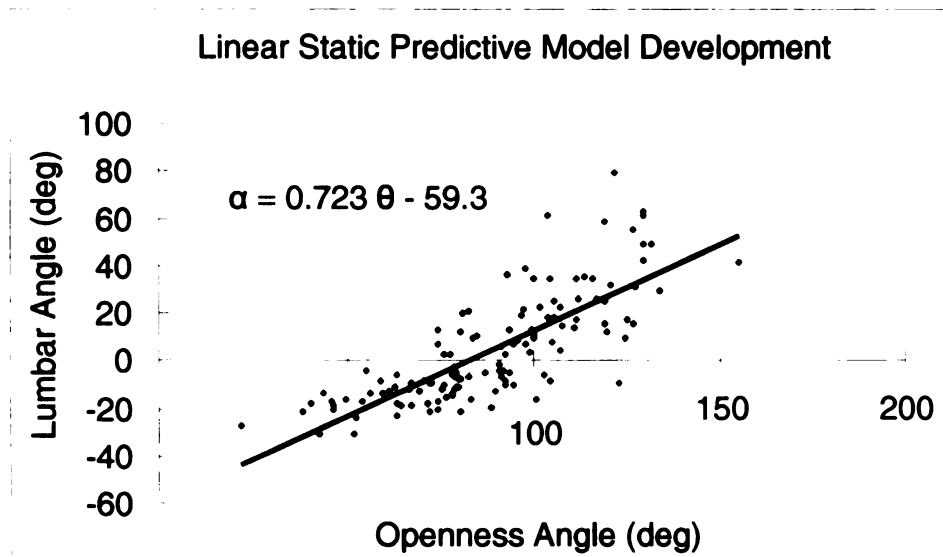


Figure 21. Graphical representation of linear population predictive model developed from all of the static openness and lumbar angle data

Figure 22 shows both the actual data from the dynamic group of subjects and the predicted values for the same openness angles that were determined by applying the model developed by the static group of subjects.

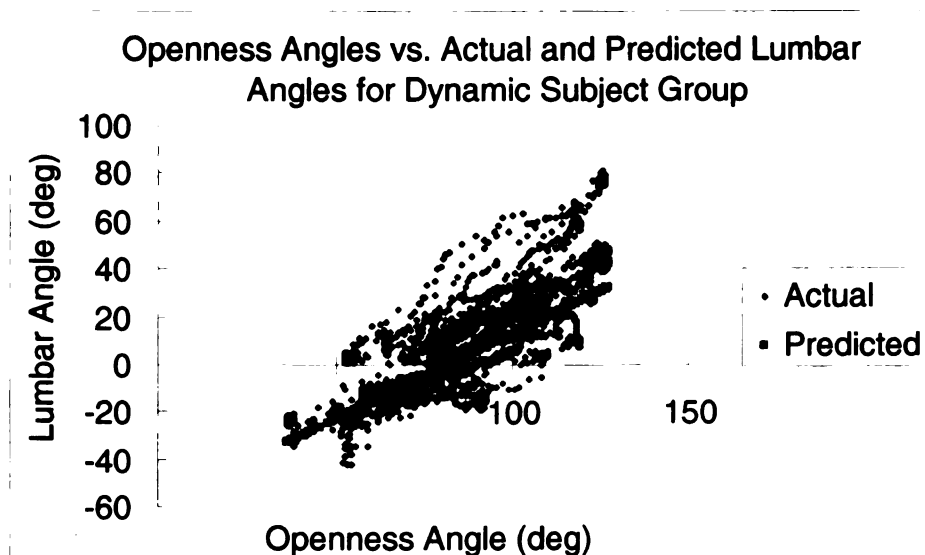


Figure 22. Predicted dynamic lumbar angle values compared to actual dynamic lumbar angle values for linear static population model applied to the openness angles of the entire dynamic data group

Comparing the lumbar angles predicted from the linear model and actual lumbar angles seen in Figure 22 with a paired t-test, the p-value was found to be less than 0.0001.

The second order polynomial model developed from the static subjects, seen in Figure 23, was found to be $\alpha = 0.004\theta^2 + 0.071\theta - 32.8$, where α is the lumbar angle and θ is the openness angle.

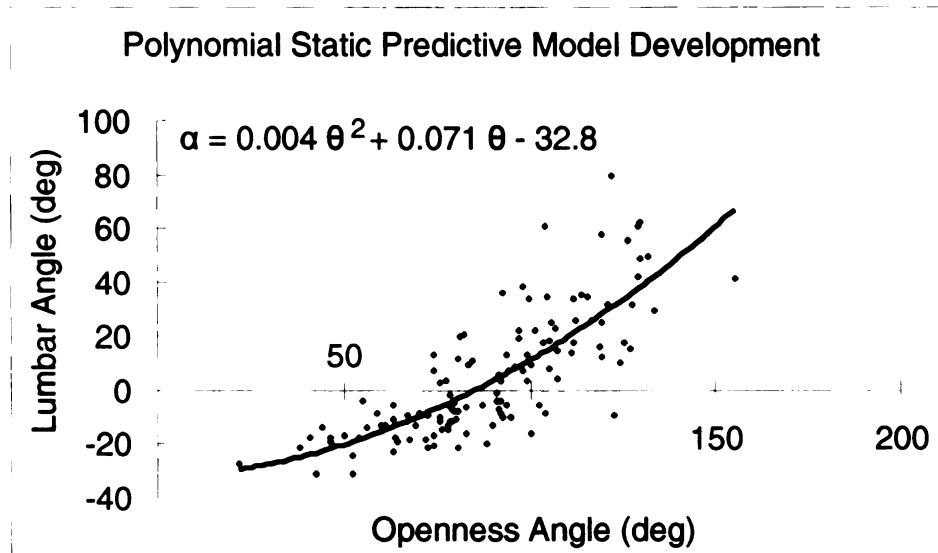


Figure 23. Graphical representation of polynomial population predictive model developed from all of the static openness and lumbar angle data

When this polynomial model was applied to the dynamic openness angles, the predicted values seen in Figure 24 were found. Also shown in Figure 24 are the actual values of lumbar angles for each corresponding openness angle.

The p-value for a paired t-test comparison between the polynomial predicted static lumbar angles and the actual lumbar angles for the dynamic data was found to be less than 0.0001.

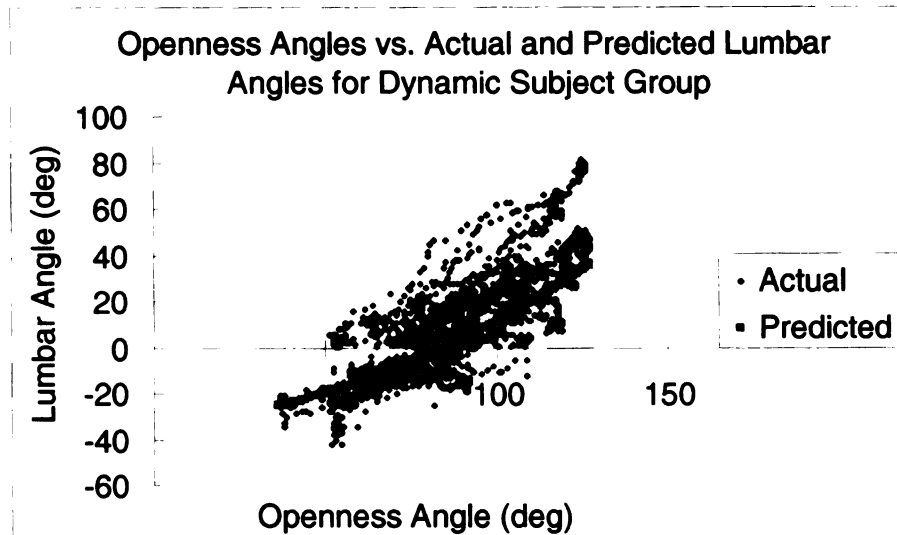


Figure 24. Predicted dynamic lumbar angle values compared to actual dynamic lumbar angle values for polynomial static population model applied to the openness angles of the entire dynamic data group

Dynamic data predicting static positions for the test population

The linear model developed from the dynamic population was $\alpha = 0.84\theta - 63.6$, where α is the lumbar angle and θ is the openness angle. This model was developed by finding the best fit regression line for all of the dynamic data and can be seen graphically in Figure 25.

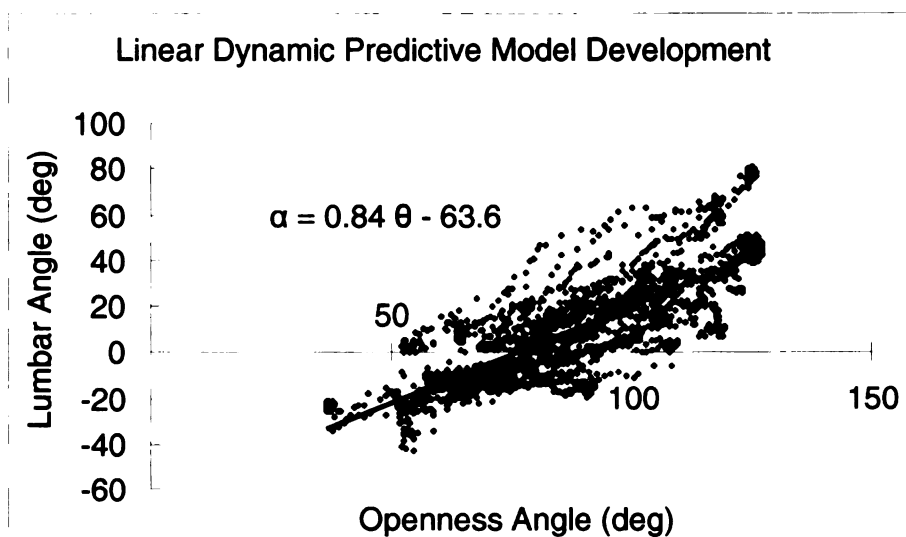


Figure 25. Graphical representation of linear population predictive model developed from all of the dynamic openness and lumbar angle data

Figure 26 shows both the actual data from the static population and the predicted values for the same openness angles that were determined by applying the model developed by the dynamic population.

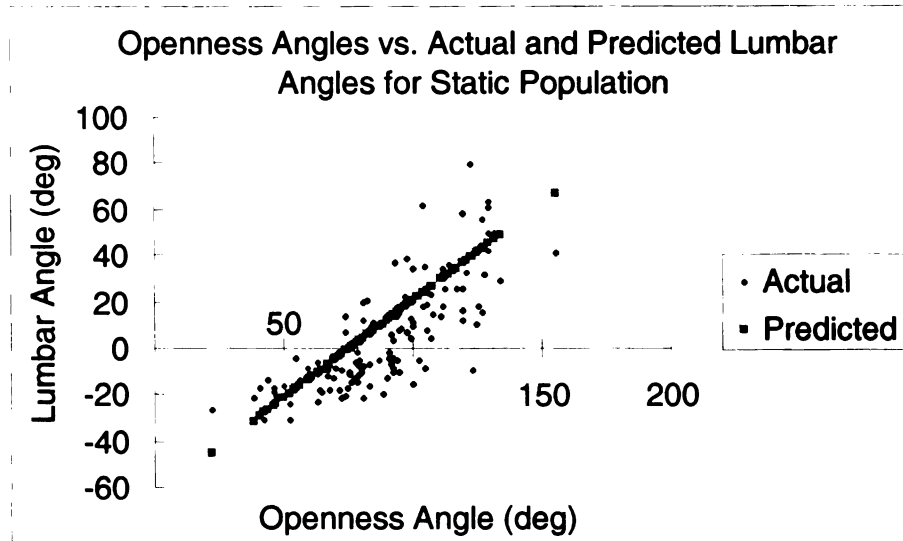


Figure 26. Predicted static lumbar angle values compared to actual static lumbar angle values for linear dynamic population model applied to the openness angles of the entire static data group

Comparing the lumbar angles predicted from the linear model and actual lumbar angles seen in Figure 26 with a paired t-test, the p-value was found to be less than 0.0001.

The second order polynomial model developed from the dynamic population, seen in Figure 27, was found to be $\alpha = 0.007\theta^2 - 0.421\theta - 12.8$, where α is the lumbar angle and θ is the openness angle.

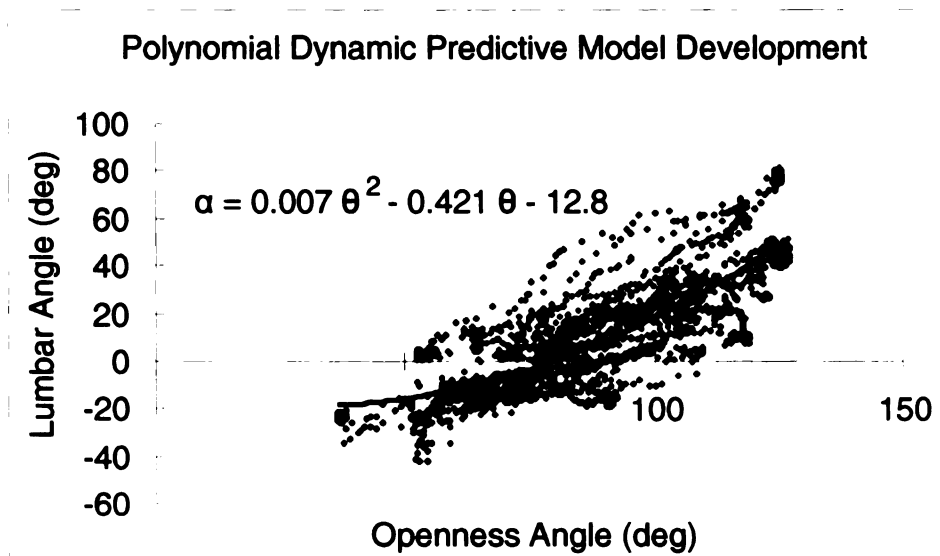


Figure 27. Graphical representation of polynomial population predictive model developed from all of the dynamic openness and lumbar angle data

When this polynomial model, derived from the dynamic population, was applied to the static population, the predicted values seen in Figure 28 were found. Also shown in Figure 28 are the actual values of lumbar angles for each corresponding openness angle.

The p-value for a paired t-test comparison between the polynomial predicted lumbar angles and the actual lumbar angles for the static population was found to be less than 0.0001.

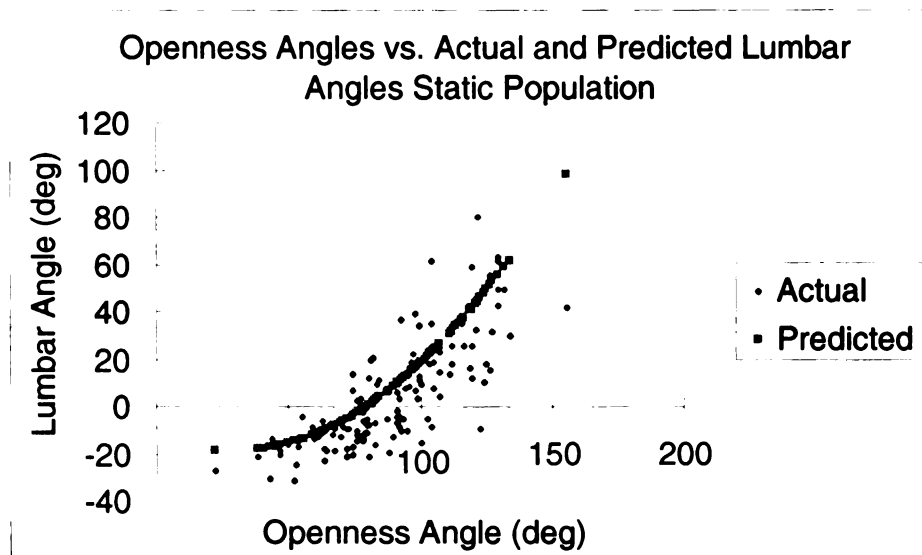


Figure 28. Predicted static lumbar angle values compared to actual static lumbar angle values for polynomial dynamic population model applied to the openness angles of the entire static data group

Static data predicting dynamic positions within a subject

The p-values associated with comparing actual dynamic lumbar angle and predicted dynamic lumbar angle from the linear and polynomial models derived from each subject's static data using a paired t-test can be seen in Table 11.

Table 11. Paired t-test values comparing predicted dynamic lumbar angles vs. actual lumbar angles for a prediction model based off the same subject's static data

	Paired T-Test Probability	
	Linear	Polynomial
S01	<0.0001	<0.0001
S04	<0.0001	<0.0001
S08	<0.0001	<0.0001
S10	<0.0001	<0.0001
S11	<0.0001	<0.0001
S12	<0.0001	<0.0001
S13	<0.0001	<0.0001
S17	<0.0001	<0.0001
S18	<0.0001	0.132
S19	<0.0001	<0.0001
S21	<0.0001	<0.0001
S23	<0.0001	<0.0001
S26	0.135	0.164
S28	<0.0001	<0.0001
S30	<0.0001	<0.0001

Note that the only instances where the p-value is above 0.0001 are in the linear and polynomial models for subject S26 and the polynomial model for subject S18.

Dynamic data predicting static positions within a subject

The p-values associated with comparing actual static lumbar angles and predicted static lumbar angles from the linear and polynomial models derived from each subject's dynamic data using a paired t-test can be seen in Table 12.

Table 12. Paired t-test values comparing predicted static lumbar angles vs. actual static lumbar angles for a subject prediction model based off of the same subject's dynamic data

	Paired T-Test Probability	
	Linear	Polynomial
S01	0.096	0.002
S04	0.410	0.405
S08	0.126	0.055
S10	0.294	0.246
S11	0.466	0.592
S12	0.073	0.072
S13	0.856	0.519
S17	0.561	0.540
S18	0.211	0.174
S19	0.894	0.215
S21	0.282	0.345
S23	0.290	0.392
S26	0.632	0.672
S28	0.069	0.377
S30	0.494	0.465

Note that only subject S01 in the polynomial model shows a p-value less than 0.01.

DISCUSSION AND CONCLUSIONS

A methodology was developed to quantify and measure the curvature of the lumbar spine during seated postural changes. Additionally, the relationships between lumbar curvature changes and changes in the relative rotations of the ribcage and pelvis were evaluated. These lumbar curvature and openness measurements were made in static and dynamic postures, and the relationships between them were evaluated using both linear and second-order polynomial models. These data and models were then evaluated statistically to determine significance and predictive capacity. The goal was to establish a reliable methodology that could be used to predict lumbar curvature of an individual while his/her back was obscured by a seatback for use in seat validation research and seat design.

Openness and Lumbar Angles

Table 4 shows the static openness angles for each subject in each position along with the total range of motion for each subject. From these data it was observed that the openness angles varied with each position. In general, the trend was for the largest openness angle to occur in the maximum lordotic posture, while the smallest openness angle occurred at a maximum kyphotic posture. Physically, this matched intuition, because in a lordotic posture, the top of thorax rotated in the posterior direction while the pelvis rotated in the opposite direction. Given the vector directions applied in defining the openness angle, this resulted in a larger angle. The opposite was also true; for a kyphotic posture the top of the thorax rotated forward, while the top of the pelvis rotated

rearward. This brought the thorax and pelvis vectors closer to parallel with each other, meaning the openness angle was smaller.

The total ranges of motion as measured by the openness angle were also noted. All of the subjects were able to produce a minimum range of 24 degrees between their maximum lordotic and maximum kyphotic positions. The average range of motion as measured by the openness angle was 53 degrees. This means that the ranges of openness angles well above the error for the system (0.38 degree) and provided adequately large range within which a relationship could be determined.

Examination of the static lumbar angles seen in Table 5 yielded similar results to the observations found with openness angles. The trend for the lumbar angles was for the largest angle to occur at the maximum lordotic posture, while the smallest angle occurred at the maximum kyphotic posture. This too made intuitive sense as the largest lumbar angles would occur when the most eccentric lumbar marker was the farthest anterior. As defined, this was positive. Movement through a “straight back” alignment of the markers produced a very small angle, and when the most eccentric marker was posterior, as was the case in kyphotic postures, the angle was negative.

In terms of total ranges of motion, as measured by the static lumbar angles, the average range of motion was 41 degrees, while the smallest range of motion was 5.8 degrees. While not as large as the ranges for the openness angle, these values were still above the thresholds of the error of the system, and supplied a sufficient range to evaluate any relationships that existed between openness and lumbar angles.

Table 6 shows the range values for the dynamic motions. As measured by the openness angle, the average dynamic range of motion was from 62 degrees to 110

degrees for a total range of 48 degrees. These values covered a similar range as the static data seen in Table 4 (61 degrees to 114 degrees, total range of 53 degrees). Similarly, the dynamic lumbar angles ranged from -13 degrees to 33 degrees for a total range of 46 degrees, which covered a similar range as the static lumbar angle range seen in Table 5 (-16 degrees to 25 degrees, total range of 41degrees). These similarities showed that the static postures were encompassing the same range of data as the dynamic motion data.

Distinct Static Positions

The data in Table 7 show low paired t-test scores ($p < 0.001$) when each position was compared to every other position as measured by both the openness angle and the lumbar angle. This meant that both measures, openness and lumbar angle, independently distinguished the four different postures, ranging from lordosis to kyphosis, in a seated position.

This information was the basis on which all subsequent data was founded and was therefore important to note. Had the positions been indistinguishable from one another using the given measures, then comparisons between these positions would not have been appropriate. However, since the openness angle distinguished postures based on anterior markers and the lumbar angle distinguished postures as measured at the lumbar spine, it was reasonable to pursue establishing a relationship between the two measures across positions.

Observations between openness and lumbar angles

Static

From the data presented in Figure 1 and summarized in Table 8, it was seen that plotting lumbar angle vs. openness angle for the static positions produced a relationship that was well approximated by both a linear relationship (average $r^2=0.829$) and a second-order polynomial relationship (average $r^2=0.935$).

Upon further inspection, it was seen that the disparity between the two average r^2 values was mainly attributed to a few subjects. The majority of the subjects displayed approximately the same r^2 value for both the linear fit and the polynomial fit, but subjects S11, S15, S18, and S20 all had linear r^2 values at least 0.25 less than the corresponding polynomial r^2 values. This apparent jump in fit values was explained by the relatively low number of data points in the static models. Mathematically, two points are required to quantify a line, three points can quantify a second-order polynomial, and four points can be fit to a third-order polynomial. When this is understood in how well a best fit line is approximating the data, it becomes much easier to have a second-order polynomial closely fit 3 points and have a small error on the fourth, than it is to have a linear model very closely fit all four points. This can also be inferred visually by observing the individual plots. Additionally, by viewing Figure 9(a-ee), it was seen that in most cases, the polynomial fit did not differ drastically when compared to the linear fit.

It should also be noted from Table 8, and visually from Figure 10, the general trend of the static position slopes of the best fit lines was positive. This meant that as the openness angle grew larger, i.e. moving from maximum kyphotic to maximum lordotic,

the lumbar angle also grew larger. Physically, this correlated to a situation where the top of the ribcage tilted rearward with respect to the pelvis and the lumbar spine accommodated this motion by moving from a kyphotic to lordotic posture.

The y-intercepts of the models had no discernable physical meaning. This was ascertained by investigating how the choices of the orientations of the ribcage and pelvis vectors that form the openness angle affected the overall openness/lumbar relationship. The ribcage and pelvis vectors were chosen because they simply rode along with each “rigid” body. It would have also been possible to choose any two other sagittal vectors that rode with the ribcage and pelvis. For example, the ribcage vector could have been chosen in the opposite direction, originating at the C7 marker and passing through the sternum. The only changes that would have occurred in the data would have been a 180 degrees shift in the openness angle and a shift in the intercept of the linear model. The slope would have remained the same because it would still be calculated as the change in lumbar angle over the change in openness angle. Once this was established it was possible to see that one is not limited to using only the vectors chosen in this study, but any sagittal vectors that ride with the ribcage and pelvis.

This observation also could become useful in practice, in that the ribcage vector could be chosen such that all of the required markers were on the anterior region of the subject. In the current configuration, the C7 marker was used because of the ease of consistent placement on the subject, but it also had potential drawbacks. For instance, with subjects who had long hair, the hair had a tendency to fall down over the C7 marker which obscured it from the cameras, leading to inconsistent data collection. In future studies this marker placement could also be obscured in practice if a chair had an

exceptionally tall seatback. While these situations are preventable with hair ties and smaller chairs, it could be beneficial for ease of data collection to move the entire ribcage vector to markers on the sternum of the subject, with the only change in results being an offset in the openness angles.

Dynamic

The same trends that were visible in the static data existed for the dynamic data. As seen in Figure 11 (a-o) and Table 9, the average r^2 values from the dynamic measurements were 0.841 for the linear model and 0.875 for the second-order model. This again meant that both models fit the data well. However, for the dynamic data a smaller difference between the linear and polynomial r^2 fits was measured. As can be seen in Figure 11 (a-o) this can be attributed to the fact that the two models nearly overlapped each other for most subjects. Thus, the conclusion was drawn that the added complexity of the second order model was not necessary and a simpler linear model would have sufficed.

Also similar to the static posture data, all of the linear slopes were positive but one. The same subject, S18, showed the only negative slope. Though it appeared out of the norm for the rest of the data collected, it was consistent across the two different types of testing. This showed a consistency in measurement that indicated that the openness/lumbar angle models being produced could have been subject specific.

On a per subject basis, Figure 12 (a-o) shows the static and dynamic data. From this, it was possible to see that in most cases, the static and dynamic data for each subject overlaid each other. While the ranges did not always match up precisely, it was possible

to see that a slope drawn for the static data would be similar to a slope drawn for the dynamic data. Further discussion of this visual observation is provided in the upcoming “Predictive Capacity” section.

Anthropometric Measures Related to Slope

The data in Table 10 showed low values for the Pearson Product Moment Correlation Coefficient. This meant that the anthropometric measures had low correlation with the relationship between the openness angles and lumbar angles. For a significance level of 0.05, the anthropometric measures did not produce a correlation coefficient that was of a critical level for the static data. In the dynamic data, only seated height and pelvic depth had correlation coefficients that reached the critical level at a significance of 0.05. This meant that seated height and pelvic depth could have an influence on the dynamic slope, but it was still not a strong possibility. At a significance level of 0.01, the critical value for 15 subjects was 0.641 [44] which no correlation values reached. This independence of correlation with the anthropometric measures meant that the linear relationship could be determined solely from the openness and lumbar angles.

Predictive Capacity

The similarities between the static posture data and dynamic data, without any dependence on anthropometric data, lead to testing of the predictive capability of each group. First, four cases for the entire test population will be discussed, followed by two cases of individual subject data.

Static data predicting static positions for the test population

The high p-value associated with the comparison between the predicted values and the actual values for the static positions indicated that the two groups were not statistically different. That meant that the first group produced a model that when applied to the second group produced results that were statistically indistinguishable from the actual values. This meant that given a group of sample individuals, a singular linear model could be developed that could predict lumbar angles of a separate population based solely off of measured openness angles.

This demonstrated that the approach of measuring the relative motion between the thorax and pelvis was a viable method for predicting lumbar curvature. This approach then has the potential to be used in a seating research environment where only openness angles are calculated to infer the lumbar curvature of the seated individual in static postures. It should be noted, though, that was on a population basis, and required that a population of subjects had been sampled, not just a single subject.

Dynamic data predicting dynamic positions for the test population

The dynamic to dynamic predictive modeling did not show the same results. The low p-value obtained through the paired t-test for this test condition indicated that the model and test pool were not from the same group. This meant that the dynamically determined linear models did not produce a total model that would predict with any certainty known lumbar angles given the openness angles of the second group. It is possible that this was because of the high number data points available. Thus a linear fit

would not have been able to quantify the dispersion of the points, due to variation. It is also possible that each subject had a specific profile that was not well captured by a total linear model.

Static data predicting dynamic positions for the test population

The low p-values ($p < 0.0001$) indicated that the actual lumbar angles and lumbar angles predicted from the static population model for the dynamic movements were statistically different. This meant that a model developed from a population of subjects in static postures should not be used to infer a population of dynamic lumbar angle movements.

Dynamic data predicting static positions for the test population

The low p-values ($p < 0.0001$) indicated that the actual lumbar angles and lumbar angles predicted from the dynamic population model for the static positions were statistically different. Just as one should not predict a dynamic population from a static population, this shows that a dynamic population model should not be used to infer static lumbar angles for a population.

For both the dynamic to static population prediction modeling and the static to dynamic population prediction modeling, it was expected that the significance in prediction power was lost when such a large and varied population was sampled. While almost all of the subjects displayed a positive trend in their individual relationship between openness angle and lumbar angle, the distinct nature of each of those relationships was lost when viewed as a total population. The result, as seen in Figure

21-Figure 28, was a broad collection of data points less focused around a single trajectory. This, in turn, could have been a factor that diminished the predictive capacity of each of the models.

Static data predicting dynamic positions within a subject

The data in Table 11, drawn from subject by subject linear and polynomial static to dynamic prediction models, showed p-values that indicated that the predicted values of lumbar angle in a dynamic environment based off of a subject's static model were statistically different from the actual lumbar angle values. Therefore, this method of prediction of the lumbar angle was not consistent enough to be used reliably.

This was in contrast to what was previously observed in Figure 12 (a-o). Though the static and dynamic data appeared to produce similar models, statistically, this direction of prediction was insufficient. This could have come from any of several reasons.

The mismatch could have been due to differences in the forces required to produce static postures as opposed to dynamic movement. Basic dynamics show that forces on an object in motion are different from the forces on the same object in static equilibrium. In the human body, this takes on an even greater meaning as those forces have to be generated by many different groups of muscles and interactions between many rigid bodies. The muscles used and distribution of forces in the static postures could have been very different from those used in the dynamic motions, which would explain the different openness and lumbar angles.

Another explanation could be that the statistical method for determining the value of the prediction was too strict. In the current models, the lumbar angle predictions laid on distinct trajectories. This amplified every difference between the predicted and actual values. For this reason, it is suggested that in future research broader prediction models be explored.

The discrepancies between the prediction models and actual data could have also been a result of people not moving through one specific trajectory when moving from lordotic to kyphotic positions and vice versa. As seen most prominently in Figure 12 for subjects S11 and S23 the dynamic trajectory appeared to form a loop. This implied that there were multiple lumbar angles for each openness angle. A single linear or polynomial model was not sufficient to capture that phenomenon.

Additionally, it would have been advantageous to have multiple sets of static and dynamic data for each subject. These could have been used to determine repeatability and test prediction models developed from one dynamic data set and applied to another dynamic data set from the same individual.

Dynamic data predicting static positions within a subject

The p-values associated with dynamic data predicting the static data within subject tell can be seen in Table 12. The only predicted values that were statistically different than the actual static lumbar angle values with a p-value less than 0.01 were the polynomial model values for subject S01. All other predicted values were not deemed to be statistically different. In practice, this means that a model based off of a dynamic “calibration” taken while the subject was seated in a backless chair could be used to

predict static lumbar angles for the same subject. With this established, it is possible to pursue such applications as predicting lumbar angles while a subject is seated in a chair with a back. Then the lumbar angles of static postures of maximum lordotic, maximum kyphotic, “straight and tall”, and “comfortable” could be compared to similar measures in seatbacks to determine how well a chair fits each user.

A summary of the prediction methods can be seen in Table 13. It should be noted that the static to static population prediction model and the dynamic to static within subject prediction model produced statistically indistinguishable predicted lumbar angles when compared to the actual lumbar angles.

Table 13. Prediction methods summary table

Prediction Model		Statistically Significant	p-value	
Static to Static	Population	No	0.969	0.827
	Individual	Insufficient Data	-----	-----
Dynamic to Dynamic	Population	Yes	<0.0001	<0.0001
	Individual	Insufficient Data	-----	-----
Dynamic to Static	Population	Yes	<0.0001	<0.0001
	Individual	No	see Table 11	
Static to Dynamic	Population	Yes	<0.0001	<0.0001
	Individual	Yes	see Table 12	

Summary of findings

From this research the primary findings of the work are stated as follows:

- Four distinct static postures can be identified by means of openness angle and the lumbar angle.
- The ranges of motion for the static postures covered the same ranges of motion as the dynamic motions as measured by both the openness and lumbar angles.

- In both static postures and dynamic motions, the relationships between openness angle and lumbar angle were positive.
- In both static postures and dynamic motions, the relationships between openness angle and lumbar angle were well defined by both linear and second-order polynomial models.
- It was possible to predict the relationship between openness and lumbar angles for a group of subjects in static seated postures based upon a model developed from a similar group of subjects seated in the same static seated postures.
- It was possible to predict the relationship between openness and lumbar angles experienced in static seated postures for a single subject based upon a linear or polynomial model determined from the same subject's dynamic motion.

In a broader sense, these results lead to two overarching outcomes. The first was that a methodology was successfully developed to quantify seated lumbar curvatures using a 3D motion capture system. The lumbar curvatures were then successfully related to visible bony landmarks on the anterior portion of the body. This is valuable because the curvature quantification can be used to inform seat designs with lumbar supports that can match lumbar curvatures of seated occupants. The data collected from this methodology also showed that it was feasible to predict postural change of individuals by monitoring the positions of the pelvis and ribcage. This is valuable in the area of seating evaluation where it is necessary to know the curvature of the lumbar region of the back while it is obscured from direct measurement.

Relation to published research

These findings fill a void in the research of seated human movement and dynamic lumbar movement. Based upon a review of the literature, studies reporting seated lumbar postural change and its quantification are limited. Several researchers [33, 14, 19, 37] have addressed changes in the lordotic curvature while standing; however these measurements used landmarks on the posterior portion of the body. The approaches presented by Ng et al. [33], Choi et al. [14], and Lee and Wong [37] would not be possible in the seated position while the occupant's back was obscured by a seatback. Thus, the methodology and associated data from the research reported in this thesis represent a new basis for the quantification of the contour of the lumbar region of the back and its relationship to the relative angular displacement between the ribcage and pelvis.

The novel nature of this research means that comparisons to other methods were difficult. Methods in previous research relied upon the precise tracking of each vertebra by means of radiographs, such as those presented by Frobin et al. [27], Harrison et al. [28], and Janik et al. [29], or by means of MRI's such as those presented by Hedman and Fernie [31], and Karadimas et al. [32] while the method developed for this thesis relied on measuring the surface contour of the lumbar region as a whole. The reason for this was that a lumbar support, which is an integral part of the seat design, will not directly support each vertebra, but rather would provide support to the entire region during postural changes. Therefore, it was not necessary to know the exact position of each vertebra, but rather the changes in contour of the entire lumbar region. This emphasis on

developing a practical method for the seated position limited the comparisons to previous research.

The need to quantify curvatures dynamically as people changed spinal curvature also meant that the use of radiographs or MRI's was not possible. Consequently, comparisons between the static results of the previous work by Frobin et al., Harrison et al., Janik et al., Hedman and Fernie, and Karadimas et al. and the results presented in this thesis were not appropriate. The method developed as part of this thesis provides a unique means to measure the lumbar contour, as a whole, dynamically, for designing and validating modern seating.

However, in terms of ranges of back motions, although not identical to this thesis's research, the data from Walsh et al. provides a means for comparison. Walsh et al. quantified the movement of the angle formed by external markers located near the L4, T7 and C7 vertebrae. Walsh et al. found the range of motion to be approximately 10-35 degrees across their sample of 10 subjects. From the research for this thesis, the range of static openness was from 24.7-85.6 degrees and the range of static lumbar angles was 5.8-88.4 degrees. The larger ranges in the current study can be attributed to the extreme kyphotic and lordotic cases that were included in this study but not in Walsh's work. In addition, both Walsh and the work reported here found the range of motion to be subject specific (i.e. some individuals achieved the full range of motion while others achieved only a subset of that range). In a broad sense, all three measures can be considered as measures of the movement of the human back and their similarity is positive.

Low Back Pain, Chair Design and Dynamic Postural Change

The importance of a well designed seat is directly related to Low Back Pain (LBP). LBP is costly to society monetarily, as well as in lost work time, impaired work efficiency, and diminished quality of life. The costs come from worker's compensation claims, hospital costs, medication, community care and more [4,5]. The National Institute for Occupational Safety and Health estimated that LBP costs \$14 billion to American industry annually [6].

LBP comes from the extremes of back activity: either high back activity or low back activity. Low back activity comes from prolonged static postures. Particular to this research, LBP has been linked to extended periods of static seating [9]. This static seating occurs in automobile seating, office seating, and wheelchairs, amongst others.

To reduce LBP from prolonged static postures, dynamic postures should be encouraged. It has been shown that dynamic postures can decrease intervertebral disc degeneration over time [8]. It has also been shown that chairs that support dynamic postures are more likely to induce back movement throughout the day [7]. The question then becomes, "How do we design chairs that support dynamic postures?"

In terms of application to seatback design, the ranges of, and relationship between the dynamic openness angles and lumbar angles developed in this research can be used to design chairs that will support a wide range of positions. For most people, the openness angle varies linearly between the maximum lordotic and maximum kyphotic curvatures meaning that the lumbar region of a chair can be designed such that the trajectory of the support curvature is linear between two maximums. Furthermore, the kinematic

orientation of the ribcage and pelvis could be used as the inputs that control the contour of the lumbar support. Then, instead of statically calibrating a chair's lumbar support for a single posture, a chair could be dynamically calibrated to the proper amount of lumbar support change for a given amount of ribcage and pelvis movement.

These findings can also be used to evaluate commercially available chairs and seats (e.g. car, trucks, busses, trains, airplanes; wheelchairs) for how well the motion of the seatback matches the motion of the occupants which then can be related to the support provided by the chair. Objective evaluations can serve the purpose of distinguishing chairs from one another in terms of promoting dynamic postures and confirming claims made by manufacturers regarding seat back movement. Chairs that do not support a wide range of postures for an array of anthropometries can be objectively identified.

To summarize, the methods and knowledge of dynamic human lumbar contours developed from this research will support informed design and evaluation of chairs in a broad range of applications, from office and automotive seating to design of seating for the disabled, and thus have potential for tremendous societal impact.

APPENDIX

A1. Subject Questionnaire

Lifestyle Questionnaire

Please be as thorough and accurate as possible when answering the following questions. If anything is unclear, please ask the test administrator for clarification on the day of testing.

1. What is your current age? _____ yrs. height _____ ft. _____ in. ,
weight _____ lbs. Male Female (circle one)

2. Are you currently under medical care? Yes _____, No _____

Explain: _____

3. Have you been injured recently in the hand/wrist/ elbow/arm or back region?

Yes _____ No _____

How long ago? _____

Is it a reoccurring pain/injury? _____ If so, how often?

Are you under current treatment for this condition? Yes _____ No _____

Has this condition impaired your daily activities? Yes _____ No _____

Explain: _____

4. Have you experienced any back or neck pain today? Yes _____, No _____

Do you know the cause? _____

5. Are you currently taking any pain medications?

Yes _____, No _____

If so, which medication(s)

What are the medications

for? _____

A1 (cont.).

6. Are you right_____ or left _____ handed?

7. What is your occupation?

8. Daily, how many hours would you say you are seated at a computer?

9. During the time you work at a computer, please estimate the % of time you:

_____ use the keyboard

-----use a mouse or similar device

-----just studying the screen

(Percentages should add up to 100)) Example: 40% keyboard, 30% mouse, 30% screen)

10. Do you know what type of office chair you currently have?

11. Do you use your armrests when you mouse? Yes No if so, describe

12. Are you pregnant? Yes ____No ____

(If the subject is pregnant, she may be excused from the testing.)

A2. Individual Subject Measurements

Subject	Height (in.)	Weight (lb)	Age (y.o.)	Sex	Hand	Seated				
						Seated Height	B. Width	Pelvic Width	Pelvic Height	Pelvic Depth
						(in.)	(cm)	(cm)	(cm)	(cm)
S01	173	810	24	M	R	85.1	39.5	23.0	7.0	15.5
S02	180	867	25	M	R	91.4	34.5	23.0	10.0	12.5
S03	163	534	26	F	R	83.8	35.0	20.0	7.5	12.5
S04	160	534	22	F	R	86.4	38.5	24.0	7.0	15.5
S05	161	494	22	F	R	87.6	30.5	25.5	5.5	12.0
S06	165	663	22	M	R	86.4	35.0	22.5	12.5	14.0
S07	175	636	20	M	R	91.4	34.0	25.0	12.0	14.5
S08	168	569	20	F	R	85.1	35.5	28.0	10.5	13.5
S09	175	703	23	F	R	88.9	38.5	25.5	10.0	17.0
S10	152	494	23	F	R	81.3	38.0	25.0	7.0	13.5
S11	150	400	23	F	R	73.7	33.5	21.0	6.5	11.5
S12	159	543	23	F	R	82.6	38.5	24.5	6.0	15.5
S13	170	605	24	F	R	86.4	35.5	22.5	7.5	15.0
S14	163	814	26	F	R	86.4	46.0	26.0	6.0	19.5
S15	171	609	20	M	R	86.4	34.0	22.5	10.5	15.5
S16	174	721	23	M	R	86.4	39.0	23.5	7.5	18.0
S17	156	609	20	F	R	82.6	36.0	21.5	6.5	16.0
S18	150	489	24	F	R	74.9	34.0	22.5	7.5	12.5
S19	150	485	24	F	R	73.7	34.5	21.0	8.0	12.5
S20	184	867	25	M	R	94.0	38.0	21.5	7.5	15.5
S21	163	552	23	F	R	86.4	37.0	22.5	8.5	15.5
S22	185	899	25	M	R	91.4	41.0	25.5	9.5	17.0
S23	169	676	26	F	R	87.6	41.5	22.0	8.0	16.5
S24	154	494	21	F	R	81.3	38.5	21.0	8.5	15.0
S25	177	689	23	M	R	86.4	38.0	22.5	10.0	15.5
S26	177	836	25	M	L	91.4	39.5	20.5	7.5	16.5
S27	173	623	24	M	R	87.6	38.0	21.5	7.0	16.0
S28	183	712	24	M	L	91.4	35.5	25.5	10.0	14.0
S29	177	867	27	M	R	88.9	38.5	24.5	8.0	18.0
S30	179	1001	24	M	R	91.4	44.0	24.5	10.0	17.0
S31	179	770	25	M	L	88.9	38.5	24.0	10.0	15.5
Min	150	400	20			73.7	30.5	20.0	5.5	11.5
Max	185	1001	27			94.0	46.0	28.0	12.5	19.5
Average	168	663	23.4			86.0	37.4	23.3	8.4	15.1
SD	10.8	151	1.89			5.09	3.19	1.91	1.78	1.93

A3. Calibration Measurements

Calibration measurements were made on two separate days to ensure accuracy of motion tracking system. The first table shows length measurements of 3 different wands with tracking markers on the each end. They are named by the measurement made by hand.

		Individual Tracking (mm)			3 Wands at Once (mm)		
		157mm	173mm	176mm	157mm	173mm	176mm
Day 1	Average	157.21	173.60	176.01	156.84	173.80	176.56
	S.D.	0.878	0.311	1.640	0.523	0.387	0.574
Day 2	Average	157.35	173.80	176.50	156.98	173.88	176.65
	S.D.	0.741	0.301	0.341	0.808	0.554	0.362

The next two tables show length and angle calculations for two calibration triangles. These consisted of a solid piece of wood with 3 markers affixed at fixed distances and angles from one another. For all data shown here, lengths are measured in millimeters and angles are measured in degrees.

		Small Triangle					
		Length AB (mm)	Length BC (mm)	Length CA (mm)	Angle ABC (deg)	Angle BCA (deg)	Angle CAB (deg)
Day 1	Average	171.23	243.42	172.00	44.96	44.70	90.34
	S.D.	0.903	1.061	0.896	0.340	0.218	0.339
Day 2	Average	171.19	243.50	172.31	44.67	45.04	90.29
	S.D.	0.946	0.901	0.726	0.246	0.298	0.381

		Big Triangle					
		Length AB (mm)	Length BC (mm)	Length CA (mm)	Angle ABC (deg)	Angle BCA (deg)	Angle CAB (deg)
Day 1	Average	410.25	428.46	469.51	68.04	54.14	57.82
	S.D.	0.561	0.715	0.670	0.118	0.098	0.126
Day 2	Average	410.60	428.46	469.68	68.04	54.17	57.79
	S.D.	0.634	0.578	0.506	0.094	0.094	0.098

A4. Lumbar radius calculation

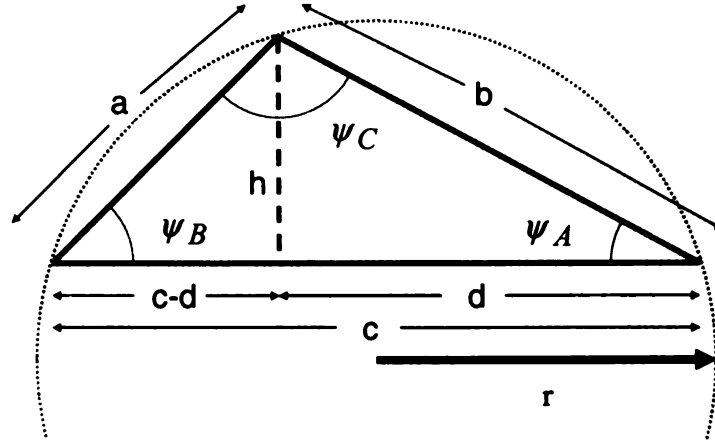


Figure 29. Diagram for radius calculation

Given a triangle with sides of arbitrary lengths a , b , and c , as seen in Figure 29, it is possible to draw a line perpendicular to side c that will give the height of the triangle, which will be called h . The triangle is now divided into two different right triangles with height h , and base lengths d and $c-d$. Using this, and Pythagorean's Theorem, it is possible to solve both triangles for h^2 as seen in equations 12 and 13.

$$h^2 = b^2 - d^2 \quad (12)$$

$$h^2 = a^2 - (c-d)^2 \quad (13)$$

Setting these two equations equal to one another allows for solving of length d in terms of the known quantities a , b , and c , seen in equation 14.

$$d = \frac{-a^2 + b^2 + c^2}{2c} \quad (14)$$

A4 (cont.).

Once d is known, it can be entered back into equation 12 such that h can be solved for in the following manner, seen as equations 15-18.

$$h^2 = b^2 - \left(\frac{-a^2 + b^2 + c^2}{2c} \right)^2 \quad (15)$$

$$h^2 = b^2 - \left(\frac{a^4 + b^4 + c^4 - 2a^2b^2 - 2a^2c^2 + 2b^2c^2}{4c^2} \right) \quad (16)$$

$$h^2 = \frac{-a^4 - b^4 - c^4 + 2a^2b^2 + 2a^2c^2 + 2b^2c^2}{4c^2} \quad (17)$$

$$h = \frac{1}{2} \sqrt{\frac{-a^4 - b^4 - c^4 + 2a^2b^2 + 2a^2c^2 + 2b^2c^2}{c^2}} \quad (18)$$

Once h is described in terms of the known values, a, b, and c, the area of the triangle can be found by using the equations 19-21.

$$A = \frac{1}{2} (base)(height) = \frac{1}{2} ch \quad (19)$$

$$A = \frac{1}{2} c \left(\frac{1}{2} \sqrt{\frac{-a^4 - b^4 - c^4 + 2a^2b^2 + 2a^2c^2 + 2b^2c^2}{c^2}} \right) \quad (20)$$

$$A = \frac{1}{4} \sqrt{-a^4 - b^4 - c^4 + 2a^2b^2 + 2a^2c^2 + 2b^2c^2} \quad (21)$$

A4 (cont.).

Equation 21 is commonly known as Heron's formula, which gives the area of a triangle given the lengths of each of the sides of the triangle. Alternative forms of Heron's formula are shown in equations 22 and 23.

$$A = \frac{1}{4} \sqrt{(a^2 + b^2 + c^2)^2 - 2(a^4 + b^4 + c^4)} \quad (22)$$

$$A = \frac{1}{4} \sqrt{(a+b+c)(a+b-c)(a-b+c)(-a+b+c)} \quad (23)$$

Another method to solve for the area of the triangle is to use equation 24.

$$A = \frac{1}{2} ab \sin \psi_C \quad (24)$$

The Law of Sines states:

$$\frac{a}{\sin \psi_A} = \frac{b}{\sin \psi_B} = \frac{c}{\sin \psi_C} = 2r \quad (25)$$

Equations 22, 24, and 25 can then be combined to solve for r in terms of the known lengths a, b, and c shown as equations 26-28.

$$A = \frac{1}{2} ab \left(\frac{c}{2r} \right) \quad (26)$$

A4 (cont.).

$$r = \frac{1}{4} \frac{abc}{A} \quad (27)$$

$$r = \frac{abc}{\sqrt{(a+b+c)(a+b-c)(a-b+c)(-a+b+c)}} \quad (28)$$

A5. Dynamic Openness and Lumbar Angles (deg)

S01												
θ	α	θ	α	θ	α	θ	α	θ	α	θ	α	
83.8	-3.3	96.3	5.1	100.6	7.4	99.6	5.2	86.6	-1.2	76.8	-5.4	
83.9	-3.4	96.8	4.7	100.8	7.1	99.5	3.5	86.2	-1.1	76.7	-4.7	
83.9	-3.2	97.0	3.4	101.0	7.8	99.3	3.0	85.7	-1.2	76.6	-2.7	
84.2	-4.1	97.3	3.4	101.1	7.6	99.4	2.9	85.0	-1.0	76.7	-4.8	
84.4	-3.9	97.6	4.4	101.2	7.0	99.0	3.8	84.3	-0.5	76.6	-3.3	
84.6	-3.0	97.7	6.1	101.2	7.3	98.6	3.9	84.1	-3.0	76.5	-2.9	
84.9	-2.9	97.9	4.5	101.2	6.9	98.2	3.3	83.7	-2.7	76.5	-4.0	
85.1	-2.6	98.0	3.7	101.3	6.9	98.1	3.0	83.2	-2.0	76.5	-4.4	
85.5	-2.0	98.1	4.4	101.2	5.5	97.6	3.2	82.8	-2.3	76.6	-4.5	
85.9	-1.3	98.2	4.4	101.1	6.6	97.1	3.4	82.6	-2.2	76.6	-4.4	
86.1	-1.3	98.3	3.7	101.0	5.9	96.7	3.4	82.4	-2.4	76.6	-4.5	
86.5	-1.4	98.5	3.5	101.0	5.4	96.1	3.0	82.0	-2.6	76.5	-4.6	
86.9	-1.8	98.6	3.6	100.9	7.1	95.6	3.1	81.8	-2.7	76.6	-4.3	
87.1	-1.4	98.8	5.8	100.8	6.3	95.0	2.6	81.4	-2.7	76.5	-4.0	
87.5	-3.0	98.9	3.6	100.7	6.4	94.4	1.9	81.1	-2.5	76.6	-4.5	
87.9	-3.4	99.0	3.6	100.6	5.9	93.7	2.5	81.0	-2.7	76.6	-4.5	
88.3	-3.0	99.2	5.0	100.6	5.6	93.3	-0.3	77.6	-3.1	76.6	-4.3	
88.5	-2.1	99.4	3.3	100.6	6.1	93.0	-0.3	77.5	-2.7	76.6	-4.5	
88.7	-2.2	99.5	5.3	100.6	7.0	92.7	1.4	77.3	-2.7	76.7	-4.6	
89.3	-0.7	99.7	6.0	100.6	6.9	92.3	0.4	77.3	-1.2	76.8	-4.5	
89.3	-0.9	100.0	7.0	100.6	6.9	91.8	0.6	77.2	-4.2	76.7	-4.6	
89.6	-0.5	100.4	7.1	100.6	5.9	91.6	2.5	77.2	-2.0	76.7	-4.7	
90.2	0.2	100.8	7.1	100.6	6.3	91.3	2.4	77.1	-5.0	76.7	-4.5	
90.4	1.0	101.0	6.1	100.6	6.3	91.0	2.5	77.0	-1.7	76.7	-4.6	
90.7	2.3	101.1	5.8	100.6	5.6	90.7	2.4	76.9	-0.8	76.7	-4.9	
91.2	1.5	101.2	6.8	100.5	6.4	90.3	1.1	76.8	-3.9	76.7	-4.7	
91.6	-0.1	101.4	6.4	100.5	6.7	89.8	0.2	76.7	-4.8	76.8	-5.4	
91.9	0.5	101.5	6.9	100.4	7.0	89.4	0.4	76.8	-3.6	76.8	-5.0	
92.1	0.7	101.5	8.5	100.6	6.4	89.1	0.7	76.7	-4.6	76.8	-3.0	
92.7	0.4	101.3	7.3	100.4	6.6	88.9	-0.1	76.8	-4.6	76.7	-5.2	
93.1	1.4	101.2	6.4	100.5	6.0	88.7	-1.0	76.8	-4.8	76.8	-4.5	
93.6	2.8	101.1	6.5	100.3	6.3	88.6	-0.8	76.8	-4.6	76.7	-4.4	
94.1	3.6	100.9	7.0	100.3	5.9	88.1	-0.1	76.8	-5.0	76.7	-4.5	
94.7	3.9	100.9	7.4	100.2	7.4	87.6	-0.7	76.7	-4.9	76.8	-4.3	
95.1	3.3	100.8	7.2	100.2	6.4	87.3	-2.2	76.7	-4.0	76.8	-4.0	
95.5	4.9	100.7	7.4	100.1	5.8	87.1	-1.7	76.7	-4.2	76.8	-4.2	
95.8	3.6	100.7	7.6	99.8	5.6	86.8	-1.6	76.7	-3.5	76.8	-3.9	

A5 (cont.).

S01	
θ	α
76.8	-4.6
76.8	-4.9
76.8	-5.4
76.8	-4.8
76.8	-5.0
76.8	-4.3
76.8	-4.3
76.8	-4.5
76.8	-4.3
76.8	-4.6
76.9	-4.7
76.9	-4.7
77.1	-5.2
77.2	-4.8
77.2	-4.3
77.2	-4.7
77.2	-4.2
77.3	-4.6
77.4	-4.8
77.5	-4.4
77.5	-4.9
77.5	-4.7
77.5	-3.1
77.6	-3.5
77.8	-6.2
78.0	-1.0
78.3	-4.6
78.5	-4.0
78.7	-4.2

A5 (cont.).

S04												
	θ	α	θ	α	θ	α	θ	α	θ	α	θ	α
	70.0	4.2	86.8	18.7	85.3	18.1	63.9	0.7	60.3	-5.6	74.2	9.2
	70.3	5.3	87.1	19.0	85.0	17.3	63.6	0.1	60.3	-4.9	74.4	7.6
	70.9	5.4	87.4	19.6	84.5	17.9	63.3	0.7	60.4	-4.6	74.6	8.9
	71.4	5.2	87.8	19.3	84.1	17.0	63.0	0.6	60.3	-4.4	74.8	9.2
	72.3	5.2	88.0	20.3	83.8	15.1	62.8	0.0	60.3	-4.4	75.1	9.6
	73.1	5.9	88.2	20.5	83.0	16.5	62.6	-3.1	60.3	-4.8	75.2	9.8
	73.8	5.1	88.3	20.0	82.2	14.4	62.4	-4.1	60.3	-5.2	75.2	7.3
	74.4	5.4	88.5	21.3	81.4	13.0	62.1	-6.1	60.5	-6.0	75.2	7.2
	75.5	6.9	88.7	21.5	80.4	11.5	61.8	-5.6	60.7	-5.6	75.2	7.4
	76.1	6.8	88.7	21.8	79.7	10.2	61.6	-5.3	60.8	-6.3	75.2	7.1
	77.0	11.5	88.9	21.0	79.0	11.4	61.1	-5.4	60.9	-5.6	75.1	7.2
	77.7	11.1	88.9	22.6	78.6	10.8	60.9	-5.8	61.1	-5.7	75.0	7.2
	78.5	7.7	89.0	21.4	78.0	11.2	60.8	-5.7	61.4	-7.0		
	79.2	10.0	89.1	22.6	77.3	11.1	60.5	-6.2	61.7	-7.9		
	80.1	11.0	89.2	23.8	76.5	11.7	60.5	-6.5	62.3	-6.0		
	80.8	11.3	89.4	23.4	75.9	11.0	60.4	-6.8	62.6	-6.2		
	81.5	12.0	89.6	25.0	75.2	11.4	60.4	-6.4	62.3	0.3		
	82.1	10.9	89.8	24.9	74.5	9.4	60.3	-6.4	62.5	-4.5		
	82.7	10.5	89.8	25.8	73.5	11.6	60.1	-6.4	62.9	-3.8		
	83.1	10.8	91.3	26.6	72.9	9.8	60.0	-6.8	63.4	-3.8		
	83.3	12.1	91.3	27.2	72.1	8.3	60.0	-6.9	63.8	-4.4		
	83.6	11.9	91.3	26.4	71.5	9.2	59.9	-6.7	64.1	-3.4		
	83.9	13.0	91.3	26.3	70.9	8.2	59.8	-6.3	64.4	-3.5		
	84.2	13.9	91.2	26.4	70.5	7.5	59.9	-5.9	64.8	2.3		
	84.5	15.5	91.3	26.5	70.1	7.5	59.9	-6.7	65.3	2.8		
	84.8	15.1	90.3	24.1	69.5	8.0	59.9	-6.2	66.1	2.3		
	85.0	14.6	89.9	23.3	69.0	6.5	60.0	-6.9	66.4	0.9		
	85.4	15.7	89.8	22.6	68.5	4.7	60.0	-7.2	66.7	1.5		
	85.5	14.7	89.5	22.2	68.2	4.0	60.0	-7.1	66.8	2.1		
	85.8	14.2	89.0	21.2	67.8	3.1	60.1	-7.5	72.8	5.8		
	86.0	15.3	88.5	21.0	67.2	5.4	60.1	-7.0	73.0	5.7		
	86.0	16.8	88.1	21.1	66.5	2.9	60.2	-5.8	73.3	6.7		
	86.2	17.0	87.4	21.7	65.8	2.8	60.2	-6.7	73.6	7.0		
	86.3	17.4	86.7	17.6	65.4	1.0	60.1	-6.4	73.7	6.9		
	86.4	16.5	86.5	17.6	65.1	-4.6	60.2	-5.6	73.9	7.1		
	86.4	17.9	86.0	17.8	64.6	0.8	60.2	-6.4	74.1	7.3		
	86.7	19.3	85.8	17.1	64.3	0.7	60.4	-5.8	74.1	7.1		

A5 (cont.).

S08										
θ	α	θ	α	θ	α	θ	α	θ	α	
87.3	4.8	101.6	28.7	102.3	30.3	95.1	17.1	61.4	-15.2	
87.3	4.9	101.6	29.0	102.3	30.1	94.0	16.3	60.8	-14.6	
87.4	4.6	101.7	29.6	102.3	30.3	93.1	12.7	60.4	-15.1	
87.4	4.6	101.7	29.7	102.2	31.7	92.0	12.9	59.8	-15.0	
87.4	4.8	101.9	28.0	102.3	32.6	91.1	14.0	59.3	-15.8	
87.6	7.6	102.0	30.0	102.3	31.8	89.9	6.5	59.1	-15.2	
87.9	5.0	102.1	28.1	102.3	31.5	88.7	10.8	58.7	-15.6	
88.6	11.1	102.2	30.0	102.3	32.8	87.8	6.5	58.4	-15.7	
89.0	8.9	102.2	30.8	102.5	33.5	86.7	8.1	57.9	-15.8	
89.4	5.5	102.3	30.2	102.3	32.3	85.4	5.0	57.7	-16.4	
89.8	5.2	102.3	28.2	102.4	31.9	84.2	2.3	57.1	-15.8	
90.3	6.3	102.3	30.3	102.4	31.0	83.1	1.5	56.9	-16.0	
90.6	6.5	102.3	30.7	102.4	31.5	82.0	4.0	56.7	-16.1	
91.1	7.9	102.3	30.3	102.5	31.3	81.2	4.4	56.7	-16.1	
91.5	8.2	102.3	30.2	102.4	31.1	80.0	6.3	56.5	-15.8	
92.0	7.2	102.2	30.7	102.4	31.4	79.0	0.5	56.5	-16.2	
92.2	7.7	102.2	30.1	102.4	31.4	77.9	2.6	56.4	-16.3	
92.8	10.9	102.2	30.0	102.4	31.3	76.8	0.6	56.3	-16.6	
93.7	12.3	102.3	30.6	102.3	31.7	76.0	1.6	56.3	-17.0	
94.1	10.4	102.1	29.6	102.4	32.8	75.0	-6.5	56.4	-15.8	
94.7	13.8	102.2	29.8	102.3	31.0	74.4	-7.5	56.5	-16.2	
95.3	15.8	102.1	30.6	102.4	31.7	73.5	-8.0	56.4	-16.0	
95.9	14.6	102.2	30.1	102.2	31.2	72.6	-8.4	56.4	-15.9	
96.3	15.4	102.2	27.7	102.2	30.9	71.7	-8.6	56.5	-16.1	
96.5	19.5	102.2	29.7	102.1	32.4	70.8	-9.9	56.7	-16.3	
96.7	18.0	102.1	28.7	101.9	32.8	69.9	-10.6	56.6	-16.3	
96.9	16.0	102.2	29.7	101.8	31.6	68.9	-12.1	56.6	-16.0	
97.2	17.7	102.1	29.0	101.7	31.8	67.9	-11.3	56.9	-16.4	
97.5	19.4	102.2	30.7	102.1	31.4	67.0	-11.1	57.2	-16.3	
98.2	21.1	102.1	30.7	101.1	30.6	66.2	-12.4	57.7	-15.6	
99.2	23.7	102.2	27.3	100.7	28.7	65.4	-13.1	58.1	-15.6	
99.9	24.2	102.2	30.7	100.4	27.2	64.9	-13.7	58.4	-15.8	
100.7	26.9	102.2	29.8	99.5	26.9	64.3	-14.2	58.5	-16.0	
101.1	27.8	102.2	30.3	98.7	24.3	63.7	-14.3	58.7	-16.3	
101.3	28.0	102.2	29.6	97.8	21.9	63.2	-14.7	58.6	-16.3	
101.4	29.1	102.2	29.7	96.9	20.7	62.5	-14.5	58.6	-17.0	
101.4	29.7	102.3	28.8	96.0	17.9	62.0	-14.8	58.6	-16.7	

A5 (cont.).

S08					
θ	α	θ	α	θ	α
58.6	-16.4	67.5	-12.9	89.0	8.0
58.5	-16.3	68.3	-12.9	89.5	8.6
58.5	-15.6	68.7	-14.0	90.0	10.6
58.6	-15.8	69.6	-12.8	90.3	8.0
58.7	-16.3	70.5	-12.4	90.7	8.8
58.8	-17.3	71.5	-10.8	91.0	9.7
58.7	-17.3	72.4	-10.1	91.3	8.6
58.8	-16.3	73.2	-8.0	91.7	8.9
59.1	-16.0	73.9	-7.5	92.0	10.3
59.1	-15.7	74.5	-12.2	92.5	15.2
59.2	-15.8	75.4	-7.1	92.6	15.7
59.3	-15.4	76.4	3.3	92.6	15.5
59.5	-15.8	77.4	-8.4	92.6	14.9
59.6	-15.9	78.2	1.7	92.2	9.5
59.7	-15.8	78.6	2.0	92.1	7.3
59.8	-15.3	78.7	2.0	92.0	11.0
59.8	-15.8	78.9	0.7	92.0	8.7
59.9	-16.0	79.2	1.0	92.0	11.3
60.0	-15.7	79.6	3.2		
60.0	-16.3	80.2	3.4		
60.1	-16.1	80.9	3.2		
60.2	-16.0	81.2	4.5		
60.3	-15.7	81.9	10.0		
60.5	-15.9	82.5	9.7		
60.7	-15.4	82.9	7.8		
61.2	-15.4	83.6	7.0		
61.6	-15.6	84.0	5.0		
62.3	-14.7	84.6	7.0		
62.6	-15.9	85.2	5.5		
63.1	-15.5	85.7	4.5		
63.9	-15.0	86.2	6.2		
64.4	-13.8	86.5	6.6		
64.9	-14.1	86.7	7.2		
65.4	-13.8	87.0	6.6		
65.8	-17.9	87.4	7.3		
66.2	-13.9	88.1	9.2		
66.7	-14.0	88.8	11.8		

A5 (cont.).

S10									
θ	α	θ	α	θ	α	θ	α	θ	α
87.7	7.8	124.4	46.8	123.3	48.3	75.0	19.8	79.7	21.8
88.1	8.7	124.4	45.3	123.0	48.0	74.9	18.4	76.8	20.6
88.4	7.9	124.4	47.1	122.8	48.7	75.1	21.0	77.8	22.5
88.8	7.2	124.5	48.0	122.6	47.3	74.8	17.9	79.1	21.8
89.6	7.9	124.5	48.7	122.0	47.5	78.3	19.8	80.6	21.7
90.5	12.4	124.4	47.7	121.5	47.3	78.0	19.2	81.8	22.8
91.8	12.4	124.3	48.3	120.9	46.5	77.7	19.3	83.2	27.2
93.0	13.8	124.3	48.9	120.2	45.7	77.6	19.8	84.6	27.9
94.5	14.3	124.2	47.8	119.5	44.9	77.5	19.6	86.0	26.3
96.1	18.5	124.1	48.7	118.7	42.3	77.5	20.5	87.1	27.4
97.7	20.6	124.1	48.7	117.7	42.4	77.5	18.7	88.3	27.3
99.2	24.2	124.1	48.5	116.4	40.6	77.5	18.3	89.5	28.0
101.3	23.0	124.1	50.8	114.2	41.2	77.5	19.4	90.7	28.0
103.4	24.3	124.0	49.8	111.9	35.5	77.3	18.6	91.9	29.2
105.1	28.1	124.0	48.6	109.8	35.8	77.4	16.0	93.1	30.4
106.8	28.8	123.9	50.1	107.1	32.2	77.3	16.0	94.1	31.6
108.8	34.9	123.9	50.6	104.6	31.7	77.3	16.4	95.3	28.8
110.3	33.2	123.8	50.6	102.0	33.1	77.4	15.4	96.0	32.3
111.7	31.7	123.8	50.0	98.9	25.5	77.3	19.3	96.9	31.6
113.1	33.0	123.8	50.0	95.8	22.9	77.4	18.8	97.9	31.5
114.4	35.2	123.7	51.3	93.0	21.7	77.5	18.5	98.9	33.7
115.5	35.2	123.6	49.9	90.7	21.9	77.6	17.7	99.7	31.8
116.5	36.5	123.6	50.9	88.3	22.0	77.8	17.2	100.8	33.7
117.3	36.6	123.4	48.7	86.1	21.5	77.9	17.7	101.6	35.3
118.5	38.7	123.5	48.4	84.1	17.7	78.0	18.0	102.4	37.8
119.5	38.0	123.3	48.8	82.4	18.2	78.1	17.6	102.9	38.1
120.5	40.2	123.2	48.8	80.8	18.7	77.9	17.0	103.3	37.4
121.2	40.5	123.3	48.3	79.1	19.3	77.8	17.6	103.2	35.4
122.0	41.5	123.3	50.1	77.8	19.7	77.8	19.6	103.3	34.6
122.4	45.5	123.3	48.8	76.6	19.2	77.9	18.1	103.4	36.0
123.1	45.5	123.2	48.8	75.6	19.7	77.9	18.2	103.3	35.7
123.7	46.3	123.3	49.5	75.1	20.0	77.8	18.4	103.1	34.7
124.0	43.8	123.4	49.1	74.6	17.1	77.8	19.3	102.8	33.0
124.2	45.1	123.4	45.5	74.2	15.1	78.1	18.9	102.7	31.7
124.3	44.8	123.4	48.3	75.1	18.2	78.2	18.4	102.5	31.4
124.3	47.6	123.3	49.5	75.2	19.0	78.6	20.6		
124.4	48.3	123.4	49.0	74.9	18.3	79.3	19.6		

A5 (cont.).

S11									
θ	α	θ	α	θ	α	θ	α	θ	α
82.3	15.4	115.8	27.8	117.7	11.5	102.5	10.8	78.0	5.3
83.0	15.5	116.1	27.1	117.4	10.9	101.2	10.8	77.8	6.4
83.6	14.7	116.2	26.7	117.1	10.6	99.8	9.8	77.7	4.8
84.4	16.2	116.6	26.6	117.0	10.4	98.5	7.0	77.6	5.7
85.3	18.8	116.6	25.4	117.0	9.7	97.4	10.0	77.8	6.1
86.3	18.9	116.6	21.0	116.9	10.5	96.4	8.9	77.8	4.0
87.3	20.3	116.8	20.1	116.9	9.9	95.2	10.0	77.8	4.4
88.3	18.1	117.0	19.3	117.0	10.0	93.8	9.5	77.7	5.3
89.2	18.2	117.2	19.5	117.2	9.5	92.6	7.1	77.5	5.4
90.3	20.1	117.1	20.8	117.1	9.9	91.7	6.4	77.3	5.3
91.2	21.3	117.3	19.7	117.0	10.1	90.9	6.7	77.3	5.1
92.5	21.9	117.4	18.4	117.1	10.1	90.0	7.2	77.3	5.6
93.4	22.5	117.4	18.0	116.9	9.7	88.9	6.1	77.1	5.9
94.2	24.0	117.6	16.0	116.9	10.3	87.9	6.9	76.7	4.9
95.2	21.8	117.7	16.8	116.8	10.1	87.1	6.3	76.5	5.3
96.1	22.3	117.8	16.2	116.9	10.6	86.4	6.5	76.4	4.7
96.8	22.8	118.0	17.9	116.5	10.8	85.7	5.7	76.1	5.2
97.3	23.6	117.9	18.6	116.6	9.5	85.3	5.1	75.6	6.1
98.1	22.7	117.9	18.2	116.2	9.2	85.2	7.7	75.3	5.8
98.9	25.3	117.9	15.6	116.0	12.0	84.8	5.7	74.8	6.3
99.7	26.2	117.9	14.4	115.8	11.8	84.2	5.7	74.2	8.8
100.7	26.1	117.7	15.2	115.5	10.3	83.9	5.9	73.7	5.5
102.1	28.9	117.7	13.2	115.4	10.8	83.6	4.6	73.3	5.8
103.9	30.2	117.7	13.1	115.1	7.3	82.9	4.2	72.9	3.8
105.5	27.7	117.7	12.3	114.9	8.0	82.6	7.0	72.6	3.4
106.5	32.8	118.0	12.1	114.4	8.8	81.7	5.5	72.4	5.5
107.7	34.0	118.2	7.2	113.8	6.8	81.2	5.1	72.1	3.5
108.6	33.1	118.3	8.4	113.3	12.3	80.7	3.4	71.8	5.5
109.5	34.3	118.3	8.0	112.6	12.2	80.2	4.7	71.2	3.6
110.1	34.6	118.5	8.1	112.1	15.1	79.8	6.0	70.7	3.8
110.5	34.3	118.8	9.7	111.1	12.8	79.6	6.1	70.2	3.6
111.5	32.5	118.9	7.5	110.0	13.7	79.3	4.3	69.8	2.9
112.0	33.3	119.1	10.6	108.9	11.7	79.2	3.7	69.8	2.6
112.8	32.9	119.1	11.3	107.8	11.6	79.0	3.7	69.3	3.3
113.6	31.5	118.8	10.5	106.8	13.1	78.8	3.3	69.1	2.9
114.5	31.0	118.3	10.0	105.2	10.2	78.8	4.3	68.7	2.5
115.2	30.1	117.9	10.1	103.9	10.7	78.2	5.1	68.4	2.9

A5 (cont.).

S11			
θ	α	θ	α
68.2	2.7	71.7	4.5
68.0	2.6	72.5	5.1
67.9	2.6	72.8	5.2
67.9	2.5	73.3	5.9
68.2	2.1	74.1	6.9
68.3	3.0	74.6	4.9
68.4	2.5	75.6	6.8
68.6	3.4	76.1	6.2
68.7	4.8	76.6	5.5
68.8	3.6	77.4	7.8
68.9	3.5	78.2	12.0
68.9	3.2	79.1	10.9
69.0	2.1	79.8	7.2
69.1	2.7	80.7	10.0
69.1	2.4	81.7	14.3
69.1	3.2	82.8	16.8
69.0	3.5	83.7	18.2
69.3	1.0	84.2	16.8
69.5	1.5	85.0	16.1
69.4	3.3	85.5	16.4
69.4	0.9	86.1	18.0
69.3	1.3	86.4	19.5
69.4	1.4	86.7	20.5
69.4	1.8	87.0	21.4
69.5	1.8	87.4	20.9
69.6	1.5	87.6	21.7
69.7	2.0	87.9	20.1
69.7	2.0	88.1	19.1
69.8	2.7	88.4	18.4
69.8	1.9	88.5	21.0
69.8	1.7	88.5	19.8
69.9	1.8	88.8	18.3
69.9	3.5	88.7	17.1
70.1	2.3	88.9	16.9
70.1	1.5	88.8	17.2
70.6	3.4	88.7	19.2
71.2	4.2	88.6	16.6

A5 (cont.).

S12												
θ	α	θ	α	θ	α	θ	α	θ	α	θ	α	
80.6	9.8	109.2	33.6	109.6	34.3	76.5	14.6	64.5	6.4	63.6	6.5	
81.3	10.8	109.3	33.8	109.5	33.9	74.7	13.4	64.2	6.4	63.4	5.9	
82.1	14.5	109.1	31.2	109.5	34.3	73.1	9.6	64.2	6.5	63.5	6.2	
82.9	12.0	109.1	32.9	109.5	34.6	71.5	9.8	64.3	9.8	63.8	5.6	
84.4	17.1	109.0	33.3	109.4	34.0	70.1	6.8	64.1	6.4	64.2	7.0	
86.1	15.2	108.9	33.1	109.4	33.1	68.7	9.6	64.1	9.5	64.9	7.4	
87.7	17.6	108.9	32.4	109.5	34.6	67.3	8.3	64.0	5.7	66.0	11.0	
88.9	19.5	108.8	32.5	109.4	35.5	66.0	7.7	64.1	5.6	67.2	11.7	
90.1	17.8	108.7	32.5	109.5	34.7	64.9	6.7	64.1	6.2	68.4	9.7	
91.9	20.2	108.6	32.4	109.5	34.3	64.2	4.6	64.0	6.1	69.5	7.2	
93.4	20.6	108.6	32.5	109.5	34.5	63.8	4.4	64.1	5.9	70.9	11.0	
94.6	22.8	108.7	32.7	109.4	35.1	63.6	8.6	64.1	5.8	72.4	10.9	
96.2	20.7	109.0	33.6	109.4	34.2	63.3	9.4	64.2	6.0	73.7	11.6	
97.3	24.0	109.1	32.9	109.4	34.1	63.3	12.3	64.1	7.3	75.5	10.4	
98.9	25.1	109.1	33.6	109.3	43.3	63.4	11.3	64.1	5.8	77.0	11.5	
100.2	27.8	109.0	35.3	109.2	33.4	63.5	9.5	64.0	6.2	78.3	14.4	
101.6	25.0	109.2	34.9	108.9	33.1	63.8	11.3	64.0	6.5	79.3	10.5	
102.5	26.5	109.2	33.3	108.6	33.4	63.8	11.1	64.1	6.4	80.7	12.1	
103.5	26.8	109.3	32.8	108.5	34.9	64.1	11.0	64.1	10.4	81.8	16.2	
104.5	29.5	109.5	33.0	108.2	36.2	64.3	7.1	64.0	5.7	83.0	13.9	
105.6	31.4	109.6	34.9	107.9	36.4	64.2	6.8	64.0	5.6	84.2	11.9	
106.4	34.0	109.6	33.4	107.5	35.8	64.3	6.5	63.9	6.0	84.8	12.6	
107.0	31.6	109.4	33.7	107.1	36.5	64.6	6.0	63.9	6.0	85.4	12.5	
107.5	32.8	109.4	33.0	106.5	37.6	64.6	5.6	63.8	5.9	85.6	11.4	
107.9	31.4	109.4	33.0	105.7	39.3	64.6	4.9	63.8	9.2	85.6	13.2	
108.4	31.2	109.3	34.9	104.2	37.6	64.8	8.7	63.8	6.2	85.0	12.8	
108.7	31.6	109.4	33.1	102.3	35.2	64.8	5.3	63.6	6.0	84.6	12.3	
109.0	31.8	109.4	33.2	100.2	38.0	64.8	8.1	63.6	8.4	84.0	10.5	
109.0	32.1	109.4	33.2	98.0	37.9	64.9	5.3	63.6	5.9	83.5	10.1	
109.2	32.3	109.4	33.4	95.1	32.1	64.8	5.2	63.5	5.8	83.0	12.1	
109.4	32.6	109.4	33.2	92.4	28.0	64.7	5.0	63.6	5.7			
109.6	33.4	109.4	33.8	90.2	26.1	64.5	4.6	63.7	6.7			
109.5	33.2	109.5	33.3	87.7	24.2	64.5	5.1	63.6	5.5			
109.4	34.0	109.5	34.1	84.7	21.3	64.5	5.1	63.6	6.1			
109.3	33.7	109.5	34.0	82.6	19.5	64.5	5.6	63.5	5.9			
109.5	34.5	109.5	33.9	80.1	15.8	64.5	6.2	63.6	6.1			
109.4	34.4	109.6	34.1	78.1	13.0	64.5	5.9	63.5	6.2			

A5 (cont.).

S13										
θ	α	θ	α	θ	α	θ	α	θ	α	
72.3	-14.8	109.4	4.2	109.2	4.1	85.3	-11.3	63.7	-18.3	
73.2	-15.6	109.4	4.8	109.2	3.8	83.3	-10.5	63.8	-18.4	
74.1	-15.9	109.4	4.4	109.2	3.3	81.1	-10.3	64.0	-18.1	
74.9	-13.9	109.4	4.5	109.2	3.8	79.2	-13.6	63.9	-18.0	
75.9	-13.8	109.4	4.0	109.1	3.2	77.4	-14.1	64.2	-18.1	
76.9	-13.2	109.4	5.0	109.1	3.8	75.9	-13.9	64.4	-18.3	
77.7	-13.9	109.5	3.9	109.2	3.6	74.3	-14.5	64.5	-18.0	
79.1	-13.2	109.5	4.2	109.2	4.0	72.3	-13.1	64.7	-18.5	
80.0	-12.2	109.5	4.5	109.2	4.3	70.0	-13.9	64.5	-17.8	
81.1	-13.9	109.5	4.0	109.1	4.2	68.0	-14.6	64.5	-18.2	
82.2	-12.5	109.5	4.4	109.1	3.6	66.3	-16.2	64.6	-18.1	
83.3	-12.1	109.4	4.6	109.1	3.3	64.5	-17.2	64.7	-18.3	
84.6	-9.0	109.4	3.8	109.0	4.0	63.0	-17.0	64.6	-17.7	
85.8	-10.3	109.3	3.8	108.9	3.7	62.1	-18.4	64.6	-17.8	
87.3	-10.5	109.4	4.5	108.9	2.9	61.8	-19.7	64.7	-17.7	
88.7	-9.5	109.3	4.0	108.7	3.7	61.8	-19.1	64.6	-18.0	
89.8	-6.0	109.4	3.3	108.7	2.6	61.8	-19.5	64.6	-17.9	
91.2	-8.0	109.4	4.1	108.4	1.7	62.1	-19.2	64.6	-18.6	
92.7	-9.1	109.4	4.4	108.2	-5.6	62.2	-19.9	64.6	-17.8	
94.1	-9.9	109.4	4.5	107.6	0.1	62.3	-18.9	64.6	-17.7	
95.5	1.9	109.5	4.5	107.3	2.4	62.4	-18.9	64.5	-16.0	
96.9	2.6	109.4	4.3	106.9	2.2	62.5	-19.1	64.4	-17.5	
98.1	2.9	109.4	4.2	106.1	3.3	62.7	-19.4	64.3	-17.9	
99.7	5.0	109.4	4.1	105.4	1.6	62.9	-18.9	64.2	-18.4	
100.6	1.4	109.4	5.4	104.7	-5.7	63.0	-20.3	64.3	-16.5	
102.0	0.3	109.4	3.9	103.9	0.9	63.0	-19.0	64.0	-17.3	
103.0	3.7	109.4	4.4	102.8	0.5	63.1	-19.0	64.0	-18.4	
104.2	5.5	109.4	4.1	101.3	-9.2	63.2	-19.4	64.1	-17.6	
104.9	5.4	109.4	4.8	100.3	-10.7	63.2	-19.6	63.8	-18.3	
105.9	5.9	109.4	4.2	98.8	-10.4	63.4	-19.5	63.7	-18.9	
106.9	4.1	109.4	5.5	97.0	-8.2	63.2	-19.8	64.0	-17.7	
107.7	5.2	109.3	3.7	95.5	-9.6	63.3	-19.8	63.7	-17.7	
108.4	4.6	109.3	4.5	93.1	-11.6	63.2	-18.9	63.7	-17.9	
108.7	2.2	109.3	4.6	91.3	-10.7	63.4	-19.2	63.7	-17.9	
109.0	3.4	109.3	3.7	89.8	-7.5	63.5	-18.3	63.8	-17.7	
109.3	3.8	109.2	4.4	88.3	-7.8	63.6	-18.2	63.8	-17.8	
109.4	3.6	109.3	4.5	87.0	-11.2	63.7	-18.1	63.5	-17.7	

A5 (cont.).

S13			
θ	α	θ	α
63.5	-17.7	79.1	-10.0
63.5	-17.7	80.3	-10.1
63.6	-18.1	81.5	-10.1
63.7	-17.8	82.2	-10.7
63.4	-17.5	82.8	-9.5
63.4	-18.0	82.9	-9.9
63.4	-19.2	82.9	-10.8
63.3	-18.0	82.5	-10.2
63.4	-18.0	82.0	-10.7
63.4	-18.0	81.4	-10.6
63.4	-18.0	81.1	-13.2
63.6	-18.0	80.8	-10.1
63.6	-17.8	80.4	-10.9
63.5	-18.0	80.2	-10.0
63.5	-17.7	80.0	-9.5
63.4	-18.2		
63.5	-18.3		
63.4	-18.0		
63.7	-17.9		
63.6	-19.4		
63.9	-18.4		
64.1	-17.6		
64.4	-18.4		
64.8	-19.2		
65.3	-19.9		
65.9	-20.9		
66.5	-18.7		
67.4	-17.4		
68.3	-15.2		
69.2	-15.3		
70.4	-16.9		
71.4	-15.8		
72.4	-12.9		
73.4	-14.2		
74.8	-11.1		
76.2	-13.6		
77.4	-10.7		

A5 (cont.).

S17											
θ	α	θ	α	θ	α	θ	α	θ	α	θ	α
99.6	16.5	126.0	39.9	126.7	43.3	118.8	43.6	86.2	14.3	80.5	11.2
100.8	25.1	126.1	40.1	126.6	43.1	117.7	42.7	86.1	14.7	80.6	12.1
102.2	24.9	126.2	43.7	126.6	44.2	116.6	45.4	86.0	14.7	80.6	11.4
103.3	25.1	126.1	44.1	126.5	42.5	115.9	41.7	86.0	15.3	80.7	11.7
104.4	29.7	126.1	44.3	126.6	42.7	115.1	42.7	85.8	16.1	80.8	11.7
105.4	22.1	126.0	44.9	126.5	41.6	114.2	40.0	85.4	15.2	80.8	11.9
106.4	27.9	125.9	44.7	126.5	42.1	112.8	35.8	85.2	14.5	80.9	12.1
107.4	27.2	125.8	44.3	126.5	43.4	111.6	33.9	84.9	15.6	80.8	11.6
108.3	32.8	125.7	44.5	126.4	42.0	110.2	37.7	84.6	14.5	81.0	12.0
108.8	29.0	125.5	44.9	126.4	44.0	108.6	34.1	84.3	15.4	81.0	11.5
109.4	28.3	125.4	45.5	126.3	43.5	106.9	29.3	83.9	13.8	81.0	11.6
110.1	27.0	125.4	45.0	126.2	42.9	105.2	24.8	83.6	13.7	81.0	11.8
110.7	29.4	125.6	48.3	126.2	44.1	103.7	31.6	83.4	14.4	80.8	11.7
111.4	29.7	125.8	48.0	126.2	42.7	102.9	31.5	83.0	13.6	80.9	11.7
112.2	29.3	125.8	48.3	126.2	43.7	102.8	18.9	82.8	13.5	80.8	8.6
113.5	32.1	125.8	48.5	126.2	43.0	102.1	22.5	82.7	12.2	80.8	10.3
114.7	30.5	125.9	50.7	126.2	43.4	101.6	25.5	82.6	12.6	80.7	12.0
115.9	32.5	126.0	50.2	126.1	42.0	100.4	19.5	82.5	13.0	80.7	11.2
117.0	32.0	126.0	50.2	126.1	43.9	99.2	23.1	82.3	13.6	80.8	11.3
118.3	38.6	126.1	49.9	126.1	43.9	97.6	15.7	82.3	13.5	80.9	11.7
119.3	37.7	126.1	49.0	126.0	42.4	96.2	19.2	82.2	13.5	80.9	11.8
120.0	35.0	126.2	48.5	126.0	42.4	95.0	17.3	82.0	13.2	80.9	12.2
120.7	38.2	126.3	48.1	125.9	42.9	94.1	19.3	81.7	10.1	80.8	12.3
121.5	36.8	126.5	48.3	125.9	43.0	92.9	18.7	81.4	12.7	81.0	12.3
122.3	39.0	126.7	48.7	125.8	43.3	91.9	18.5	81.1	10.9	81.1	9.9
122.9	42.9	126.8	47.5	125.7	42.9	91.0	18.2	81.0	11.0	81.0	9.6
123.5	41.9	127.0	47.5	125.6	44.7	90.5	18.3	80.9	10.3	81.0	9.6
123.8	40.5	127.0	44.7	125.4	42.7	89.9	16.9	80.9	11.5	81.1	11.2
124.1	40.4	127.0	43.2	125.1	44.3	89.5	15.2	80.9	11.3	81.4	9.4
124.3	39.9	127.1	44.1	125.0	42.9	89.0	14.3	80.8	11.4	81.6	9.5
124.5	40.3	127.1	44.3	124.7	43.8	88.6	15.8	80.7	11.5	81.9	10.1
124.6	40.4	127.1	46.7	124.2	47.7	87.9	14.1	80.7	11.4	82.3	10.6
124.8	39.8	127.0	44.0	123.5	49.8	87.5	13.7	80.5	11.3	83.2	10.2
124.9	39.1	127.0	42.1	122.7	50.5	87.1	13.3	80.5	10.8	84.1	13.6
125.1	39.4	126.9	42.2	121.9	47.8	86.8	12.1	80.5	11.4	85.1	15.3
125.3	40.1	126.8	42.4	121.2	43.7	86.5	12.5	80.4	11.7	86.2	15.3
125.6	39.3	126.7	42.8	119.9	41.4	86.4	12.4	80.5	11.3	87.4	16.7

A5 (cont.).

S17	
θ	α
88.3	18.3
89.4	17.2
90.5	18.1
91.3	17.7
92.0	18.0
92.9	16.9
93.6	18.4
94.5	20.8
95.4	19.2
96.4	17.0
97.5	18.0
98.7	19.5
99.3	21.0
99.9	21.9
100.6	23.0
101.3	23.7
101.7	24.6
102.3	24.5
102.8	24.7
103.4	24.4
104.1	27.2
104.7	22.7
105.1	23.1
105.7	27.8
106.2	25.0
106.7	33.7
107.2	31.9
107.4	33.1
107.8	33.4
108.1	26.5
108.2	29.7
108.4	30.3

A5 (cont.).

S18										
θ	α	θ	α	θ	α	θ	α	θ	α	
71.6	-12.2	89.7	-13.9	91.7	-15.0	89.4	-12.7	59.9	-10.2	
72.0	-12.9	89.8	-14.5	91.6	-15.4	89.3	-14.3	59.5	-10.9	
72.8	-11.3	90.0	-16.7	91.6	-15.4	89.2	-13.4	58.9	-10.5	
74.3	-11.0	90.1	-14.7	91.5	-18.0	88.9	-14.0	58.4	-11.1	
75.9	-12.0	89.9	-16.3	91.4	-17.0	88.7	-13.4	58.2	-11.4	
78.0	-10.5	90.0	-14.8	91.3	-16.4	88.7	-12.8	58.1	-11.8	
79.5	-13.9	90.2	-14.3	91.0	-18.5	88.2	-13.3	58.0	-11.3	
80.5	-13.5	90.2	-14.2	91.1	-18.8	87.8	-12.6	57.9	-10.9	
81.2	-12.5	90.4	-14.6	90.8	-19.0	87.1	-11.5	57.9	-9.9	
81.2	-13.4	90.4	-14.2	90.8	-18.2	86.5	-12.7	57.7	-10.1	
82.0	-13.2	90.5	-14.4	90.8	-18.1	85.9	-10.2	57.5	-9.7	
82.7	-12.5	90.9	-14.4	90.7	-18.1	85.2	-12.9	57.3	-10.3	
83.2	-14.7	90.9	-14.1	90.7	-18.5	84.3	-13.0	57.5	-10.1	
83.4	-15.1	91.0	-14.7	90.6	-18.6	83.5	-12.7	57.4	-10.2	
83.7	-16.7	91.2	-14.3	90.6	-18.7	82.2	-12.9	57.3	-9.5	
84.1	-16.5	91.4	-14.4	90.5	-18.0	80.8	-13.5	57.1	-9.2	
84.6	-17.2	91.5	-16.7	90.5	-19.3	79.0	-13.0	57.1	-9.7	
85.0	-17.2	91.6	-14.1	90.5	-16.0	76.9	-11.6	57.2	-10.2	
85.5	-17.6	91.7	-14.1	90.4	-19.0	75.1	-16.5	57.1	-11.4	
86.2	-17.3	91.7	-14.5	90.4	-17.7	73.3	-12.6	57.2	-10.9	
86.3	-18.5	91.8	-12.8	90.3	-17.7	72.2	-12.3	57.2	-11.9	
86.5	-18.2	91.9	-14.5	90.2	-17.2	70.8	-11.7	57.2	-11.6	
86.8	-16.4	92.0	-15.0	90.2	-14.1	69.6	-12.6	57.2	-11.3	
87.4	-17.7	92.1	-14.2	90.1	-16.6	68.2	-11.6	57.1	-10.2	
87.9	-16.2	92.1	-12.8	90.2	-12.4	66.7	-11.5	57.2	-12.6	
88.3	-16.0	92.1	-14.6	90.0	-15.0	65.7	-11.4	57.2	-11.4	
88.6	-15.6	92.2	-14.4	90.0	-14.2	64.7	-10.5	57.4	-7.0	
88.9	-16.5	92.2	-15.3	89.9	-13.7	63.7	-9.6	57.3	-13.4	
89.2	-14.6	92.2	-14.2	89.8	-13.3	63.1	-11.1	57.4	-10.0	
89.3	-16.2	92.2	-14.4	89.9	-12.7	62.6	-9.3	57.6	-9.1	
89.4	-13.2	92.2	-14.4	89.7	-12.5	62.3	-12.5	57.9	-11.4	
89.5	-15.2	92.2	-14.6	89.7	-12.5	62.0	-10.2	58.2	-9.5	
89.6	-13.8	92.1	-14.7	89.7	-14.6	61.5	-10.2	58.2	-11.7	
89.6	-14.8	92.1	-15.2	89.6	-13.6	61.1	-11.6	58.3	-10.9	
89.7	-13.9	92.0	-15.2	89.6	-13.2	60.6	-11.0	58.4	-13.2	
89.6	-13.5	91.9	-15.3	89.6	-13.1	60.4	-10.4	58.6	-9.7	
89.7	-13.8	91.8	-15.0	89.5	-12.9	60.0	-10.3	58.7	-11.5	

A5 (cont.).

S18					
θ	α	θ	α	θ	α
58.9	-10.6	62.9	-10.2	75.6	-8.4
59.1	-11.7	63.4	-7.8	75.6	-7.8
59.3	-11.5	64.1	-6.3	75.5	-8.4
59.5	-11.0	64.4	-8.5	75.3	-5.5
59.6	-13.3	64.9	-9.8	74.9	-9.7
59.7	-12.7	65.1	-8.6	74.5	-7.9
59.9	-12.6	65.2	-9.1	74.2	-6.4
60.0	-10.9	65.4	-9.4	74.1	-6.0
60.2	-11.1	65.5	-11.1	74.2	-6.1
60.3	-11.1	65.7	-10.8		
60.6	-9.2	65.9	-11.2		
60.5	-11.2	66.2	-10.9		
60.6	-13.5	66.7	-11.2		
60.7	-10.3	67.3	-12.6		
60.9	-10.9	67.9	-12.9		
60.9	-10.5	68.2	-12.0		
61.1	-11.0	68.5	-12.1		
61.0	-10.6	69.0	-11.7		
61.2	-11.0	69.2	-12.0		
61.2	-10.8	69.6	-11.8		
61.3	-13.3	69.8	-11.1		
61.4	-12.5	70.0	-11.0		
61.3	-10.6	70.8	-10.5		
61.5	-9.9	71.1	-10.0		
61.4	-10.6	71.3	-10.9		
61.6	-10.2	71.6	-9.7		
61.5	-11.3	72.2	-10.4		
61.6	-8.1	72.6	-10.8		
61.5	-10.8	73.0	-10.9		
61.5	-10.3	73.2	-11.4		
61.5	-10.5	73.5	-11.7		
61.6	-10.2	73.8	-11.6		
61.8	-11.4	74.3	-10.0		
61.8	-10.7	74.6	-11.8		
61.9	-10.9	75.0	-8.5		
62.1	-12.6	75.2	-8.1		
62.4	-11.1	75.4	-8.1		

A5 (cont.).

S19												
θ	α	θ	α	θ	α	θ	α	θ	α	θ	α	
70.5	-5.9	84.9	0.0	86.4	1.9	83.8	-4.7	68.6	-6.7	67.9	-6.0	
70.6	-5.7	85.2	-4.1	86.4	-4.2	83.7	-5.0	68.4	-6.3	67.7	-5.6	
70.7	-6.3	85.3	-4.5	86.5	0.7	83.5	-5.2	68.2	-6.8	67.6	-6.5	
70.9	-5.4	85.4	-4.4	86.5	-4.8	83.4	-5.0	68.1	-6.7	67.4	-6.6	
71.1	-5.7	85.5	-4.6	86.6	-4.2	83.1	-4.4	68.0	-6.1	67.4	-6.5	
71.3	-6.0	85.6	-4.0	86.5	-4.4	82.7	-5.1	68.0	-6.4	67.3	-6.1	
71.7	-6.9	85.8	-4.4	86.6	-4.8	82.3	-4.7	68.0	-6.4	67.4	-6.6	
72.0	-7.2	85.9	-3.8	86.5	-4.5	81.7	-4.2	68.0	-7.0	67.3	-6.7	
72.5	-8.6	85.9	-3.9	86.5	-4.5	81.3	-1.8	68.1	-7.0	67.2	-6.3	
72.6	-8.6	86.1	1.6	86.5	-4.5	81.0	0.3	68.2	-6.1	67.2	-6.9	
72.9	-8.7	86.1	2.4	86.5	-4.2	80.7	-2.2	68.3	-5.4	67.2	-7.0	
73.3	-9.2	86.2	2.0	86.5	-4.5	80.4	-4.6	68.3	-6.5	67.3	-8.2	
73.6	-8.4	86.3	1.8	86.5	-4.2	78.9	-4.6	68.3	-6.6	67.4	-6.3	
74.3	-7.5	86.3	2.1	86.5	-4.4	78.3	-4.5	68.3	-6.5	67.3	-6.8	
74.5	-7.7	86.4	2.1	86.4	-4.6	77.8	-5.1	68.3	-6.2	67.3	-6.5	
74.7	-6.2	86.5	1.8	86.4	0.1	77.1	-5.1	68.3	-8.9	67.3	-7.1	
75.4	-6.3	86.6	1.8	86.4	0.0	76.5	-5.0	68.5	-5.7	67.4	-6.5	
75.7	-5.9	86.6	1.9	86.4	2.0	75.8	-3.8	68.3	-7.0	67.4	-6.6	
75.9	-5.8	86.7	-3.7	86.4	2.1	75.3	-3.5	68.3	-6.8	67.5	-6.7	
77.9	-6.1	86.7	0.3	86.3	2.4	74.9	-4.0	68.3	-7.1	67.6	-6.8	
78.1	-6.2	86.8	0.3	86.3	2.2	74.5	-4.4	68.3	-6.9	67.8	-5.9	
78.3	-6.2	86.8	0.2	86.2	2.4	74.0	-4.7	68.4	-6.7	67.8	-7.1	
78.8	-5.8	86.8	0.6	86.1	-3.7	73.7	-4.6	68.5	-6.4	67.9	-5.8	
79.1	-5.9	86.8	-4.2	86.1	0.0	73.3	-6.6	68.5	-6.7	68.1	-5.9	
79.5	-5.9	86.9	0.3	86.0	2.7	72.8	-8.1	68.6	-6.1	68.1	-7.1	
79.9	-5.5	86.9	0.3	85.8	4.5	72.3	-7.5	68.4	-6.0	68.1	-6.4	
80.4	-4.0	86.8	0.2	85.8	2.3	71.9	-6.5	68.4	-6.9	68.2	-6.5	
80.9	-4.2	86.8	-4.3	85.7	2.3	71.4	-7.0	68.5	-5.7	68.5	-6.5	
81.5	-2.8	86.6	-3.9	85.6	2.5	71.1	-7.5	68.4	-6.3	68.6	-6.1	
83.1	-3.8	86.7	-4.2	85.5	1.7	70.7	-7.1	68.3	-6.6	68.6	-5.8	
83.4	-5.7	86.6	0.1	85.4	1.9	70.6	-7.2	68.3	-6.9	69.0	-6.3	
83.7	-7.8	86.4	-3.9	85.2	-2.9	70.3	-7.7	68.3	-6.9	69.3	-6.3	
83.9	-4.1	86.4	2.1	85.0	-2.7	69.9	-8.1	68.3	-6.8	69.7	-5.5	
84.1	-6.0	86.3	2.0	84.8	-3.3	69.6	-7.6	68.3	-6.9	69.9	-5.7	
84.3	-3.4	86.3	1.4	84.6	-2.9	69.1	-5.8	68.2	-6.8	70.1	-5.3	
84.5	-4.7	86.4	2.0	84.3	-3.2	68.9	-6.9	68.3	-5.0	70.6	-7.3	
84.7	-3.8	86.4	1.4	84.0	-4.5	68.6	-6.2	68.0	-5.8	71.2	-6.4	

A5 (cont.).

S19	
θ	α
71.6	-6.3
72.3	-6.9
72.7	-4.5
73.0	-6.1
73.0	-6.4
73.1	-5.9
73.0	-6.2
73.0	-4.6
72.8	-3.6
72.8	-3.3
73.0	-4.0

A5 (cont.).

S21									
θ	α	θ	α	θ	α	θ	α	θ	α
74.2	-9.6	107.1	50.2	117.1	60.0	117.2	67.4	63.3	-9.0
74.7	-9.1	109.6	47.9	117.1	61.5	116.9	58.8	61.9	-4.1
75.3	-7.0	110.3	50.2	117.1	62.0	116.7	59.7	59.3	-8.1
75.7	0.1	110.8	51.3	117.2	61.6	116.4	63.1	60.7	-10.7
76.6	0.7	111.8	52.2	117.1	61.3	116.0	63.8	59.5	-14.3
77.3	2.6	112.6	53.2	117.1	61.5	115.6	63.3	59.6	-19.6
77.7	3.2	113.7	51.7	117.1	61.6	115.4	63.1	59.3	-14.4
78.3	4.4	114.2	51.7	117.1	62.1	115.0	62.1	58.8	-34.2
79.1	6.3	114.6	54.5	117.1	61.0	114.5	62.7	61.5	-24.4
79.6	7.9	115.2	53.4	117.2	61.7	113.7	62.4	55.9	-16.4
80.8	9.9	115.4	55.5	117.2	61.6	113.8	65.8	55.4	-16.8
83.6	12.7	115.8	56.9	117.2	59.9	111.9	61.4	55.4	-18.6
86.5	13.2	115.9	56.7	117.3	61.2	109.1	61.7	54.4	-14.8
87.1	13.3	116.2	57.5	117.3	61.2	110.1	61.2	51.5	-30.4
87.9	15.2	116.4	57.9	117.4	60.1	109.2	61.0	51.5	-28.0
88.8	19.5	116.6	58.6	118.3	61.6	106.5	59.6	51.8	-26.6
89.5	22.6	116.6	59.1	118.4	57.6	105.8	59.1	52.0	-26.5
90.1	24.5	116.7	59.0	118.5	57.6	104.8	58.9	53.5	-25.1
90.8	26.0	116.8	58.9	118.6	57.7	103.9	58.7	54.0	-23.8
91.8	25.5	116.8	59.2	118.6	64.5	102.9	62.9	54.4	-24.2
93.0	28.5	116.9	59.8	118.7	66.7	100.0	62.6	54.3	-37.4
95.4	32.2	116.9	59.7	118.7	67.0	97.0	61.4	54.2	-34.6
96.8	32.2	117.0	59.9	118.8	58.9	95.6	57.8	52.1	-22.7
97.8	35.7	116.9	64.2	118.8	56.0	94.4	55.3	51.1	-23.5
100.3	38.6	116.8	64.9	117.8	57.7	93.1	51.0	51.5	-24.2
101.3	41.0	116.9	65.0	117.8	58.7	91.9	48.6	52.9	-41.9
102.2	42.9	116.7	64.5	117.9	58.8	88.5	45.1	52.1	-40.8
102.9	43.7	116.7	64.6	117.9	58.7	85.3	42.2	52.4	-38.3
103.7	45.5	117.1	66.0	117.9	58.7	84.3	36.9	52.5	-35.5
104.3	46.3	117.1	64.7	117.9	58.8	83.1	34.1	52.5	-34.9
104.4	46.7	117.1	64.2	117.9	58.3	82.2	28.0	52.6	-33.1
104.7	46.2	117.0	64.8	117.8	58.4	81.2	23.4	52.8	-30.2
105.0	48.0	117.1	65.1	117.8	66.3	77.7	28.7	52.8	-22.8
105.4	48.2	117.1	64.7	117.8	58.6	74.9	27.9	53.0	-23.8
107.4	48.9	117.1	62.8	117.7	59.3	74.0	25.2	52.9	-24.2
109.6	49.1	117.1	62.9	117.5	67.4	72.9	18.3	52.5	-25.0
108.3	49.6	117.1	64.6	117.3	67.9	61.5	-7.7	52.9	-26.1

A5 (cont.).

S21					
θ	α	θ	α	θ	α
53.1	-24.2	54.1	-24.5	76.2	11.8
52.9	-23.9	54.0	-24.4	77.3	15.8
53.0	-23.4	53.9	-24.5	77.0	18.1
53.1	-22.9	54.0	-24.6	78.0	20.9
53.2	-22.7	54.1	-24.6	79.1	23.5
53.4	-22.5	54.1	-24.9	82.0	26.0
53.3	-22.3	54.2	-25.0	85.0	28.7
53.6	-22.5	53.9	-25.0	85.7	28.7
53.3	-23.1	53.6	-24.4	86.1	30.1
53.4	-23.5	53.6	-24.2	86.8	32.4
53.5	-22.9	53.6	-23.7	87.3	34.8
53.5	-23.6	53.6	-23.7	87.9	36.7
53.5	-24.1	53.7	-23.7	88.5	37.9
53.8	-24.0	53.5	-29.2	89.0	37.5
53.6	-23.8	53.7	-30.9	91.3	38.0
53.4	-23.8	53.3	-33.1	92.2	39.1
53.6	-23.6	53.7	-35.6	92.7	40.2
53.6	-23.5	54.4	-37.7	94.7	41.6
53.5	-23.1	54.5	-42.4	94.9	41.8
53.4	-22.8	55.2	-21.8	95.0	42.2
53.5	-23.3	55.3	-34.6	95.1	42.3
53.5	-22.8	55.9	-22.6	95.2	43.1
53.5	-23.5	55.8	-19.6		
53.5	-23.2	56.0	-21.6		
53.5	-23.9	58.3	-24.8		
53.5	-23.4	58.5	4.2		
53.8	-23.6	60.5	-14.7		
53.9	-23.6	64.3	-18.8		
53.9	-23.4	62.6	-8.8		
54.2	-23.6	64.9	-12.6		
54.2	-23.6	64.4	1.2		
54.3	-23.5	65.3	10.8		
54.3	-23.7	68.4	2.3		
54.3	-24.0	71.3	4.9		
54.3	-23.7	70.7	6.8		
54.3	-24.0	72.2	8.1		
54.2	-24.4	73.4	10.9		

A5 (cont.).

S23												
θ	α	θ	α	θ	α	θ	α	θ	α	θ	α	
76.0	9.5	122.2	69.6	124.5	74.1	106.3	56.9	53.1	1.1	52.4	1.8	
77.1	9.7	123.0	71.7	124.6	74.3	103.9	53.4	52.3	0.5	52.6	2.5	
78.2	21.4	123.9	76.1	124.6	75.0	101.3	51.0	53.8	2.3	52.6	1.4	
80.8	13.8	124.4	78.2	124.7	75.4	98.5	55.7	53.7	1.6	52.6	3.7	
82.5	16.8	124.7	79.5	124.7	75.5	95.1	53.9	53.8	1.9	52.5	3.0	
85.0	18.1	124.9	80.9	124.8	74.8	91.6	52.5	53.8	1.8	52.4	3.2	
85.7	18.4	125.0	81.4	125.6	75.6	89.5	53.5	53.8	2.5	52.5	3.8	
87.0	21.3	125.1	81.5	125.6	76.4	85.3	50.6	53.8	1.8	52.4	3.8	
88.0	23.3	125.0	80.6	125.6	77.0	81.8	46.7	53.7	1.9	52.4	4.2	
88.6	23.2	124.8	79.7	125.6	79.2	80.7	46.3	53.6	2.3	52.4	4.5	
89.7	21.5	124.6	79.8	125.6	78.9	80.1	44.6	53.7	2.0	52.4	4.0	
90.5	24.7	124.4	80.4	125.7	78.2	79.6	41.0	53.7	1.9	52.4	3.5	
91.1	25.7	124.4	79.6	125.6	78.0	78.7	39.7	53.5	2.3	52.4	4.9	
93.0	26.0	124.4	79.4	125.5	78.9	77.8	34.7	53.6	1.7	52.4	4.4	
93.7	28.1	124.4	77.7	125.5	78.9	75.3	32.8	53.6	1.4	52.4	4.6	
94.6	30.7	124.4	78.3	125.5	78.9	74.3	28.1	53.6	0.8	52.4	4.6	
95.3	28.0	124.3	78.2	125.5	78.6	73.2	25.8	53.7	0.6	52.5	3.9	
96.3	30.0	124.4	78.2	125.5	79.7	72.1	22.5	53.8	1.3	52.5	4.7	
97.8	30.6	124.2	77.4	125.5	78.7	70.8	20.2	53.8	2.5	52.4	4.3	
100.2	35.2	124.2	75.5	125.4	79.6	68.7	14.1	53.9	1.8	52.3	4.3	
101.1	33.1	124.1	75.5	125.4	80.1	67.5	23.1	53.9	2.6	52.4	4.5	
102.2	35.0	124.0	74.8	125.4	78.6	65.4	10.8	53.8	2.4	52.5	4.9	
103.3	35.1	124.0	74.8	125.4	79.4	64.4	12.0	54.2	1.8	52.4	4.4	
104.2	39.3	124.1	74.0	125.3	78.7	63.3	14.7	53.0	1.8	52.5	5.1	
104.9	42.1	124.1	72.8	125.3	77.5	61.9	12.9	54.0	2.3	52.5	5.0	
107.2	39.8	124.1	71.8	125.2	78.6	61.3	9.9	54.3	1.3	52.5	4.9	
108.8	43.5	124.1	71.8	125.1	78.8	58.7	3.3	54.2	2.0	52.6	4.5	
110.3	44.2	124.2	73.0	125.0	76.7	56.9	1.7	54.1	1.2	52.9	5.0	
111.8	48.9	124.4	74.3	124.7	77.7	56.0	2.1	54.1	2.1	54.7	5.6	
113.0	49.3	124.4	74.5	122.5	76.5	55.9	4.6	54.4	2.4	55.2	4.3	
114.2	48.9	124.3	74.2	121.1	70.8	55.6	5.4	53.4	1.8	56.2	3.6	
115.4	51.0	124.4	74.8	118.5	66.4	54.2	2.3	52.4	1.3	52.2	2.4	
117.0	53.8	124.4	74.6	117.2	66.0	54.9	0.6	52.5	1.6	54.0	3.9	
118.0	56.4	124.4	74.6	115.6	62.8	53.5	-25.6	52.5	1.5	55.0	8.4	
118.8	59.5	124.5	74.4	113.8	59.0	52.8	2.2	52.5	1.1	55.7	8.2	
120.0	63.7	124.5	75.7	110.9	55.5	52.5	2.9	52.6	2.2	56.4	10.8	
121.3	66.4	124.6	74.8	108.5	53.8	52.2	-8.5	52.5	-10.5	57.4	9.3	

A5 (cont.).

S23	
θ	α
58.2	10.8
60.1	15.9
61.1	10.2
61.6	13.3
62.2	16.9
62.7	12.3
63.6	11.8
64.1	17.9
64.1	12.4
64.4	13.0
65.4	13.6
67.3	13.3
68.1	13.4
69.0	12.7
69.9	15.2
70.6	15.8
71.2	14.8
72.7	16.4
73.1	15.7
73.2	14.6
73.4	13.8
73.4	11.8
73.4	12.2
73.5	12.1
73.4	10.8

A5 (cont.).

S26												
θ	α	θ	α	θ	α	θ	α	θ	α	θ	α	
74.4	-7.1	122.9	26.4	83.5	4.6	61.6	-14.3	63.5	-13.2	81.3	2.0	
75.2	-4.9	122.9	26.9	81.7	3.5	61.7	-14.7	63.5	-14.5			
75.9	-7.5	122.8	27.5	80.2	0.3	61.7	-14.3	63.6	-14.3			
77.5	-2.6	122.0	32.2	78.4	-1.4	61.7	-15.0	63.4	-13.4			
79.3	-2.9	121.7	35.1	76.2	-3.2	62.2	-13.9	63.3	-12.9			
80.7	5.9	121.5	34.7	74.9	-4.3	62.2	-14.2	63.3	-11.9			
82.1	6.4	121.2	33.0	73.4	-5.8	62.5	-15.2	63.5	-13.7			
83.9	1.3	120.9	34.3	72.1	-5.8	62.6	-15.0	63.8	-12.3			
85.7	4.5	120.6	35.3	70.6	-6.3	62.6	-13.1	64.4	-13.0			
87.2	6.7	120.4	34.4	69.0	-6.7	62.5	-15.5	65.1	-10.9			
88.7	9.7	120.0	34.2	67.3	-8.6	62.7	-12.4	65.8	-10.3			
90.2	7.6	119.8	33.8	65.6	-6.6	63.0	-12.2	66.8	-7.6			
91.8	6.6	119.6	33.7	63.8	-9.1	63.2	-13.8	67.9	-7.5			
93.0	10.4	119.4	33.6	62.4	-12.5	63.3	-13.6	68.8	-8.8			
94.6	17.7	119.3	31.0	61.7	-9.2	63.6	-12.3	70.1	-5.8			
95.7	19.6	119.2	33.7	61.4	-12.0	63.7	-11.9	70.8	-4.8			
97.0	18.4	119.0	34.4	61.4	-11.7	63.7	-12.6	71.8	-4.1			
98.2	16.9	118.8	35.7	61.5	-11.2	64.4	-12.6	72.8	-4.9			
99.6	15.9	118.4	34.1	61.7	-11.1	64.2	-13.2	73.6	-3.4			
100.6	16.0	117.9	32.3	61.8	-11.3	64.1	-13.2	74.6	-5.1			
101.6	18.6	117.2	31.1	61.9	-12.6	64.0	-13.6	75.6	-7.7			
102.3	16.6	116.0	32.0	61.9	-12.8	63.9	-13.7	76.6	-5.7			
119.9	28.0	114.6	32.8	62.0	-13.5	64.0	-13.2	77.5	-5.3			
120.6	27.8	112.7	33.9	61.8	-13.1	64.1	-11.4	78.5	-4.7			
121.1	27.2	110.9	30.7	62.0	-16.0	64.1	-14.0	79.4	2.2			
121.4	26.7	108.6	28.2	61.9	-13.6	64.1	-13.7	80.3	3.8			
121.7	27.2	106.4	32.2	61.7	-11.0	64.2	-12.4	80.9	4.1			
121.9	25.9	104.2	33.3	61.5	-11.7	64.2	-11.9	81.4	2.9			
122.0	27.8	101.7	25.3	61.5	-11.1	64.1	-12.3	81.8	2.3			
122.2	26.9	98.8	23.3	61.6	-10.2	64.2	-12.4	82.2	-6.0			
122.4	27.2	96.8	21.6	61.7	-10.5	64.2	-12.3	82.4	-3.1			
122.4	27.8	95.1	26.9	61.9	-13.8	63.6	-12.8	82.7	-1.4			
122.5	26.8	92.9	26.8	61.9	-11.4	63.6	-12.1	82.7	0.6			
122.6	27.5	90.8	25.3	61.7	-10.8	63.7	-12.3	82.5	0.3			
122.8	27.4	89.1	20.2	61.7	-12.6	63.7	-11.7	82.3	4.0			
122.9	26.2	87.4	13.9	61.6	-12.9	64.3	-11.7	82.0	4.1			
122.8	26.9	85.5	7.6	61.6	-12.4	63.7	-12.4	81.6	2.2			

A5 (cont.).

S28											
θ	α	θ	α	θ	α	θ	α	θ	α	θ	α
55.4	-25.4	107.2	12.9	104.8	17.8	83.7	-7.3	36.6	-23.0	36.6	-24.1
56.8	-23.8	107.1	13.9	104.8	17.6	80.2	-12.1	36.6	-23.2	36.6	-24.6
57.2	-25.7	106.9	12.8	105.0	18.7	77.3	-14.1	36.7	-23.0	36.5	-24.1
58.0	-24.6	106.8	13.4	105.1	12.7	75.4	-14.7	36.7	-23.2	36.5	-24.4
58.8	-25.3	106.9	13.1	105.1	12.5	72.6	-16.4	36.6	-22.3	36.5	-24.2
60.2	-21.4	106.9	12.8	105.1	13.5	70.8	-17.2	36.6	-25.5	36.5	-24.9
61.9	-22.5	106.8	12.7	105.2	12.6	67.6	-19.8	36.6	-23.6	36.6	-24.4
64.9	-22.1	106.7	12.9	105.2	12.6	64.8	-17.7	36.6	-23.1	36.6	-24.4
67.9	-21.9	106.7	12.6	105.3	14.0	61.6	-23.1	36.6	-23.5	36.6	-24.6
71.1	-21.4	106.6	12.6	105.2	13.8	58.7	-27.4	36.7	-23.9	36.6	-24.5
73.0	-16.0	106.5	12.2	105.2	21.9	56.7	-25.0	36.7	-23.5	36.6	-24.6
74.7	-16.6	106.5	12.2	105.2	13.6	54.5	-26.7	36.7	-23.7	36.7	-23.2
78.1	-14.1	106.4	12.4	105.2	13.5	51.1	-23.9	36.7	-23.4	36.9	-24.4
80.6	-13.1	106.3	12.8	105.2	14.0	48.9	-27.4	36.8	-23.1	36.9	-22.8
83.5	-13.1	106.3	12.4	105.1	13.9	45.6	-26.1	36.8	-22.9	37.2	-25.8
85.2	-8.7	106.2	12.8	105.1	20.1	44.1	-28.2	36.8	-23.0	38.0	-28.2
87.1	-8.7	106.3	19.3	105.1	13.6	42.9	-27.4	36.9	-25.7	37.8	-34.5
88.8	-6.5	106.3	14.6	105.1	13.1	41.6	-27.3	36.7	-22.2	38.8	-32.8
91.8	-1.8	106.3	13.3	105.0	13.3	40.7	-28.8	36.9	-23.5	40.3	-30.4
93.4	0.5	106.3	13.6	105.0	19.4	39.4	-25.4	36.9	-25.7	42.1	-24.3
95.9	1.2	106.2	18.0	105.0	18.3	39.1	-26.0	36.9	-23.1	43.1	-22.9
97.4	9.3	106.2	13.7	105.0	19.7	38.1	-23.0	36.9	-23.4	44.1	-23.2
98.8	10.1	106.1	18.2	104.9	18.9	37.9	-23.6	36.9	-23.4	45.3	-18.3
99.9	11.7	106.1	13.1	104.7	18.8	37.9	-20.9	36.8	-23.4	47.7	-20.4
101.3	11.5	106.0	13.2	104.5	20.1	38.0	-22.2	36.8	-23.3	48.8	-19.1
102.2	9.6	105.9	12.4	104.0	17.8	37.8	-21.3	36.9	-22.9	49.6	-17.0
103.2	17.0	105.8	11.9	103.5	16.9	37.1	-22.3	36.8	-23.4	50.2	-17.3
104.1	15.0	105.8	12.1	102.5	14.6	37.0	-22.6	36.7	-23.2	50.5	-18.3
104.8	12.0	105.6	11.7	101.1	13.5	36.8	-22.0	36.7	-23.3	50.8	-17.1
106.5	13.3	105.4	11.5	100.0	11.2	36.7	-21.6	36.7	-23.9	51.0	-19.4
107.2	13.4	104.6	11.5	98.5	11.4	36.6	-21.2	36.7	-23.0	51.1	-17.2
107.5	14.0	104.4	11.1	97.1	7.0	36.5	-22.1	36.7	-22.6	51.2	-19.4
107.6	13.4	104.4	15.9	94.3	3.7	36.5	-21.6	36.8	-22.2	51.2	-18.3
107.7	13.5	104.5	16.3	92.5	2.6	36.6	-22.0	36.7	-23.6	51.3	-23.4
107.7	13.7	104.5	16.9	89.9	0.0	36.6	-22.2	36.6	-23.7		
107.6	13.4	104.6	17.0	87.8	-3.9	36.7	-21.9	36.6	-22.8		
107.4	13.2	104.6	17.2	85.6	-4.3	36.8	-22.3	36.6	-23.5		

A5 (cont.).

S30									
θ	α	θ	α	θ	α	θ	α	θ	α
78.2	5.6	108.6	24.5	114.9	21.9	113.0	18.7	67.9	-14.6
79.0	11.7	108.9	18.1	114.8	22.9	113.0	22.0	67.7	-17.1
79.5	13.3	109.4	21.6	114.7	22.8	112.6	19.1	67.4	-16.7
79.9	10.6	109.7	21.8	114.7	22.2	112.0	17.4	66.8	-15.4
80.7	7.2	110.2	20.9	114.7	22.3	111.4	22.4	66.8	-15.0
81.6	7.9	110.5	21.0	114.7	22.1	110.4	22.8	66.5	-14.5
82.5	10.2	110.6	20.0	114.7	22.4	109.4	25.4	66.5	-14.7
83.5	11.8	111.0	21.0	114.6	22.3	108.3	15.8	66.6	-14.8
85.1	12.2	111.2	21.6	114.6	22.4	107.0	16.7	66.5	-14.1
86.3	14.0	111.4	21.6	114.6	23.0	105.6	17.5	66.5	-17.7
87.4	12.8	111.6	21.6	114.5	22.8	104.2	20.7	66.4	-15.4
88.7	15.7	111.9	18.8	114.5	22.5	102.4	17.4	66.1	-16.1
89.7	15.7	112.3	19.5	114.5	21.9	101.0	15.1	65.9	-16.5
90.6	18.2	112.4	20.3	114.5	22.3	99.3	16.7	65.7	-16.5
91.5	19.6	112.6	20.4	114.4	22.1	97.3	13.5	65.4	-14.6
92.2	18.0	112.8	20.1	114.4	22.0	95.1	8.9	65.5	-16.5
93.1	23.8	112.9	19.6	114.3	21.4	93.3	10.2	65.2	-15.5
94.1	18.8	113.0	19.7	114.3	22.4	91.3	9.4	65.1	-14.7
95.0	19.2	113.1	21.1	114.2	21.4	88.9	2.8	65.0	-14.9
96.1	19.8	113.2	19.5	114.1	21.1	86.8	0.4	65.0	-15.4
97.1	25.3	113.4	19.8	114.0	21.7	84.9	0.4	64.9	-15.5
97.9	21.7	113.6	19.5	114.0	21.6	82.8	3.6	64.9	-15.0
98.6	22.5	113.8	20.0	114.0	21.9	80.6	2.8	64.7	-14.9
99.5	22.9	113.9	22.2	114.0	21.0	78.2	-15.2	64.6	-15.2
100.0	19.1	114.1	22.9	113.9	21.0	75.8	-15.3	64.6	-15.9
100.8	20.4	114.3	23.3	114.1	25.4	73.7	-15.7	64.8	-15.3
101.6	21.9	114.3	24.3	114.0	26.0	72.0	-17.8	64.5	-15.8
102.2	16.9	114.7	24.2	114.3	23.2	71.2	-14.9	64.3	-15.7
103.2	27.6	114.9	23.6	114.1	22.8	70.8	-15.0	64.3	-15.9
104.0	22.8	114.9	22.0	114.1	22.1	70.7	-14.2	64.2	-15.1
104.8	12.7	115.0	20.1	114.2	22.9	70.7	-14.2	64.3	-15.0
105.5	20.6	115.3	20.3	114.2	27.5	70.5	-14.9	64.0	-14.2
105.9	26.8	115.2	20.9	114.2	27.2	70.5	-16.8	64.1	-15.0
106.3	22.4	115.2	21.1	114.1	27.4	70.2	-14.2	64.1	-15.0
106.9	25.4	115.1	22.4	113.3	14.4	69.5	-13.9	64.0	-15.3
107.6	28.8	115.0	23.4	113.2	21.4	69.1	-13.9	64.2	-15.1
108.3	27.1	115.0	23.7	113.2	20.0	68.6	-14.3	64.0	-15.6

A5 (cont.).

S30			
θ	α	θ	α
64.0	-15.3	65.1	-16.8
64.0	-15.3	65.3	-14.6
64.1	-15.7	65.7	-13.9
64.2	-15.6	66.2	-13.5
64.5	-16.6	66.6	-13.5
64.5	-16.3	67.4	-14.4
64.7	-16.5	67.9	-13.5
64.8	-16.6	69.1	-13.4
64.9	-16.5	70.2	-11.8
64.6	-16.5	71.1	1.3
64.7	-16.4	72.2	1.2
64.5	-17.1	73.4	1.7
64.6	-17.3	74.7	0.8
64.6	-16.7	75.9	2.0
64.6	-16.9	76.8	2.5
64.6	-17.1	77.8	8.3
64.7	-16.1	79.0	8.7
64.7	-15.4	80.1	7.1
64.8	-16.8	81.0	8.3
64.9	-16.7	81.8	10.1
64.9	-16.2	82.2	10.8
65.1	0.2	82.8	11.3
64.9	-13.7	83.0	11.1
65.0	-14.4	83.5	11.0
64.8	-14.8	83.8	11.6
64.8	-16.9	83.9	11.0
64.6	-16.8	84.1	16.1
64.6	-16.7	84.0	15.5
64.9	-16.1	83.9	13.3
64.9	-16.6	83.7	13.4
65.0	-16.7		
65.1	-17.0		
65.0	-17.5		
65.0	-17.5		
65.0	-17.4		
65.0	-16.3		
65.0	-16.8		

BIBLIOGRAPHY

1. Kopec, J., E. Sayre, and J. Esdaile, *Predictors of back pain in a general population cohort*. Spine (Phila Pa 1976), 2004. **29**(1): p. 70-7; discussion 77-8.
2. Schneider, S. and S. Zoller, *[Physical movement - Is it good for the back? : Nationwide representative study on different effects of physical activity at the workplace and in leisure time.]*. Orthopade, 2009.
3. Lis, A., et al., *Association between sitting and occupational LBP*. Eur Spine J, 2007. **16**(2): p. 283-98.
4. Murphy, P. and T. Courtney, *Low back pain disability: relative costs by antecedent and industry group*. Am J Ind Med, 2000. **37**(5): p. 558-71.
5. Maniadakis, N. and A. Gray, *The economic burden of back pain in the UK*. Pain, 2000. **84**(1): p. 95-103.
6. NIOSH, *Proposed National Strategy for the Prevention of Musculoskeletal Injuries*. National Strategies for Prevention of Leading Work-Related Diseases and Injuries, 1986.
7. van Dieen, J.H., M.P. de Looze, and V. Hermans, *Effects of dynamic office chairs on trunk kinematics, trunk extensor EMG and spinal shrinkage*. Ergonomics, 2001. **44**(7): p. 739-50.
8. Pope, M., K. Goh, and M. Magnusson, *Spine ergonomics*. Annu Rev Biomed Eng, 2002. **4**: p. 49-68.
9. Li, G. and C. Haslegrave, *Seated work postures for manual, visual and combined tasks*. Ergonomics, 1999. **42**(8): p. 1060-86.
10. Pynt, J., J. Higgs, and M. Mackey, *Historical perspective milestones in the evolution of lumbar spinal postural health in seating*. Spine (Phila Pa 1976), 2002. **27**(19): p. 2180-9.
11. van Deursen, L., et al., *Sitting and low back pain: the positive effect of rotary dynamic stimuli during prolonged sitting*. Eur Spine J, 1999. **8**(3): p. 187-93.
12. Schiltenswolf, M. and S. Schneider, *Activity and low back pain: a dubious correlation*. Pain, 2009. **143**(1-2): p. 1-2.

13. Ben-Galim, P., et al., *Hip-spine syndrome - The effect of total hip replacement surgery on low back pain in severe osteoarthritis of the hip*. Spine, 2007. **32**(19): p. 2099-2102.
14. Choi, A.R., et al. *Development of a Spine Kinematic Model for the Clinical Estimation of Abnormal Curvature*. in IFMBE. 2007. Seoul, Korea.
15. Lehman, G.J., *Biomechanical assessments of lumbar spinal function. How low back pain sufferers differ from normals. Implications for outcome measures research. Part I: Kinematic assessments of lumbar function*. Journal of Manipulative and Physiological Therapeutics, 2004. **27**(1): p. 57-62.
16. Morel, E., et al., *Sagittal balance of the spine and degenerative spondylolisthesis*. Revue De Chirurgie Orthopedique Et Reparatrice De L Appareil Moteur, 2005. **91**(7): p. 615-626.
17. Dunne, L.E., et al. *A System for Wearable Monitoring of Seated Posture in Computer Users*. in IFMBE. 2007.
18. Pynt, J., M.G. Mackey, and J. Higgs, *Kyphosed seated postures: Extending concepts of postural health beyond the office*. Journal of Occupational Rehabilitation, 2008. **18**(1): p. 35-45.
19. Cholewicki, J. and S.M. McGill, *Mechanical stability of the in vivo lumbar spine: Implications for injury and chronic low back pain*. Clinical Biomechanics, 1996. **11**(1): p. 1-15.
20. Frigo, C., et al., *The upper body segmental movements during walking by young females*. Clinical Biomechanics, 2003. **18**(5): p. 419-425.
21. Granata, K.P. and B.C. Bennett, *Low-Back Biomechanics and Static Stability During Isometric Pushing*. Hum Factors, 2005. **47**(3): p. 536-549.
22. Keller, T.S., C.J. Colloca, and J.G. Beliveau, *Force-deformation response of the lumbar spine: a sagittal plane model of posteroanterior manipulation and mobilization*. Clinical Biomechanics, 2002. **17**(3): p. 185-196.
23. Sun, L.W., et al., *Modelling and simulation of the intervertebral movements of the lumbar spine using an inverse kinematic algorithm*. Medical & Biological Engineering & Computing, 2004. **42**(6): p. 740-746.
24. Pazos, V., et al., *Reliability of trunk shape measurements based on 3-D surface reconstructions*. European Spine Journal, 2007. **16**(11): p. 1882-1891.

25. Lee, R.Y.W., J. Laprade, and E.H.K. Fung, *A real-time gyroscopic system for three-dimensional measurement of lumbar spine motion*. Medical Engineering & Physics, 2003. **25**(10): p. 817-824.
26. Allbrook, D., *Movements of the Lumbar Spinal Column*. Journal of Bone and Joint Surgery-British Volume, 1957. **39**(2): p. 339-345.
27. Frobin, W., et al., *Precision measurement of segmental motion from flexion-extension radiographs of the lumbar spine*. Clinical Biomechanics, 1996. **11**(8): p. 457-465.
28. Harrison, D.E., et al., *How do anterior/posterior translations of the thoracic cage affect the sagittal lumbar spine, pelvic tilt, and thoracic kyphosis?* European Spine Journal, 2002. **11**(3): p. 287-293.
29. Janik, T.J., et al., *Can the sagittal lumbar curvature be closely approximated by an ellipse?* Journal of Orthopaedic Research, 1998. **16**(6): p. 766-770.
30. Morl, F. and R. Blickhan, *Three-dimensional relation of skin markers to lumbar vertebrae of healthy subjects in different postures measured by open MRI*. European Spine Journal, 2006. **15**(6): p. 742-751.
31. Hedman, T.P. and G.R. Fernie, *In vivo measurement of lumbar spinal creep in two seated postures using magnetic resonance imaging*. Spine (Phila Pa 1976), 1995. **20**(2): p. 178-83.
32. Karadimas, E.J., et al., *Positional MRI changes in supine versus sitting postures in patients with degenerative lumbar spine*. J Spinal Disord Tech, 2006. **19**(7): p. 495-500.
33. Ng, J.K.F., et al., *Range of motion and lordosis of the lumbar spine - Reliability of measurement and normative values*. Spine, 2001. **26**(1): p. 53-60.
34. Li, G. and P. Buckle, *Current techniques for assessing physical exposure to work-related musculoskeletal risks, with emphasis on posture-based methods*. Ergonomics, 1999. **42**(5): p. 674-695.
35. Bierma-Zeinstra, S.M.A., et al., *Measuring the Sacral Inclination Angle in Clinical Practice: Is There an Alternative to Radiographs?* Journal of Manipulative and Physiological Therapeutics, 2001. **24**(8): p. 505-508.
36. Black, K.M., P. McClure, and M. Polansky, *The influence of different sitting positions on cervical and lumbar posture*. Spine, 1996. **21**(1): p. 65-70.
37. Lee, R.Y.W. and T.K.T. Wong, *Relationship between the movements of the lumbar spine and hip*. Human Movement Science, 2002. **21**(4): p. 481-494.

38. Walsh, P., et al. *Marker-Based Monitoring of Seated Spinal Posture Using a Calibrated Single-Variable Threshold Model*. in *EMBS Annual International Conference*. 2006. New York City, USA.
39. Engsberg, J.R., et al., *Relationships Between Spinal Landmarks and Skin Surface Markers*. *Journal of Applied Biomechanics*, 2008. **24**: p. 94-97.
40. Stinton, S., et al., *Development and validation of a non-invasive spinal motion measurement system*, in *Annual Meeting for the American Society of Biomechanics*. 2009: Penn State University.
41. Troke, M., et al., *A new, comprehensive normative database of lumbar spine ranges of motion*. *Clinical Rehabilitation*, 2001. **15**(4): p. 371-379.
42. Seidel, G.K., et al., *Hip Joint Center Location from Palpable Landmarks - A Cadaver Study*. *Journal of Biomechanics*, 1005. **28**(8): p. 995-998.
43. Bush, T.R. and P.E. Gutowski, *An approach for hip joint center calculation for use in seated postures*. *Journal of Biomechanics*, 2003. **36**(11): p. 1739-1743.
44. Devore, J.L. and N.R. Farnum, *Applied statistics for engineers and scientists*. 2nd ed. 2005, Belmont, CA: Thomson Brooks/Cole. xvii, 605 p.

MICHIGAN STATE UNIVERSITY LIBRARIES



3 1293 03063 5449